LUMINESCENCE PROPERTIES OF ELECTRON-HOLE-DROPLETS

IN PURE AND DOPED GERMANIUM

Thesis by

Martin Chen

In Partial Fulfillment of the Requirements

for the Degree of

Doctor of Philosophy

California Institute of Technology

Pasadena, California

1977

(Submitted May 9, 1977)

To Mom, Dad, Stan and T.T.

ACKNOWLEDGEMENTS

ABSTRACT

This work contains 4 topics dealing with the properties of the luminescence from Ge.

The temperature, pump-power and time dependences of the photo-luminescence spectra of Li-, As-, Ga-, and Sb-doped Ge crystals were studied. For impurity concentrations less than about $10^{15}cm^{-3}$, emissions due to electron-hole droplets can clearly be identified. For impurity concentrations on the order of $10^{16}cm^{-3}$, the broad lines in the spectra, which have previously been attributed to the emission from the electron-hole-droplet, were found to possess pump-power and time dependent line shape. These properties show that these broad lines cannot be due to emission of electron-hole-droplets alone. We interpret these lines to be due to a combination of emissions from (1) electron-hole-droplets, (2) broadened multiexciton complexes, (3) broadened bound-exciton, and (4) plasma of electrons and holes. The properties of the electron-hole-droplet in As-doped Ge were shown to agree with theoretical predictions.

The time dependences of the luminescence intensities of the electron-hole-droplet in pure and doped Ge were investigated at 2 and 4.2°K. The decay of the electron-hole-droplet in pure Ge at 4.2°K was found to be pump-power dependent and too slow to be explained by the widely accepted model due to Pokrovskii and Hensel et al. Detailed study of the decay of the electron-hole-droplets in doped Ge were carried out for the first time, and we find no evidence of evaporation of excitons by electron-hole-droplets at 4.2°K. This doped Ge result is unexplained by the model of Pokrovskii and Hensel et al. It is

shown that a model based on a cloud of electron-hole-droplets generated in the crystal and incorporating (1) exciton flow among electron-hole-droplets in the cloud and (2) exciton diffusion away from the cloud is capable of explaining the observed results.

It is shown that impurities, introduced during device fabrication, can lead to the previously reported differences of the spectra of laser-excited high-purity Ge and electrically excited Ge double injection devices. By properly choosing the device geometry so as to minimize this Li contamination, it is shown that the Li concentration in double injection devices may be reduced to less than about 10^{15}cm^{-3} and electrically excited luminescence spectra similar to the photo-luminescence spectra of pure Ge may be produced. This proves conclusively that electron-hole-droplets may be created in double injection devices by electrical excitation.

The ratio of the LA- to TO-phonon-assisted luminescence intensities of the electron-hole-droplet is demonstrated to be equal to the high temperature limit of the same ratio of the exciton for Ge. This result gives one confidence to determine similar ratios for the electron-hole-droplet from the corresponding exciton ratio in semi-conductors in which the ratio for the electron-hole-droplet cannot be determined (e.g., Si and GaP). Knowing the value of this ratio for the electron-hole-droplet, one can obtain accurate values of many parameters of the electron-hole-droplet in these semiconductors spectroscopically.

Parts of this thesis either have been or will be published under the following titles:

Chapter 2: <u>Low Temperature Photoluminescence Spectra of Doped Ge</u>, M. Chen, D.L. Smith and T.C. McGill, Phys. Rev. <u>B15</u>, __ (1977).

Chapter 3: <u>Transients of the Photoluminescence Intensities of Electron-Hole-Droplets in Pure and Doped Ge</u>, M. Chen, S.A. Lyon, D.L. Smith and T.C. McGill, (to be published).

Chapter 4: <u>Properties of the Electron-Hole Condensate in Ge Double Injection Diodes II</u>, M. Chen, V. Marrello, T.C. McGill and J.W. Mayer, Phys. Rev. <u>B13</u>, 1617 (1976).

Chapter 5: <u>Ratio of TO- to LA-Phonon-Assisted Luminescence Intensities from the Exciton and Electron-Hole Condensate in Ge</u>, D.L. Smith, M. Chen and T.C. McGill, Solid State Commun. <u>18</u>, 1485 (1976).

Publications during the course of this work and not included in this thesis are:

<u>Exciton Effects on the Intervalence Band Transitions in Excited Ge</u>, D.L. Smith, M. Chen and T.C. McGill, Phys. Rev. <u>B14</u>, 3504 (1976).

<u>Multiphonon Absorption in the Alkali Earth Fluorides</u>, M. Chen, M. Hass and T.C. McGill, in <u>Optical Properties of Highly Transparent Solids</u>, (Plenum Press, New York, 1975), pp. 99-107.

vii

TABLE OF CONTENTS

Chapter 1

INTRODUCTION

I. BACKGROUND

It is well known that an electron and a hole in a pure semicon-
ductor crystal, through their mutual Coulomb attraction, can form a
bound pair. This bound pair can move about in the semiconductor and is
called a free-exciton (FE) or simply an exciton. The binding energy of
an exciton relative to a free pair of electron and hole depends upon
the effective masses of the electron and the hole as well as the di-
electric constant of the semiconductor and is usually between 1 and 20
meV. At low temperatures, the thermal energy of the carriers is less
than the binding energy of the exciton and a large fraction of the
carriers are bound into excitons.[1] In 1968 Keldysh[2] suggested the
existence of a highly correlated and high-density plasma phase of
electron-hole pairs. Each electron (hole) in this plasma sees on the
average more positive (negative) charge than a corresponding electron
(hole) bound in the exciton. The resulting reduction in the potential
energy may outweigh the gain in the kinetic energy which arises from
the close packing of fermions. This highly correlated, high-density
phase of electron-hole pairs is called the electron-hole liquid.
Theoretical calculations taking into account the band structure of the
semiconductors show that the electron-hole liquid is indeed more favor-
able energetically than the "excitonic gas" phase for a number of semi-
conductors, among them are Ge, Si[3], GaP, CdS, ZnS, and AgBr[4].

Figure 1 shows the band structure of an indirect semiconductor (Ge).
Electrons and holes are typically generated far away in k-space from
the extrema of the conduction and valence bands. Carrier -phonon
interaction tends to drive the electrons towards the bottom of the

Figure 1

The band structure of Ge. A typical excitation
of an electron-hole pair by a photon is shown
by the vertical line. The dashed lines sche-
matically illustrate the thermalization of the
excited carriers via phonon scattering; in ac-
tuality, many phonons may be needed to relax
the carriers completely. The extremum points
of the bands are labelled according to the ir-
reducible representations of the space group O_h^7.
The splitting between the Γ_8^+ and Γ_7^+ states is
0.29 eV. If spin is neglected, then the sym-
metry of the conduction band minimum is L_1.
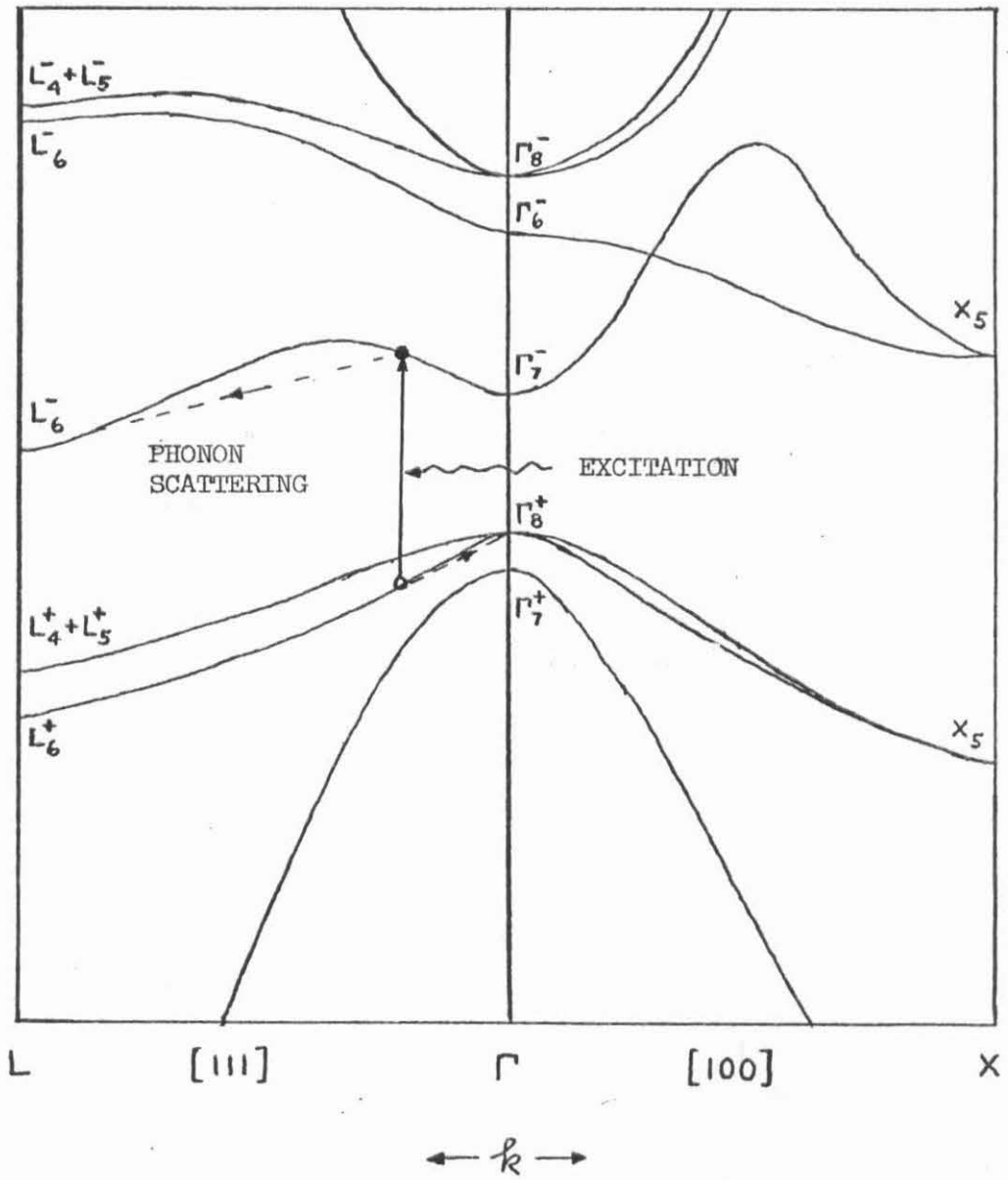
Figure 1

conduction band and the holes towards the top of the valence band.
The carrier-phonon scattering time is about a nanosecond[5] and is
much shorter than the lifetime of the carriers in indirect semiduc-
tors (usually on the order of microseconds). Thus, the carriers can
thermalize and the relative concentration of excitonic gas and electron-
hole liquid can be deduced from thermodynamic considerations. As for
any gas-liquid system, one expects to find a first-order phase transi-
tion with a critical point for the excitonic-gas-electron-hole-liquid
system. The equilibrium points of the excitonic gas and electron-hole
liquid should follow the universal, classical gas-liquid phase
diagram[6] as shown in Figure 2. If the temperature of the semi-
conductor is held constant and below the critical temperature, and the
concentration of electrons and holes is increased, the horizontal line
labelled as (a) is traced out. At low injection densities, only
excitons are formed. The exciton concentration increases with in-
crease of injection density until the density on the coexistence curve
is attained. Then, the exciton density is fixed on the coexistence
curve while droplets of electron-hole liquid begin to form. Further
increases in the injection density result in increases in the frac-
tional volume of the crystal occupied by the electron-hole-droplets
(EHD) at constant liquid and gas density. At extremely high injection
levels (which are practically hard to attain), part of the crystal may
be completely filled with electron-hole liquid. A vertical line such
as the one labelled (b) can be traced out by keeping constant injection
density while changing the temperature of the semiconductor. Below the
critical temperature, the electron-hole system spontaneously separates

6
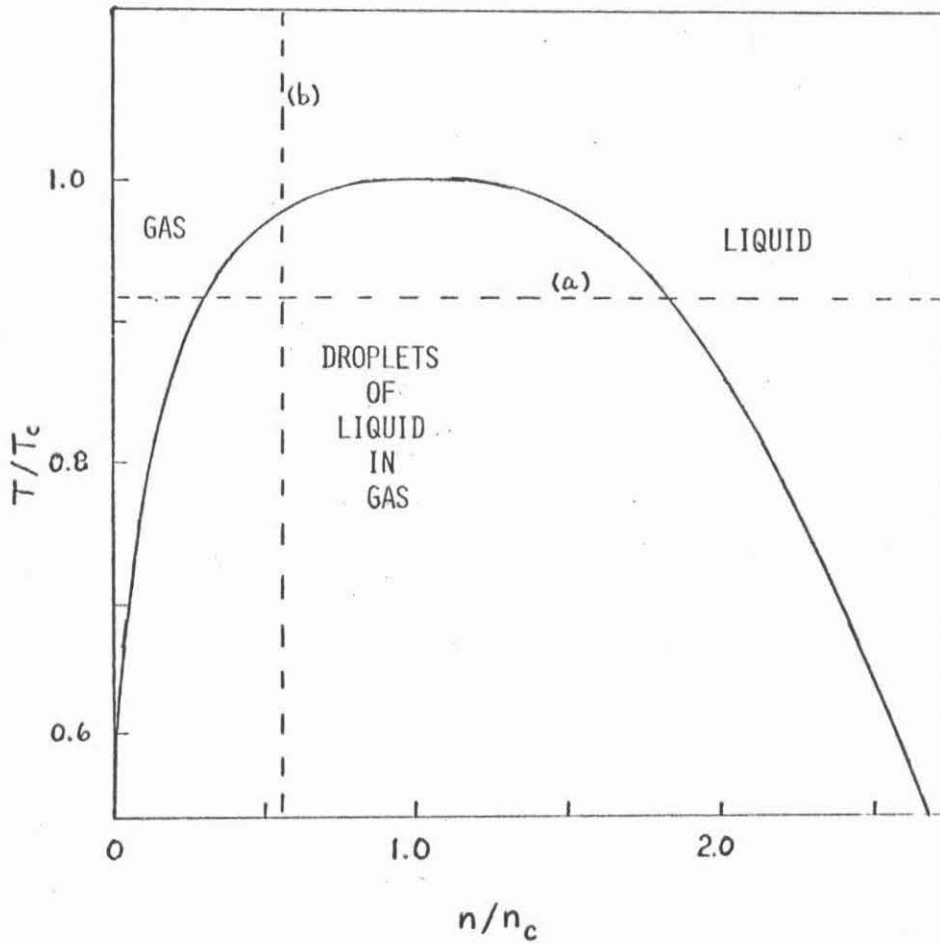
Figure 2. The classical, universal
gas-liquid phase diagram
(from reference 5)

into a low density excitonic gas phase and droplets of electron-hole
liquid.

Radiative recombination of electrons and holes in the EHD occurs
at different characteristic energies from that of the FE. Although
features in the photoluminescence spectrum of Ge due to the EHD were
observed as early as 1966 by Haynes[7], correct interpretation of these
features was first given by Pokrovskii and Svistunova[8] in 1970. Since
the electron-hole condensation phenomenon is a fundamental aspect of
carrier behavior in semiconductors, it has received considerable at-
tention since 1970 and much information about the EHD, particularly in
Ge[9], has been gathered.

Phonon assistance is required for the radiative recombination of
electrons and holes in indirect semiconductors. Usually several dif-
ferent phonons can provide the necessary crystal momentum so that the
luminescence spectrum contains several phonon-assisted EHD and FE lines.
The observed EHD line can be fitted to a simple theoretical lineshape
for the EHD to yield the binding energy of an electron-hole pair in the
liquid relative to the free exciton and the density of electron-hole
pairs in the liquid[10]. Both the binding energy and the pair density
show a quadratic dependence on temperature, indicating that carriers in
the EHD can be described as two inter-penetrating Fermi-liquids[10].
Excitons lose their identity when they are in the EHD. The liquid side
of the phase diagram can be determined by studying the luminescence
line of EHD's as a function of temperature[11]. The lifetime of the EHD
and the FE may be determined by looking at their decay as a function of
time following the turning-off of excitation[12].

Since the liquid density is high, the regions of the semiconductor occupied by EHD's have slightly different index of refraction than the rest of the crystal. Thus, infrared light passing through the crystal is both absorbed and scattered by the EHD's. The radius of the EHD can be deduced from the light scattering pattern while the EHD concentration can be estimated from the magnitude of the light absorption[13]. Results of lightscattering experiments have provided direct confirmation of the existence of EHD's.

When droplets are generated near a junction in a semiconductor, they can drift into the junction and be pulled apart by the large built-in electric field **there**. The break-up of individual droplets can be observed as current-noise spikes. Such experiments have shown that the number of electron-hole pairs in a droplet in Ge is 10^6 to 10^8 [14].

Some of the measured properties of the EHD in Ge and Si are listed in Table I.

Most studies of the EHD to date have been on high-purity Ge crystals, i.e., impurity concentrations less than $10^{14} cm^{-3}$. In this way, the electron-hole liquid can be studied with minimal complication from impurities. However, a knowledge of the influence of impurities on the behavior of the excited electrons and holes in doped crystals would be interesting and important for three reasons. First, only a few semiconductors can be grown with high purity at present. By studying the effect of impurities on the carrier behavior in a controlled manner in Ge, one obtains a basis for understanding the behavior of electrons and holes generated in semiconductors whose impurity content cannot be

	Germanium	Silicon
Pair density, n (cm^{-3})	2.4×10^{17} $(1-5.3\text{x}10^{-3}T^2)$	3.3×10^{18} $(1-4.5\text{x}10^{-4}T^2)$
Critical density, n_c (cm^{-3})	8×10^{16}	$\sim 2 \times 10^{18}$
Critical temperature, T_c (°K)	6.5	~28
Binding energy per pair, ϕ (meV)	$1.8 + 1.6\text{x}10^{-2}T^2$	$8.2 + 5.9\text{x}10^{-3}T^2$
Lifetime, τ (μsec)	37	0.2
Radiative efficiency	~50%	$\sim 10^{-3}$
Radius, r (μm)	2 to 20	
Compressibility, χ (cm^3/erg)	2×10^{-3}, $\chi/\chi_{H_2O} \sim 10^8$	
Methods of excitation	optical; electrical; electron beam	

Table I

Properties of the EHD in pure Ge and Si

reduced to an insignificant level at present. Second, by examining

how the properties of the electron-hole system change with impurity

concentration, one can extrapolate back to pure Ge and gain informa-

tion for pure Ge. Third, deliberately doped semiconductors play cen-

tral roles in devices today. Properties of electrons and holes in-

jected into doped semiconductors are, therefore, of practical interest.

II. OUTLINE OF THESIS AND SUMMARY OF MAIN RESULTS

In Chapter 2, the results of an investigation of the photo-

luminescence spectra of Li-, As-, Ga-, and Sb-doped Ge are reported.

The temperature, time, and pump-power dependences of these spectra were

studied. We found that impurity-induced emissions are quite noticeable

in the doped Ge spectra. For impurity concentrations of less than

about $10^{16} cm^{-3}$, the line due to electron-hole-droplets can easily be

identified and little impurity effect on this line is observed. For Ge

with impurity concentrations between 10^{16} and $10^{17} cm^{-3}$, we found that

the broad lines in the spectra, which have similar shape to the EHD line

and have been interpreted to be due to EHD emission previously[14], are

in fact due to two or more emission processes. One of these processes

is probably emission from the EHD, the others are impurity-induced. We

found that the phonon-assisted lines of Ge:As are least affected by the

impurity-induced emissions. We interpret these lines to be mostly due

to EHD emission. Analyses of their line shapes yielded the pair

density of the EHD and the work function of a pair in the liquid phase

relative to a pair in the gas phase. Both the pair density and the

work function of the EHD decrease linearly with impurity concentration

and are in quantitative agreement with theoretical calculations. Examination of possible causes of the impurity-induced emissions shows at least three possibilities: broadened multiexciton complexes (several excitons bound to one neutral impurity), broadened bound-exciton and plasma emissions.

The decay of the EHD luminescence intensity following the turn-off of excitation has been the subject of a number of studies[12]. The results of these studies have all been interpreted in terms of a model which views each droplet as being isolated from all other droplets. Although this model can explain many experimental observations, there were inconsistencies between the various reports. It is shown in Chapter 3 that these inconsistencies are due to the different excitation powers used by the different investigators. The previously accepted model is shown to be incapable of explaining these inconsistencies. Detailed study of the decay transients in doped Ge were carried out for the first time and the results we obtained were also not explainable in terms of the accepted model. A more detailed though still somewhat idealized model is presented. This model explains the experimental results for both pure and doped Ge.

In Chapter 4, the results of a study of electrically excited luminescence spectra from Ge double injection diodes are reported. Earlier studies[16] of double injection devices had shown that the spectra from these diodes differ from the photoluminescence spectra in several respects. We show that double injection diodes used in the earlier studies were contaminated by Li. By choosing device geometry so that Li contamination is minimized, we are able to produce double

injection spectra similar to photo-excited luminescence spectra.

In Chapter 5, we report the determination of the relative inten-
sities of the LA- and TO-phonon-assisted luminescence lines of the ex-
citon and the electron-hole-droplets, $\gamma_E(T)$ and γ_{EHD}, respectively.
The predictions of Smith and McGill[17] on the values of these relative
intensity ratios have been explicitly verified. This allows one to
determine γ_{EHD} from $\gamma_E(T)$ in many semiconductors in which γ_{EHD} cannot
be determined directly. In the case of Si and GaP, accurate line-fits
of the droplet line, which can yield many useful parameters for the
electron-hole liquid in these semiconductors, is not possible without
the value of γ_{EHD}.

SUMMARY OF MAIN RESULTS

Chapter 2:

1. Extensive data on the photoluminescence spectra of doped-Ge
were obtained. The dopants studied were Li, As, Ga and Sb. These data
included temperature and pump-power dependences of the spectra and time-
resolved spectra.

2. Many possible processes which may contribute to these spectra
were considered. The processes that are likely to contribute to the
spectra in view of our data include emission from (a) EHD, (b) broad-
ened multiexciton complexes, (c) broadened bound-excitons, and (d)
plasma of electrons and holes.

3. The LA-phonon-assisted emission of Ge:As was found to be
dominated by emissions from EHD's. Analyses of this line yielded den-
sities and work functions of the EHD in doped Ge which are in agreement

with theoretical calculations.

Chapter 3:

1. Decays of the photoluminescence intensities of the EHD of pure
and doped Ge were studied at 2 and 4.2°K.

2. These data show conclusively the inadequacy of a widely ac-
cepted model of the decay of EHD's.

3. A new model is proposed which explains the data.

Chapter 4:

It is demonstrated that EHD's can be created electrically in a
double injection diode when the impurity concentration in the active
volume of the diode is kept to less than about 10^{15}cm^{-3}.

Chapter 5:

It is demonstrated for Ge that the ratio of the LA- to TO-phonon-
assisted intensities of the EHD lines can be obtained from the same
ratio for the exciton at high temperatures. This fact is useful for
determining properties of the EHD in a number of other semiconductors.

III. DROPLET LUMINESCENCE LINE SHAPE

In examining the luminescence spectra from Ge, frequent references will be made to the line shape of the electron-hole-droplet. Therefore, a brief discussion of the thoeretical EHD line shape will first be given.

A simple model for the EHD luminescence line shape which works well was proposed by Pokrovskii[18]. In this model, it is assumed that the carrier-carrier interaction inside an EHD results only in a uniform reduction of the band gap. Thus, in the macroscopic volumes of the Ge crystal occupied by EHD's, the band gap is E_g', which is smaller than the band gap E_g of unexcited Ge. This reduction in the energy gap is illustrated in Figure 3(a). Electrons and holes in the EHD are treated as being free, except that they are confined by the edge of the EHD. Since the thermalization times within the conduction and valence bands are very short compared to the recombination time, the electrons and holes in the EHD can separately be characterized by Fermi-Dirac distributions with quasi-Fermi levels ε_F^e and ε_F^h. The situation depicted in Figure 3 is for the temperature of absolute zero. In this case, the electrons occupy all conduction band levels up to ε_F^e and no levels above ε_F^e; and a corresponding distribution applies for the holes.

The carrier distribution in momentum-space forms the basis for the model of EHD luminescence line shape, as illustrated in Figure 3(b). For simplicity, only the band extrema occupied by carriers, viz., the conduction band minimum at the L-point or the (111) zone-edge and the valence band maximum at the Γ-point or the zone-center, are shown. Each electron can recombine with any hole with the assistance of a
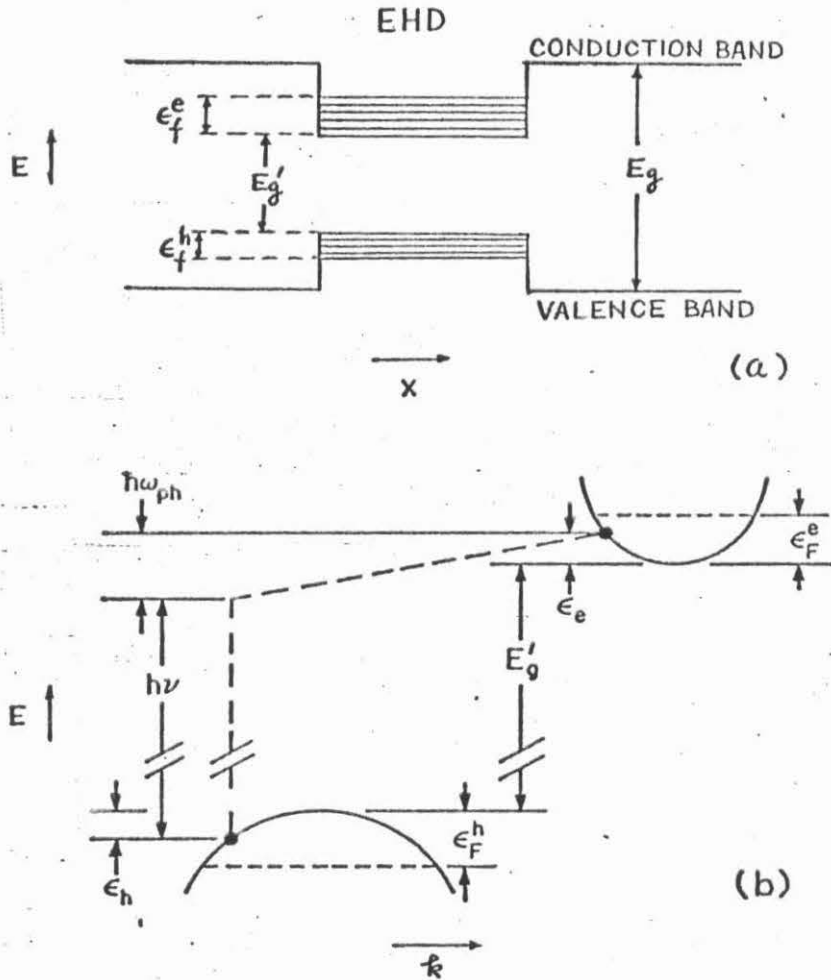
LUMINESCENCE MODEL
FOR
ELECTRON-HOLE LIQUID

Figure 3

(a) Schematic illustration of energy levels of a droplet in real space.
(b) Schematic illustration of electron-hole distribution of a droplet in k-space. A typical recombination transition of an electron-hole pair is shown.

suitable phonon to provide for crystal momentum conservation. The shape of each phonon-assisted droplet line is given by

$$I(h\nu) \sim \sum_{\vec{k}_e, \vec{k}_h} f_e(\varepsilon_e) f_h(\varepsilon_h) |M(\vec{k}_e, \vec{k}_h, \nu_{ph})|^2$$

$$\cdot \; \delta(E_g' + \varepsilon_e + \varepsilon_h - h\nu_{ph}(\vec{k}_e, \vec{k}_h) - h\nu) \tag{1}$$

In Eqn. (1), $I(h\nu)$ is the intensity of the EHD luminescence line at photon energy $h\nu$, $\vec{k}_e$ ($\vec{k}_h$) and ε_e (ε_h) are respectively the electron (hole) momentum and energy as defined in Figure 4(b), $M(\vec{k}_e, \vec{k}_h, \nu_{ph})$ is the matrix element for the phonon-assisted transition, and ν_{ph} is the frequency of the momentum-conserving phonon. The occupation probability $f_e(\varepsilon_e)$ of the electron state at energy ε_e is

$$f_e(\varepsilon_e) = \frac{1}{\exp\left[(\varepsilon_e - \varepsilon_F^e)/kT \right] + 1} \tag{2}$$

where k is the Boltzmann constant and T is the absolute temperature. The probability of occupation of the hole states is given by Eqn. (2) with ε_e and ε_F^e replaced by ε_h and ε_F^h. For Ge (and similar arguments work for other semiconductors as well), ε_F^e and ε_F^h are ~ 3 meV and k_F^e and k_F^h are $\sim 10^{-2}$ G, where G is the width of the Brillouin zone in the (111) direction. These small k_F's allow two simplifications of Eqn. (1) to be made. The different phonons required to conserve momentum for recombination have a momentum spread of at most $k_F^e + k_F^h$ and, therefore, are never far from the L-point zone-edge. Thus, $h\nu_{ph}$ can be taken to

be a constant and equal to the L-point phonon energy. For the same reason, the k-independent part of the matrix element for the transition is the dominant part of that matrix so that $M(\vec{k}_e, \vec{k}_h, \nu_{ph})$ can be taken to be a constant. The expression for $I(h\nu)$ then reduces to

$$I(h\nu) \sim \int d\varepsilon_e d\varepsilon_h \rho_e(\varepsilon_e) \ \rho_h(\varepsilon_h) f_e(\varepsilon_e) f_h(\varepsilon_h)$$

$$\cdot \ \delta(E_g' + \varepsilon_e + \varepsilon_h - h\nu_{ph} - h\nu). \tag{3}$$

In Eqn. (3) we have also replaced the sum over $\vec{k}_e$ and $\vec{k}_h$ in Eqn. (1) by integrals over the electron and hole densities of states, $\rho_e(\varepsilon_e)$ and $\rho_h(\varepsilon_h)$, which are taken to vary as $\varepsilon_e^{1/2}$ and $\varepsilon_h^{1/2}$, respectively.

It is clear from Figure 3(b) that the lowest energy photon emitted by a pair in the EHD results from recombination of an electron at the bottom of the conduction band and a hole at the top of the valence band. At zero temperature the highest energy photons emitted in recombination come from electrons and holes at their respective Fermi levels. Thus, the EHD linewidth is a strong function of $\varepsilon_F^e + \varepsilon_F^h$. Since the Fermi energies are determined by electron and hole densities, the EHD line-width can be used to obtain the pair density in an EHD. At finite temperatures, the carrier distributions are smeared out near the Fermi energies. This smearing affects the linewidth slightly but at the same time allows one to determine the temperature of the carriers by fitting the high-energy edge of the EHD line.

Figure 4 shows a comparison of the theory with an experimental EHD line of high-purity Ge[19]. It can be seen that the two curves
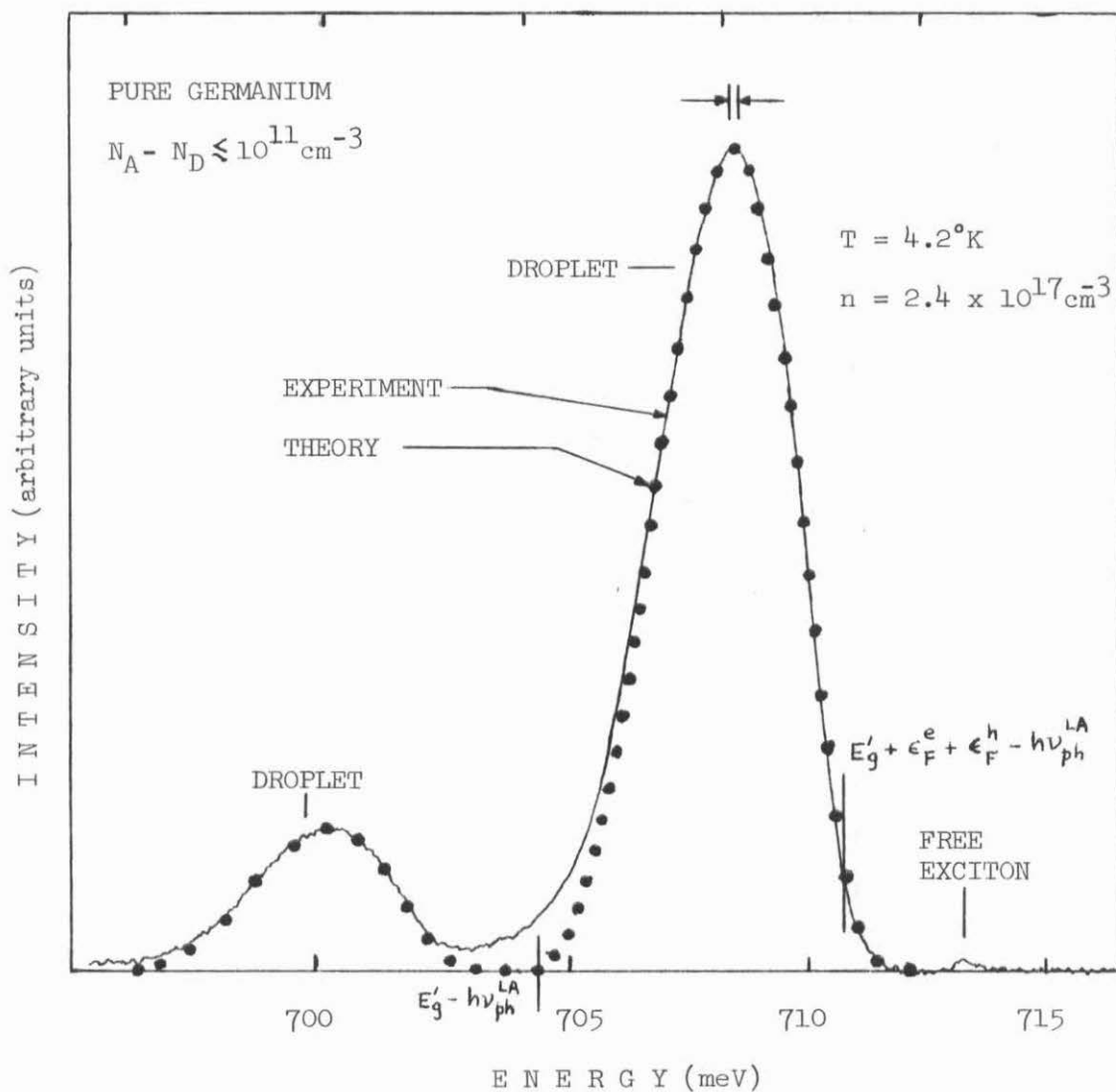
Figure 4

Photoluminescence spectrum of pure Ge at
a bath temperature of 2°K. The two broad
lines are due to emissions from electron-
hole-droplets. The more intense line is
assisted by the LA-phonon and the weaker
one is assisted by the TO-phonon. The
theoretical points are generated using
equation (3) with T=2°K and n=2.4x10^{17}cm^{-3}.

agree very well. The slight discrepancy at the low-energy edge of the line is due perhaps to two-phonon processes or recombinations which result in an excited droplet.

One can estimate the pressure exerted by the excitonic gas on an EHD by putting the density of excitons from the phase diagram[11] into the ideal-gas equation. One finds from this calculation that the excitonic pressure on a droplet is always very small so that experimentally one cannot access the finite-pressure region of the complete (density vs. temperature vs. pressure) phase diagram. In other words, the projection of the complete phase diagram onto the zero-pressure plane, such as the one shown in Figure 2, is sufficient to describe the electron-hole gas-liquid system. The droplet density or linewidth is completely determined at any given temperature by the "reduced" phase diagram as shown in Fig. 2. Above the EHD formation threshold, change of excitation intensity merely results in a change in the total volume of the liquid at constant liquid density if the temperature of the semiconductor is held constant. Similarly, when droplets are allowed to decay by turning off the excitation, the droplets decay at constant density until they get so small that the surface energy becomes significant. One would expect then that the droplet line shape would not change during decay. The fact that the droplet line shape should be independent of excitation and time is indeed observed for pure Ge. This fact provides a convenient criterion for determining if doped Ge spectra include emission from droplets.

REFERENCES

1. See, for example, R.S. Knox, Theory of Excitons, (Academic Press, New York, 1963).

2. L.V. Keldysh, in Proc. 9th Int. Conf. Semicond. Phys, Moscow, 1968 (Nauka, Leningrad, 1968), p.1303.

3. P. Vashista, S.G. Das and K.S. Singwi, Phys. Rev. Lett. 33, 911 (1974), and references contained therein. It was found that the multi-valley degeneracy of the conduction band minimum in many semiconductors is essential to the binding of the electron-hole liquid.

4. G. Beni and T.M. Rice, Phys. Rev. Lett. 37, 874 (1976). In this calculation, the coupling of the carriers to phonons was found to be important for GaP, CdS, ZnS and AgBr.

5. J.C. Hensel and K. Suzuki, Phys. Rev. B9, 4219 (1974).

6. E.A. Guggenheim, J. Chem. Phys. 13, 253 (1945).

7. J.R. Haynes, Phys. Rev. Lett. 17, 860 (1966).

8. Y.E. Pokrovskii and K.I. Svistunova, Fiz. Tek. Polup. 4, 491 (1970) [Sov. Phys.-Semicond. 4, 409 (1970)].

9. See, for example, C.D. Jeffries, Science 189, 955 (1975), and references contained therein.

10. G.A. Thomas, T.G. Phillips, T.M. Rice and J.C. Hensel, Phys. Rev. Lett. 31, 386 (1973).

11. G.A. Thomas, T.M. Rice and J.C. Hensel, Phys. Rev. Lett. 33, 219 (1974).

12. R.M. Westervelt, T.K. Lo, J.L. Staehli and C.D. Jeffries, Phys. Rev. Lett. 32, 1051 (1974), and references contained therein.

13. J.C.V. Mattos, K.L. Shaklee, M. Voos, T.C. Damen and J.M. Worlock, Phys. Rev. B13, 5603 (1976), and references contained therein.

14. J.M. Hvam and O. Christensen, Solid State Commun. 15, 929 (1974), and references contained therein.

15. R.W. Martin and R. Sauer, Phys. Status Solidi B62, 443 (1974), and references contained therein.

16. V. Marrello, T.C. McGill and J.W. Mayer, Phys. Rev. B13, 1607 (1976).

17. D.L. Smith and T.C. McGill, Phys. Rev. B14, 2448 (1976).

18. Y.E. Pokrovskii, Phys. Status Solidi <u>A11</u>, 385 (1972).

19. The computer program for the generation of the line shape of the
    EHD, as given by eqn.(3) was kindly provided by R.B. Hammomd. More
    extensive discussion of the EHD line shape can be found in R.B.
    Hammond, T.C. McGill and J.W. Mayer, Phys. Rev. <u>B13</u>, 3566 (1976).

Chapter 2

PHOTOLUMINESCENCE SPECTRA OF DOPED Ge

I. INTRODUCTION

The study of electron-hole droplets (EHD) in Ge and Si has received considerable attention in recent years[1]. In relatively pure Ge with impurity concentration $N_i \lesssim 10^{14} cm^{-3}$, the existence of EHD have been demonstrated by light scattering[2] and junction noise[3] experiments. In Ge with $N_i \sim 10^{15} cm^{-3}$, no light scattering results are available but junction noise experiments strongly suggest that EHD do exist[4]. Below 10°K, photoluminescence spectra of moderate-heavily doped Ge (we mean by moderately heavy doping impurity concentration of 10^{16}-$10^{17} cm^{-3}$ in this thesis) are dominated by a broad line whose shape and position are nearly the same as those of the EHD line in pure Ge. This led the early investigators[5,6] to suggest that EHD do form in heavily doped Ge. Also, the decay lifetimes of the EHD in heavily doped Ge:As and Ge:Sb were found to be shorter than the lifetime of EHD in pure Ge[7]. In As- and P-doped Ge, a broad line in addition to the usual phonon-assisted lines was observed. This line is similar to the EHD line and is located where EHD recombination without phonon assistance is expected. This line was attributed to recombination from EHD with the impurity atoms taking up the "excess momentum"[6,7].

An unusual property of the "EHD" line in moderate-heavily doped Ge is its pump-power-dependent line shape, first reported by Novikov et al[6]. While the line was essentially identical to that of the EHD in pure Ge at high pump powers, it shifted towards higher energy and became narrower at lower pump powers. They attributed this to the formation at low pump powers of small droplets for which the surface energy contribution is observable. Extensive investigations of the

line shape versus pump power were carried out by Martin and Sauer[8]. They reported that with increasing excitation power, the EHD line broadened on both the low- and high-energy side. The full width at half maximum (FWHM) of the line varied smoothly with pump power, exceeding that of the EHD line in pure Ge at sufficiently high pump powers. Martin and Sauer offered Novikov's explanation for the behavior at low pump powers and Martin suggested[9] that the results at high pump powers are due to a complete filling of part of the doped Ge sample with the electron-hole liquid. One difficulty with this interpretation, noted by Martin and Sauer, is that one would expect to see a range of pump powers for which normal size droplets are created but without sample filling. The FWHM of the line for this pump-power range should be independent of excitation. This prediction is not observed experimentally.

Karuzskii et al.[10] have studied the luminescence decay and magneto-oscillation behavior of the LA-phonon-assisted and the no-phonon "EHD" lines (henceforth referred to as the LA and NP lines, respectively) in Ge:As. They found very different results for the two lines. They suggested that the LA line is due to the EHD while the NP line is possibly due to emissions from "multiexciton complexes" which are thought to be objects composed of a single neutral-impurity and many bound excitons[11].

Theoretical calculations[12,13] of the properties of the EHD in doped Ge have been reported by several authors. These theories predict only slight modifications of the pair density and binding energy of a droplet for doping concentration between 10^{15} and $10^{17} cm^{-3}$. However

due to the unexplained pump-power dependence of the EHD-like line in doped Ge, no unambiguous comparison of theory with experiment exists. On the whole, the understanding of the spectra in moderate-heavily doped Ge is rather poor.

In this chapter, we present comprehensive experimental data which suggest that the broad EHD-like line in moderate-heavily doped Ge are in fact the result of two or more spectroscopically unresolved emissions. Since the temperature, pump-power and time dependences of these processes differ, their sum has a complicated behavior. The phonon-assisted lines in Ge:As were found to have very little contributions from impurity-induced emissions below 4.2°K. We interpret these lines to be due mainly to EHD emissions. Fitting the theoretical line shape to these lines yielded pair densities and binding energies of the EHD as functions of impurity concentration which are in agreement with theoretical predictions. Possible origins of the impurity-induced emissions will be discussed.

II. EXPERIMENT

(a) Samples

The pure Ge samples used in this study were of ultra-high purity. The net shallow impurity concentrations in these samples, $|N_A-N_D|$, were less than about $10^{11} cm^{-3}$. The pure as well as some of the doped Ge samples were obtained from the General Electric Research Laboratories[14]. Other doped Ge samples were purchased from the Nucleonic Products Co.[15]. Samples from these two sources were found to yield in general longer carrier lifetimes than samples from a few

other sources and are probably the best obtainable today.

To minimize heating of the samples by the excitation pulses, large slices of Ge were cut for use as samples. The areas of these slices ranged between 75 to 500 mm^2. It was also necessary to minimize the effect of the backsurface, i.e., the surface opposite to the excited one, on the excited carriers. To this end, 2 mm was chosen to be the minimum sample thickness. It will be shown later that a 2 mm separation between the excited surface and the backsurface suffices to eliminate any effect of the backsurface on the excited electrons and holes. The surfaces of the samples that were to be excited were prepared by successive lapping with 40; 15; and 5-μm alumina grits followed by a mechano-chemical polish. To minimize further surface damage, they were then lightly etched in a 5:1 HNO_3:HF solution. Prior to each experiment they were rinsed with methanol and dried. The other surfaces of the samples were simply lapped and etched.

The Li-doped Ge samples were made by diffusing Li into high-purity Ge crystals (~ 5 mm thick). The diffusions were carried out at 350°C for about 30 min. Differential resistivity measurements[16,17] on samples so prepared showed that there is a dead layer at the surface about 100 μm thick. Below the dead layer is a 400 μm layer in which the Li concentration decreases from $6X10^{16}$ to $2.5X10^{16}$cm^{-3}. Beneath this layer the doping profile is exponential with the doping level dropping about one decade per 200 μm. Figure 1 shows the differential resistivity data. Following the diffusion, the samples were lapped with 5-μm grits to remove the heavily pitted dead layer created by the Li-diffusion process. They were then etched in a 3:1 HNO_3:HF

Figure 1

Results of differential resistivity measurements
of Li-doped Ge. Lithium diffusion was carried out
at 350°C for about 30 minutes. The circles are
the sheet resistivity data versus distance from
the surface. The triangles are the carrier con-
centrations obtained from the sheet resistivities
using the standard procedure (see references 16
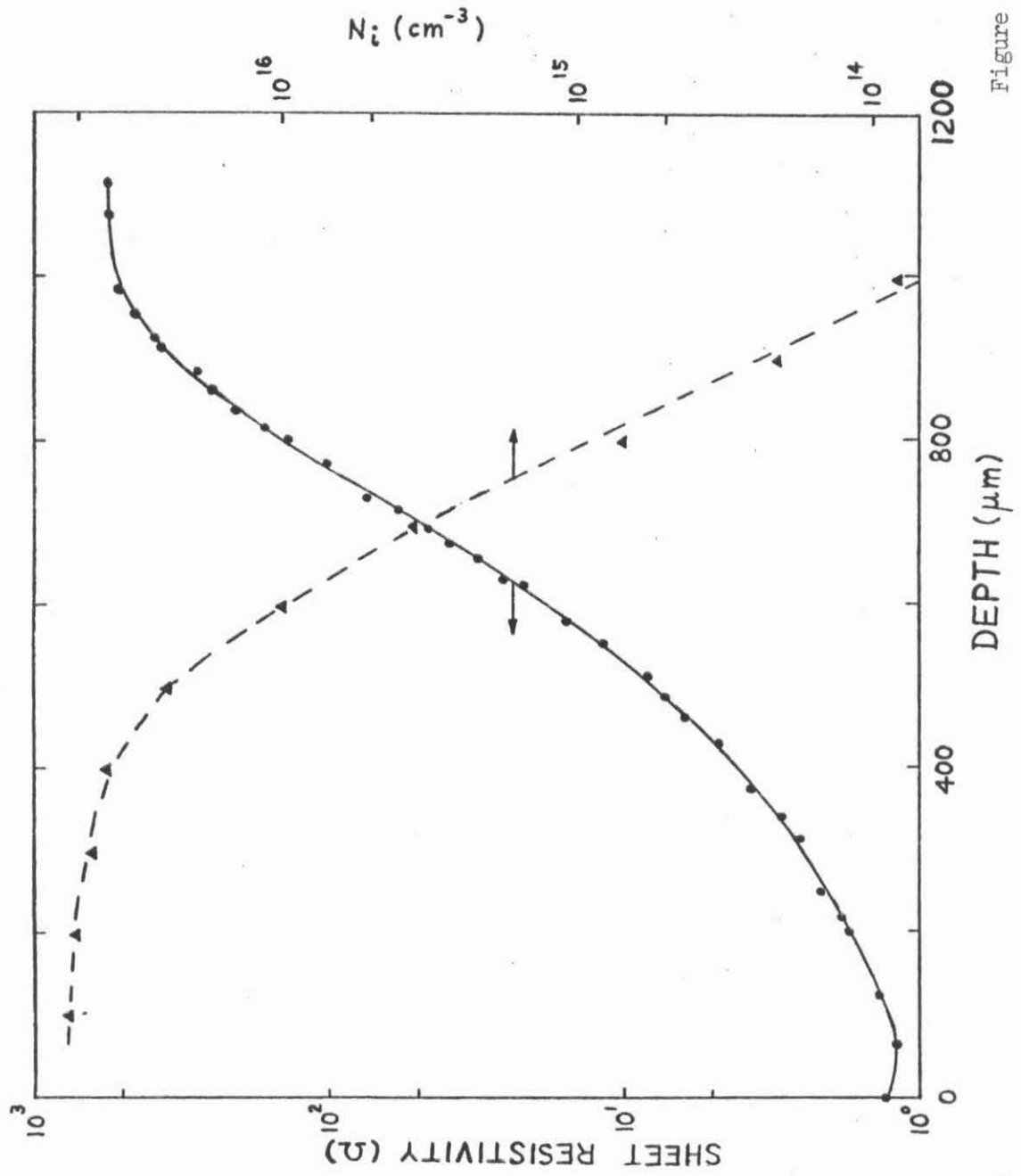and 17).

Figure 1

solution and photoluminescence measurements were performed on the doped side. The lapping, etching and measurement steps were repeated several times to cover the range of concentration of Li at the surface of 5.5×10^{16} to $5 \times 10^{14} cm^{-3}$.

(b) Experimental Apparatus

A schematic diagram of the experimental apparatus used is shown in Figure 2. Photo-excitation was provided by RCA SG2007 GaAs laser diodes. Although these diodes have a nominal maximum pulse width of 2 μsec, they can be driven with current pulses as long as 100 μsec at reduced currents without noticeable degradation. The sample under study was mechanically attached to a copper sample-holder block, and the laser is mounted a few mm's perpendicularly above the sample's flat face. The sample holder was then placed inside a Janis variable-temperature dewar. Temperatures above 4.2°K were achieved with heated He-vapor regulated by an Artronix model 5301 temperature-controller. Below 4.2°K, a vacuum regulated liquid He bath was used for cooling. Temperature drift during the recording of a single spectrum was typically less than 5%. A calibrated Ge-sensor in contact with or in close proximity to the sample was used to monitor the temperature.

The recombination radiation from the illuminated face of the sample was collected and focused by two lenses onto the entrance slit of a Spex 1400-II grating spectrometer. The lens combination has a magnification factor of three. The maximum slit opening on our Spex is 3 mm which allowed, at most, radiation within a 30 Å (1.2 meV) bandwidth and emerging from a 1-mm strip from the sample surface to be
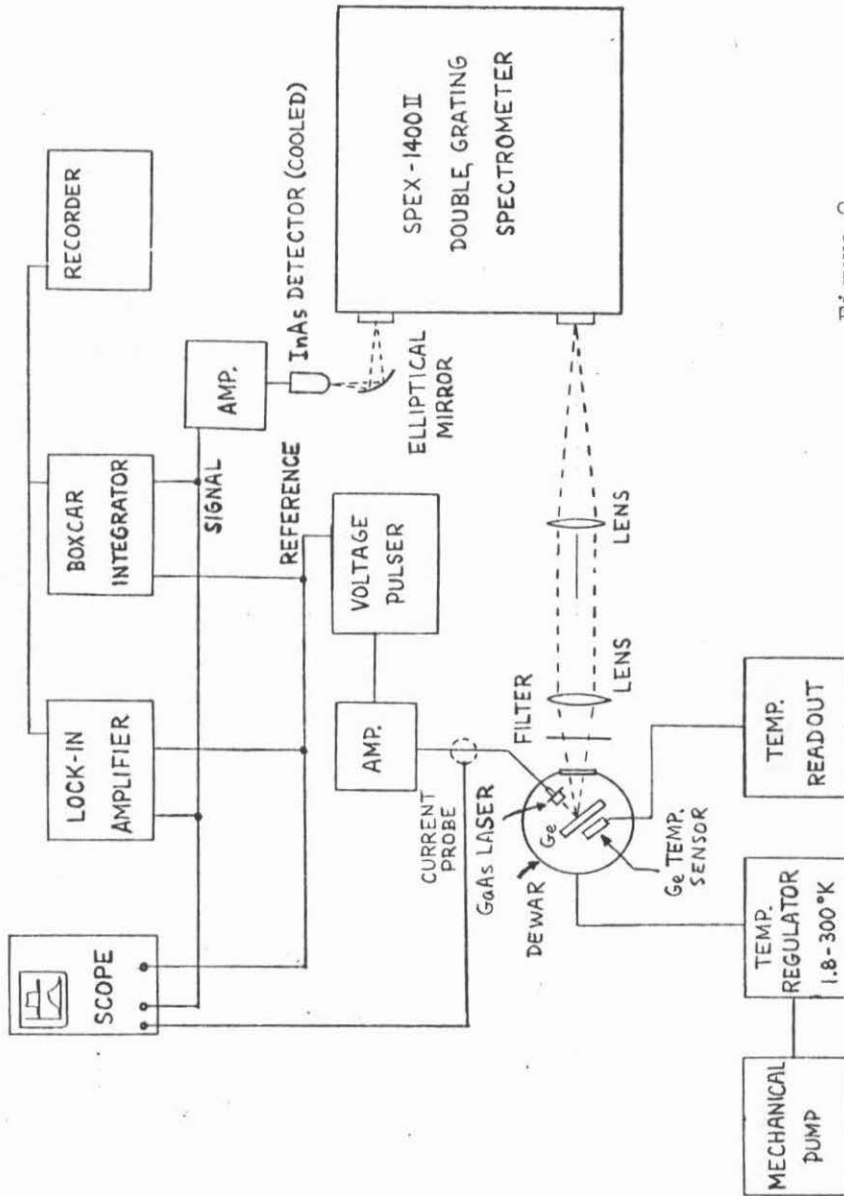
Figure 2

Schematic diagram of experimental set-up

collected. The output from the spectrometer was focused onto the detector with an elliptical mirror. An InAs photovoltaic detector operated at either dry-ice or liquid-N_2 temperatures was used. The InAs detector output was fed through a current amplifier to either a lock-in amplifier or a boxcar integrator. The processed signal was recorded on a strip chart recorder.

The outputs of the lasers used were calibrated at 5°K using a calibrated Si-photodiode. The laser spot on the sample was about 1 mm in diameter as determined with an infrared image converter. The spot size varied somewhat depending on the sample thickness. Laser powers quoted in this study have not been corrected for reflection losses at the surfaces of the Ge samples. (This loss is about 36% per surface.) Since the risetime of GaAs laser (~10 nsec) is much shorter than our detection system response time, measurement of the GaAs laser pulse yields the risetime of our detection system. The 0-90% response time was less than 5 μsec and was independent of the light level incident upon the detector for the range of light levels involved here.

Time-resolved spectra were measured using a boxcar integrator with a gate width of 2 μsec. Throughout this chapter we will define the delay time, t, to be the time between the beginning of the current pulse through the GaAs laser and the leading edge of the boxcar gate pulse.

Luminescence-scan measurements were done by imaging a polished face of the sample onto the entrance slit of the spectrometer and translating the sample.

III. EXPERIMENTAL RESULTS

(a) Ge:Li

Figure 3 shows the photoluminescence spectra at various temperatures of Li-doped samples along with spectra from a pure sample. The spectra presented in this section are not time resolved.

In Figure 3(a), the spectrum of pure Ge at 4.2°K shows the well known[11] LA-phonon-assisted EHD and free exciton (FE) lines at 708.6 and 713.2 meV, respectively. The TO-phonon-assisted replica of the FE and EHD (not shown) lines appear at about 8 meV below their respective LA lines. As the temperature is raised above 4.2°K, the intensity of the EHD line drops quickly so that at 6°K, which is close to the critical temperature of the electron-hole liquid[18], the FE signal dominates the spectrum. The LA- and TO-phonon-assisted FE lines are easily discernible at 50°K though not fully resolvable. The shift of the peak of the line to lower energy at 50°K is due to a reduction of the energy gap at that high temperature[19].

The spectra from the sample with a concentration of Li of $5 \times 10^{14} cm^{-3}$ at the surface, Figure 3(b), show essentially the same features as those from the high-purity Ge. In particular, the EHD line shape and position at 4.2°K are identical to those in the high-purity Ge. At 6°K, a shoulder is seen at the low-energy edge of the FE line. It is unlikely that this shoulder is due to EHD for two reasons. First, the peak of the EHD line at 6°K is at approximately 709.4 meV[18], as indicated by the arrow on the 6°K spectrum in Figure 3(b). Even if some correction is made for the apparent peak-shift due to the interference of the strong FE line, the shoulder is peaked at too high an

Figure 3

Photoluminescence spectra of pure and Li-doped Ge at various temperatures. The GaAs laser power, pulse-width, and duty cycle are indicated in that order below the title. Next to the title is the spectral resolution. Where resolution differed from that indicated near the title, it is indicated near the peak of the appropriate spectrum. The arrow in the 6°K spectrum in (b) indicates the peak of the EHD line as given in reference 18 .
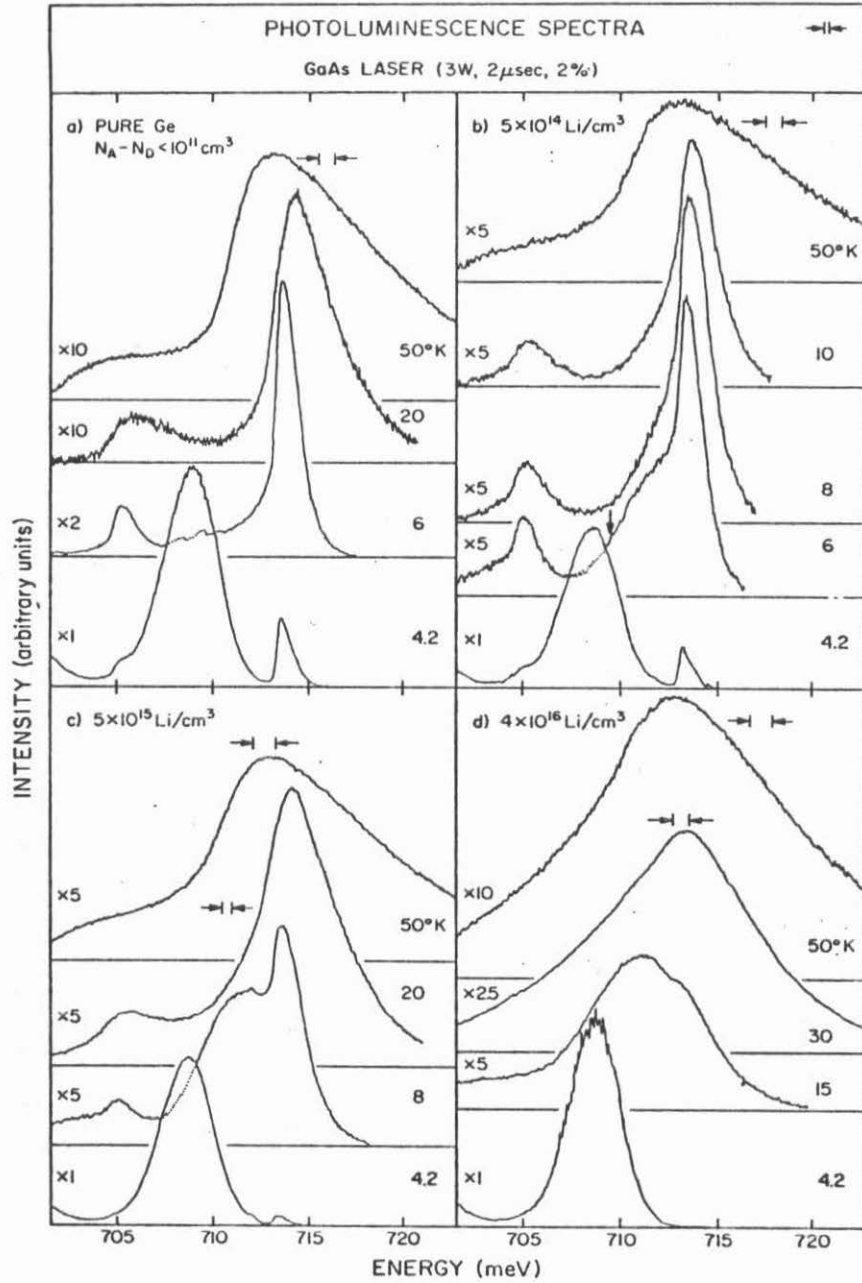
Figure 3

energy to be the EHD line. Second, the FE line in Figure 1(b) has a low-energy tail even at 8°K, which is a temperature well above the critical temperature for droplet formation. (Theoretical calculation[13] suggests that the critical temperature of EHD should not be changed by a doping level of $5X10^{14}cm^{-3}$.) Thus, the shoulder on the FE line must be due to impurity-induced emission.

When the Li concentration at the surface of the sample is $5X10^{15}cm^{-3}$, Figure 3(c), three significant changes occur in the photoluminescence spectra. First, the FE intensity at 4.2°K is greatly reduced compared to that in less heavily doped Ge. Second, a bound-exciton (BE) line can be detected between the EHD and FE lines. The BE line is located at about 712 meV, approximately 1 meV below the FE line in accordance with Haynes' Rule[20]. Third, the "EHD" line shifts continuously with increasing temperature towards the FE line. It perturbs the low energy edge of the FE line even at 20°K. There is similarity between the spectrum at 8°K in Figure 3(c) and the spectrum at 6°K in Figure 3(b). This similarity and the discussion in connection with Figure 3(b) in the preceding paragraph lead us to suspect that the "EHD" line at 8°K in Figure 3(c) is due in part to impurity-induced emission.

For the surface with $4X10^{16}cm^{-3}$ of Li, we obtained the spectra shown in Figure 3(d). First, at 4.2°K only the broad line resembling the EHD line is seen. It is not accompanied by either FE or BE emission, as is the case in the lighter-doped Ge. Second, this broad line shifts continuously towards the FE line with increasing temperature, and the FE line is unambiguously resolved only for T $\gtrsim$ 15°K. This broad line is seen even at 50°K where it fills the valley, present in

the 50°K pure Ge spectrum, between the LA- and TO-phonon-assisted FE lines.

It is difficult to interpret even the low-temperature (say $T \lesssim 5°K$) emission lines in Figure 3(d) to be due to EHD alone. In Figure 4 we show the linewidth of the "EHD" line at 5°K as a function of pump-power for different surface Li concentrations. There is no observable pump-power dependence of the linewidth of the broad line for impurity concentration up to $5 \times 10^{15} cm^{-3}$. This is as expected for a EHD emission line. In contrast, the data from the sample with $4 \times 10^{16} cm^{-3}$ of Li at the surface show clear pump-power dependence. Martin and Sauer[8] have reported quantitatively similar results for Ge:In, Ge:Ga and Ge:Sb. In addition, they showed that, at very high pump-powers, the linewidth of the broad line in moderate-heavily doped Ge exceeds that of the EHD line in pure Ge.

(b) Ge:As

The temperature dependence of the spectra from a Ge sample with $4 \times 10^{15} As/cm^3$ is very similar to that of the $5 \times 10^{15} Li/cm^3$ sample shown in Figure 3(c). In addition, we have observed no pump-power or time dependence of the EHD line. Similar behaviors were observed for Ge doped with about $10^{15} cm^{-3}$ of Ga or Sb. In the rest of this and the next two subsections, we will report only the data from moderate-heavily doped Ge whose spectra show unexpected properties.

A 4.2°K spectrum from a Ge:As sample with $5 \times 10^{16} As/cm^3$ is shown in Figure 5. Features in this spectrum include the LA line (708.5 meV) and the NP line (736 meV) as well as the TO- and TA-phonon-assisted
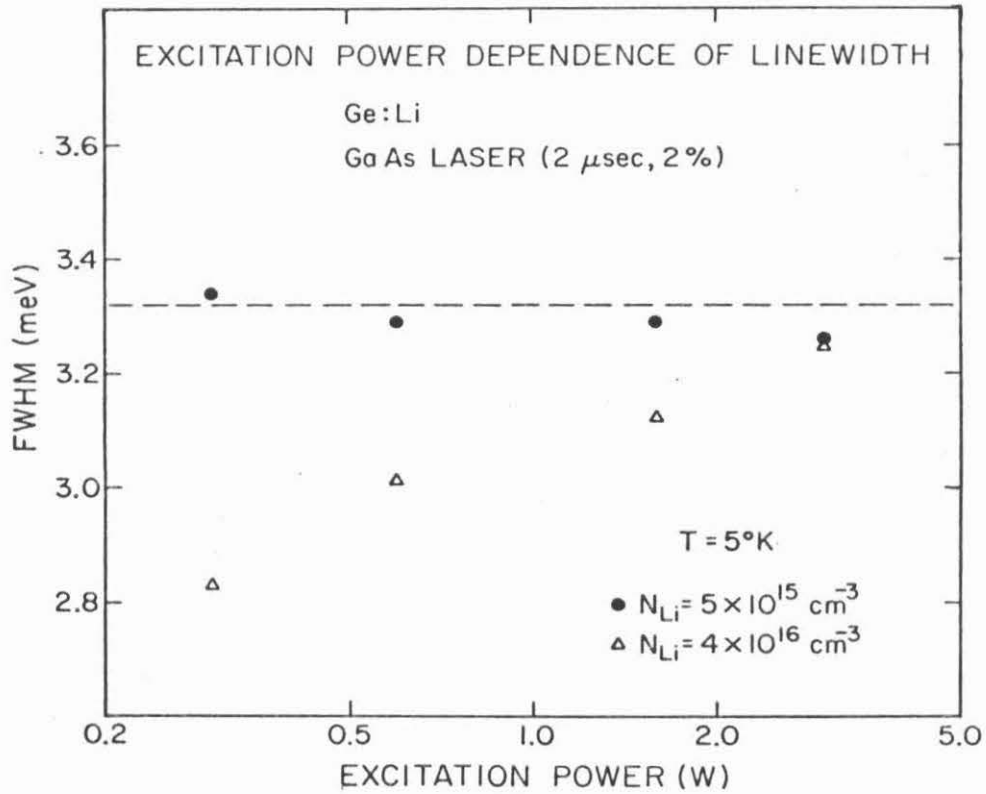
Figure 4

Excitation power dependence of the linewidth of the LA-phonon-assisted line of lightly and heavily doped Ge:Li at 5°K. The dashed line shows the (pump-power independent) EHD linewidth in high-purity Ge.

Figure 5

Photoluminescence spectrum of a moderate-heavily As-doped
Ge. The various phonon-assisted "EHD" lines are identified.
The inset shows the LA-phonon-assisted and the no-phonon
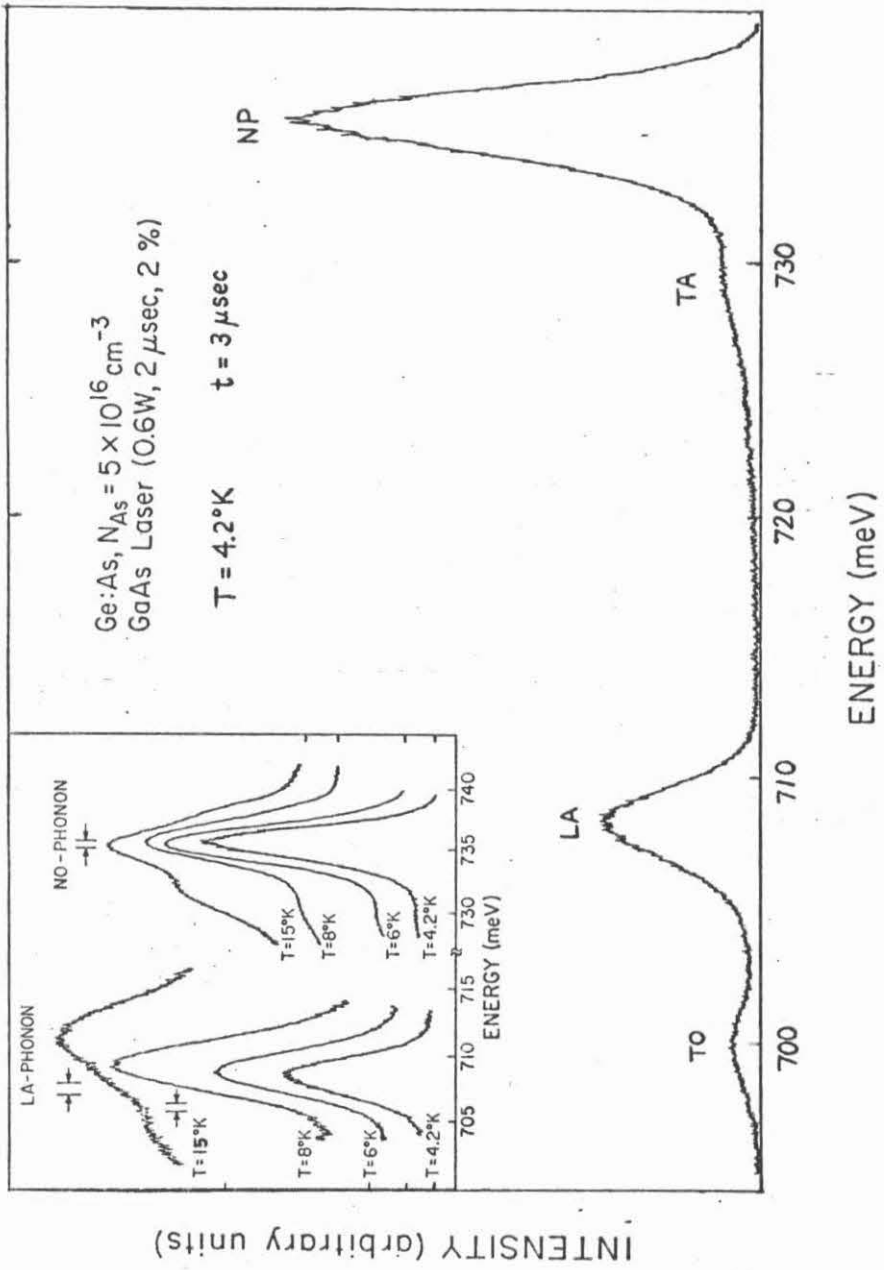lines at various temperatures.

Figure 5

satellites of the LA line at 700 and 729 meV, respectively. The

temperature dependences of the LA and NP lines are shown in the inset

in Figure 5. The temperature dependence of the LA line is similar to

that shown in Figure 3(d) for the moderate-heavily doped Ge:Li. The NP

line is partially masked by the TA-phonon-assisted line[7] and the bound

exciton line (739 meV) at high temperatures so that its behavior as a

function of temperature cannot be accurately determined.

　　　We have found that time-resolved spectra can yield a wealth of

information about these lines. All spectra reported in the rest of this

paper are time resolved. They were obtained in the manner described at

the end of Section II. In Figure 6 we have the time-resolved spectra

at 2, 4.2, 6 and 8°K of a 2×10^{16} As/cm^3 sample showing both the LA and

NP lines. We will discuss these two lines separately.

　　　At 2 and 4.2°K, the LA-phonon assisted line has relatively simple

behavior. The FWHM and peak position of the line are nearly indepen-

dent of the delay time. The BE[21,22] line can be discerned at 4.2°K

for long delay times. Some shift of the peak of the line is detectable

at 6 and 8°K, suggesting that, as the temperature is raised, some im-

purity-induced emission appear.

　　　In contrast to the LA line, the NP line has very complicated

behavior as a function of time. First, the peak of the NP line shifts

noticeably with time at 2 and 4.2°K. At 2°K the total shift of the

spectrum at $t = 35$ μsec from that at $t = 3$ μsec is 0.7 meV. At 4.2°K,

the shift is 1.3 meV between the spectra at $t = 30$ μsec and $t = 3$ μsec.

Part of the NP line peak shift at 4.2°K is due to the BE line which

becomes clearly noticeable for long time delays. Second, at 8°K, the

Figure 6

Time-resolved photoluminescence spectra of Ge:As
showing the LA-phonon-assisted and the no-phonon
lines at four different temperatures. Excitation
power used was 0.6 W, except for the LA-phonon-
assisted lines at $8°K$ for which 1.3 W was used.
The number associated with each spectrum is the
time delay t as defined in Sec.II. Relative
intensities of the spectra are arbitrary so that
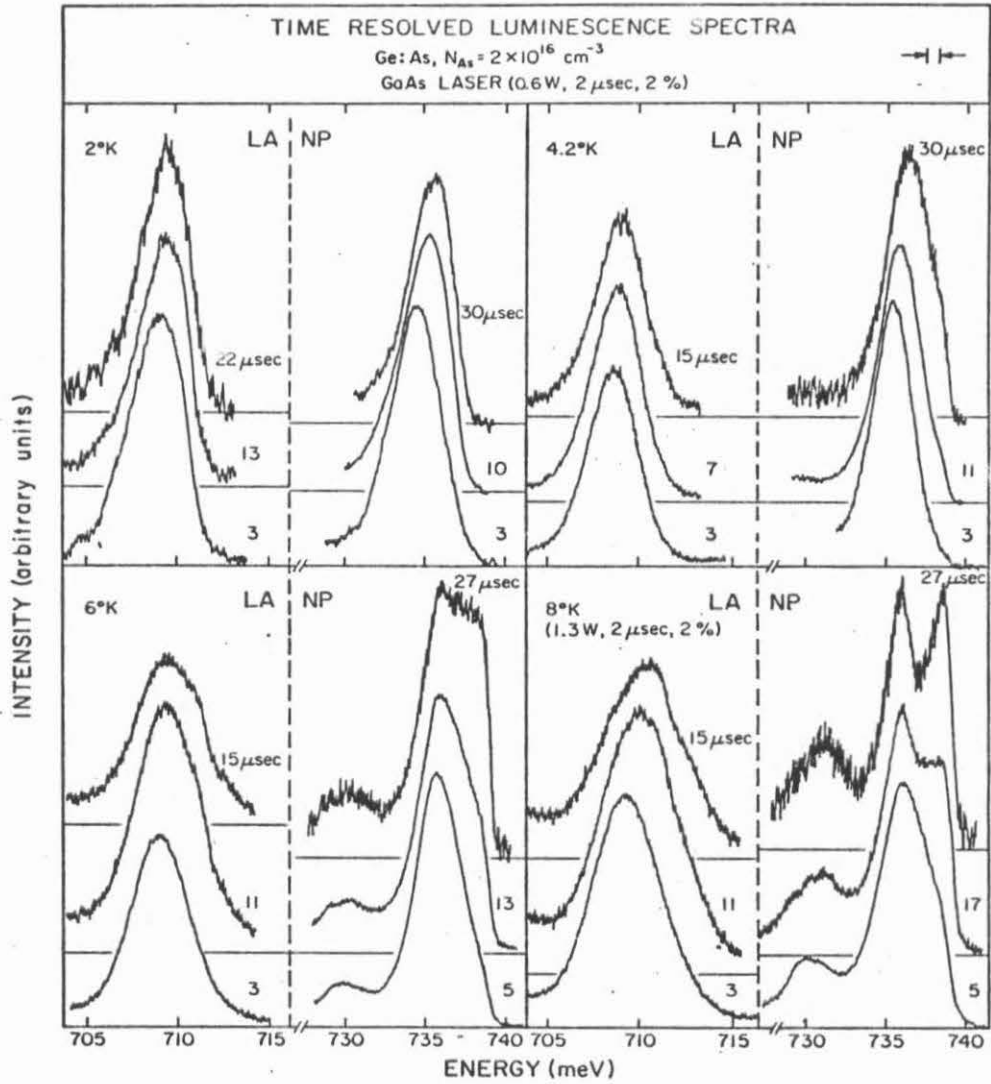the heights of different spectra should not be
compared.

TIME RESOLVED LUMINESCENCE SPECTRA
Ge: As, $N_{As} = 2 \times 10^{16}$ cm^{-3}
GaAs LASER (0.6W, 2 μsec, 2 %)

Figure 6

NP line, which resembles the EHD line at short delay times, decays con-
tinuously into a very narrow line at 736.1 meV. At t = 27 μsec, its
FWHM is about 2.2 meV and its shape is different from the theoretical
EHD lineshape[11]. The line at 739 meV is due to the BE. In the
corresponding spectrum (t = 27 μsec) at 6°K, the region between the
NP and BE lines is filled by some impurity induced emission. The 6 and
8°K spectra shows that different parts of the broad EHD-like NP line
decay at different rates so that the NP line is caused by at least
two (besides the BE line) emission processes. It is natural to expect
that the NP line at 2 and 4.2°K is also due to two or more emission
processes and that the shift of the NP line peak noted above is due
to the changing relative intensity of the various emissions.

The decay transients of the sample were measured using 100-μsec
excitation pulses. This pulse length allows the intensity of the "EHD"
lines to approach steady state before the laser is shut off. The decay
transients were obtained through the spectrometer. For the LA line,
the spectrometer was set at 708.6 meV while for the NP line, it was
set at 736 meV. (Bandpass in both cases is about 1.2 meV.) The
results are shown in Figure 7. The LA line decays exponentially with
a lifetime of 23 μsec. The NP line decay is slower and is non-
exponential. The negative curvature of the NP line is an experimental
artifact caused by the limited bandpass of our spectrometer and the
considerable shift of the NP line position as shown in Figure 6. If
the spectrometer is set to the high energy side of the NP peak at
t = 100 μsec, then the decay is much slower. These results are con-
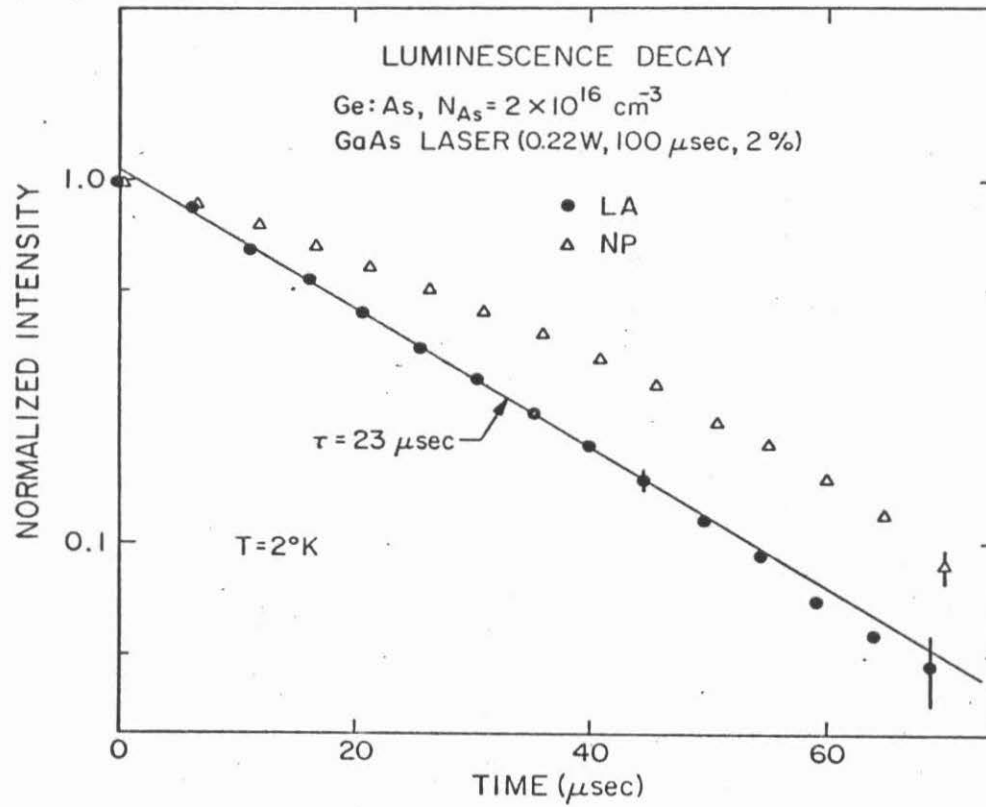sistent with the observation of Karuzskii et al.[10] who found that

Figure 7

Photoluminescence-intensity decay of the no-phonon and LA-phonon-assisted lines in Ge:As at 2°K. The time zero is the time the GaAs laser is turned off.

the NP line decays with two time constants. The decay transient at
4.2°K is quite similar to the decay at 2°K. This similarity has also
been observed in Ge doped with only 10^{15}cm^{-3} of impurities and is
markedly different from the results in pure Ge (see Chapter 3).

Information on the origin of the "EHD" line can be obtained by
looking at its luminescence decay as a function of temperature. Such
data for the LA line using pulsed excitation are presented in Figure
8. At 2 and 4.2°K, when the time-resolved spectra above suggest that
the peaks are due to EHD, the decays are as expected for the EHD; viz.,
the decay transients show both bulk recombination and "surface evapora-
tion" effects[23]. If the broad line at T > 6°K is due to the EHD,
we would expect the decay transients to show more and more downward
curvature as temperature is raised and evaporation becomes more impor-
tant. Instead, the decay transients for T > 6°K are more nearly ex-
ponential. The slight decrease of the decay rate for T $\gtrsim$ 6°K at long
delay times is real and would be more prominent if the line did not
shift with delay time out of the pass-band of our spectrometer. These
observations suggest, as did time-resolved spectra, that the LA line
of Ge:As is due mainly to EHD for T $\lesssim$ 4.2°K but is more complicated at
higher temperatures.

We note that under different excitation conditions the decay
transients are different. A dashed line corresponding to the data
points for the LA line given in Figure 7 is drawn in Figure 8. Compari-
son of the dashed line with the 2°K data points in Figure 8 shows that
the luminescence decay of the LA line is slower when 100-μsec excita-
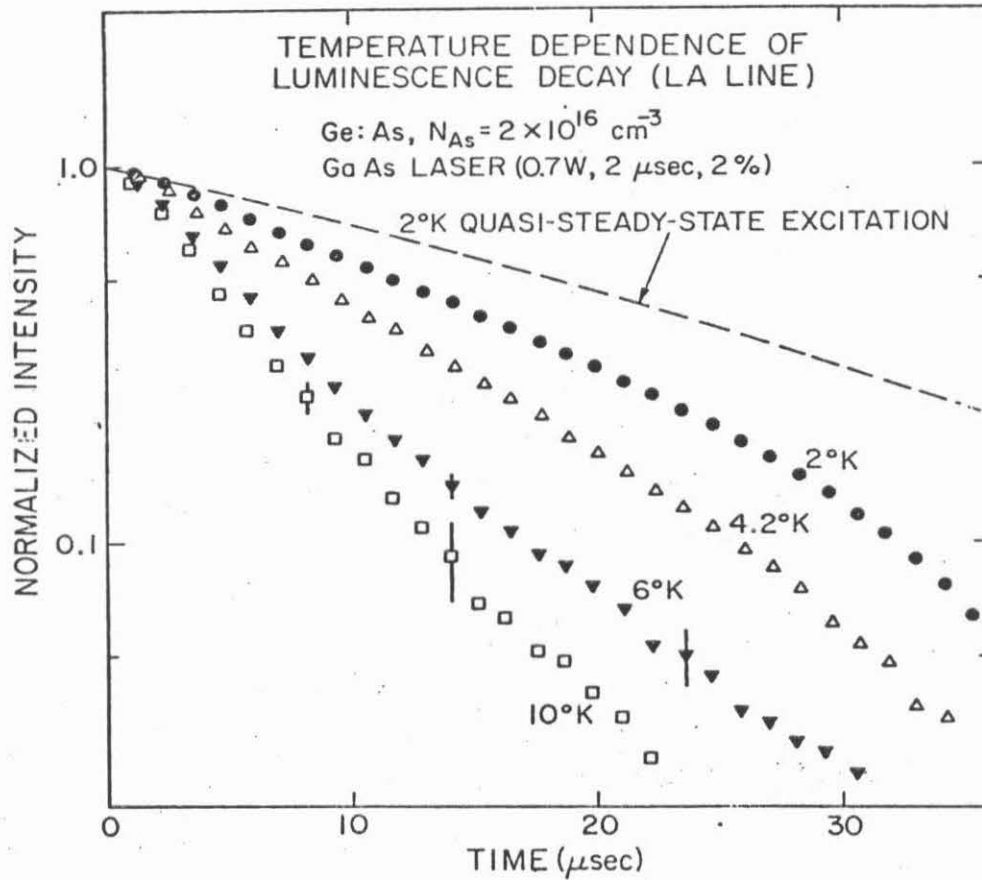tion pulses are used. This difference in the decay transients is also

Figure 8

Decay of the photoluminescence intensity of the LA-phonon-assisted line of Ge:As at various temperatures. Pulsed GaAs laser excitation was used. The result for the LA line in Fig.7 is reproduced here as the dashed line for comparison purpose. The zero of time is approximately the time that the intensity of the LA line reached its maximum.

47

observed for pure Ge and is consistent with changes in the spatial dis-
tribution of EHD's caused by different excitations (see Chapter 3).

In Figure 9, the pump power dependence of the LA and NP lines at
2°K is shown. The LA line has essentially pump-power independent line
position and FWHM, while the NP line broadens and shifts toward lower
energy with increasing pump power.

(c) Ge:Ga

The temperature dependence of the spectra from moderate-heavily
doped Ge:Ga is qualitatively similar to that shown in Figure 3(d) for
Ge:Li.

Figure 10 shows time-resolved spectra of a Ge sample with
$2.5 \times 10^{16} Ga/cm^3$ at 2, 4.2, and 8°K. We make two observations. First, a
considerable shift of the peak position with increasing delay time t
is observed. The rate of peak-shift increased with temperature-
increase.   At 2°K the total amount of shift
between t = 3 and 22 µsec is about 0.5 meV. While at 8°K the shift
amounted to about 1 meV between t = 2 and 9 µsec. Free- and bound-
exciton positions, which can be accurately determined in less heavily
doped crystals, are marked in the 8°K spectrum. It is seen that at
8°K the EHD-like line shifts towards the BE line position at long delay
times. Second, there is a large change with delay time of the FWHM of
the line at 2°K. At t = 3 µsec, the lineshape resembles the well known
EHD lineshape with a FWHM of 3.0 meV. (In pure Ge the droplet line-
width at 2°K is 3.3 meV.) However, at t = 22 µsec, the line becomes
much narrower and its high-energy edge becomes quite sharp. We have

Figure 9

Excitation-power dependence of the photoluminescence
spectrum of Ge:As taken at a fixed delay time of $3\,\mu$sec.
Both the LA-phonon-assitsted and the no-phonon lines
are shown. The excitation power is indicated at the
right baseline of each spectrum. Relative intensities
of the spectra are arbitrary.

EXCITATION POWER DEPENDENCE
OF LUMINESCENCE SPECTRA

Ge:As, $N_{As} = 2 \times 10^{16}$ cm^{-3}
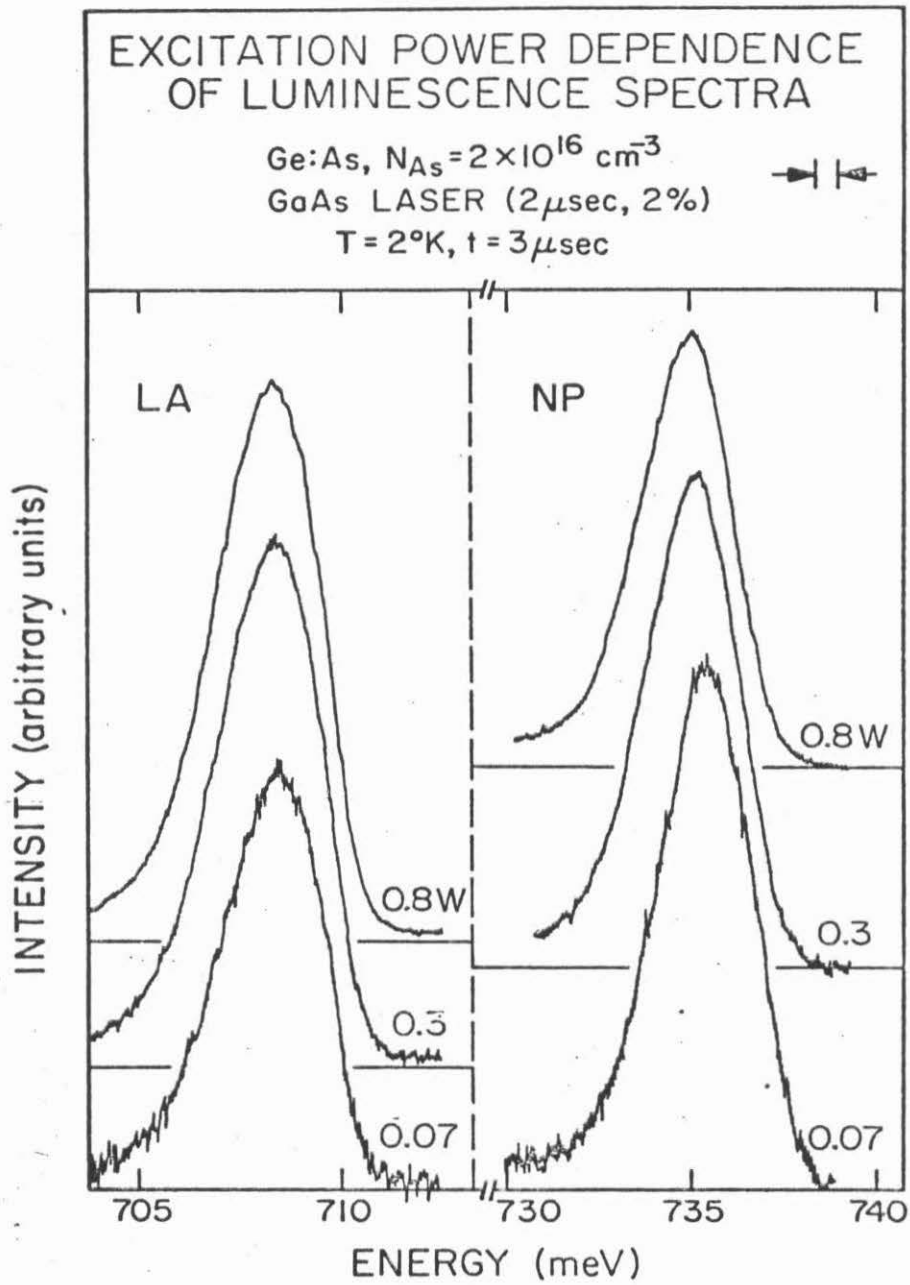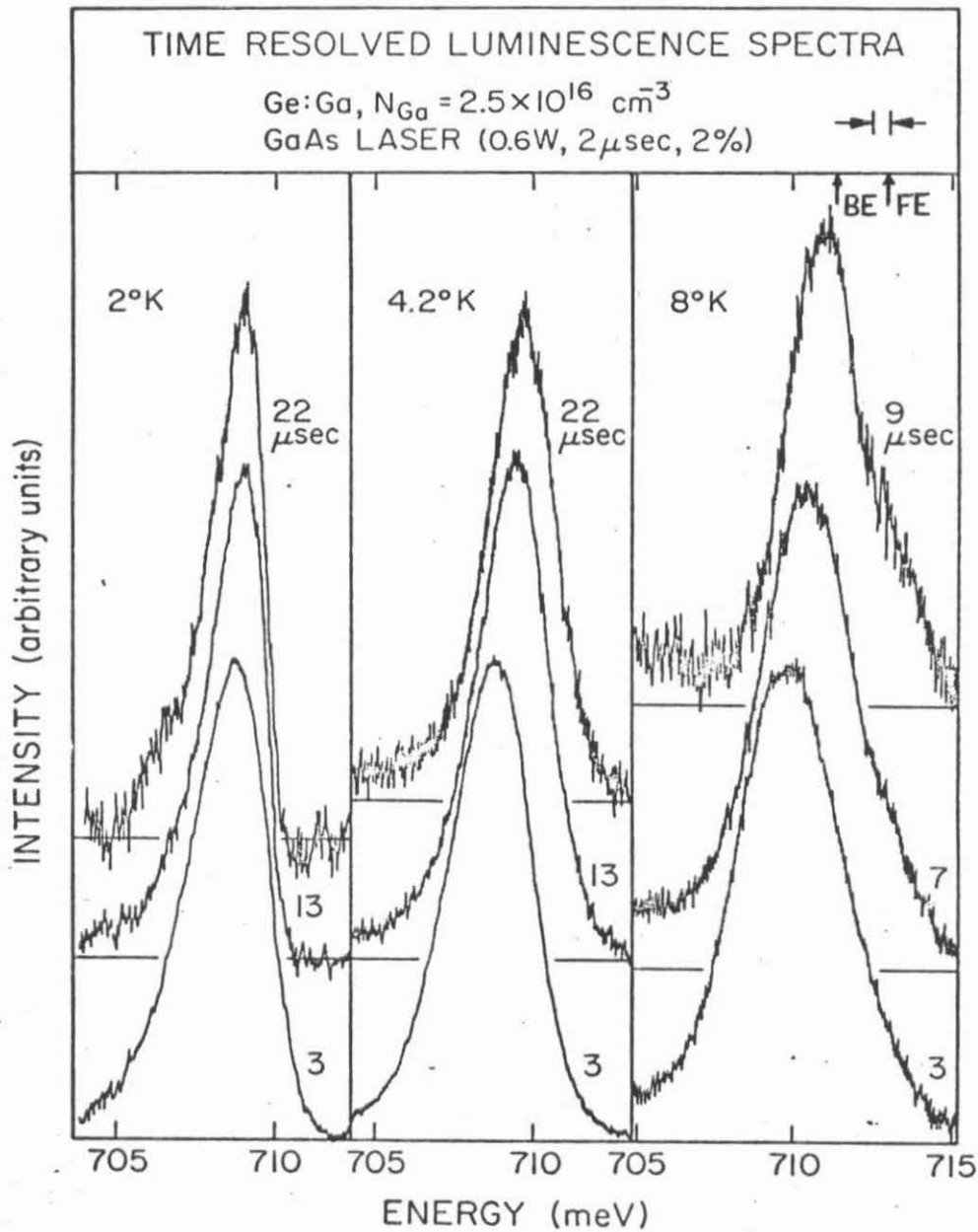GaAs LASER (2μsec, 2%)
T = 2°K, t = 3μsec

Figure 9

Figure 10

Time-resolved spectra of LA-phonon-assisted line of Ge:Ga
at three temperatures. The delay time t is shown to the
right of each spectrum. Relative intensities of the
spectra are arbitrary.

found it difficult to fit this spectrum using the theoretical EHD line shape. The t = 22 μsec spectrum is not due to the BE either, as the energy of the line does not match that of the BE.

The luminescence decay transients of the $4 \times 10^{16} Ga/cm^3$ sample at 2 and 4.2°K are shown in Figure 11. At both temperatures two distinct decay rates are observed. The results can be fit quite well by sums of two exponentials, i.e., $I(t) \sim \exp(-t/\tau_1) + A \exp(-t/\tau_2)$. The values of the parameters obtained are: at 2°K,

$$\tau_1 = 20 \text{ μsec} , \qquad \tau_2 = 76 \text{ μsec} , \qquad A = 1.4;$$

and at 4.2°K,

$$\tau_1 = 20 \text{ μsec} , \qquad \tau_2 = 59 \text{ μsec} , \qquad A = 1.1 .$$

The decay transients for a pump power of 0.09 W was unchanged within the noise level. The decay transient data using pulsed excitation for temperatures up to 10°K are presented in Figure 12. Comparing the data in Figure 8 with that in Figure 12, we note that the decay at 4.2°K is qualitatively different in the Ge:As sample and the Ge:Ga sample. While the decay plotted on a semilog plot shows a negative curvature in the Ge:As case, the decay transients show a positive curvature in the Ge:Ga sample. On the other hand, the decay for Ge:Ga doped sample are similar to those of the Ge:As sample for $T \gtrsim 6°K$. This similarity suggests impurity-induced emission always plays a role in Ge:Ga sample and plays a role in LA line of the Ge:As sample for $T \gtrsim 6°K$.

52

Figure 11

Photoluminescence-intensity decay of the LA-phonon-
assisted line of Ge:Ga at two temperatures. The
zero of time marks the shutting-off of the laser.
The straight lines are lines drawn through the
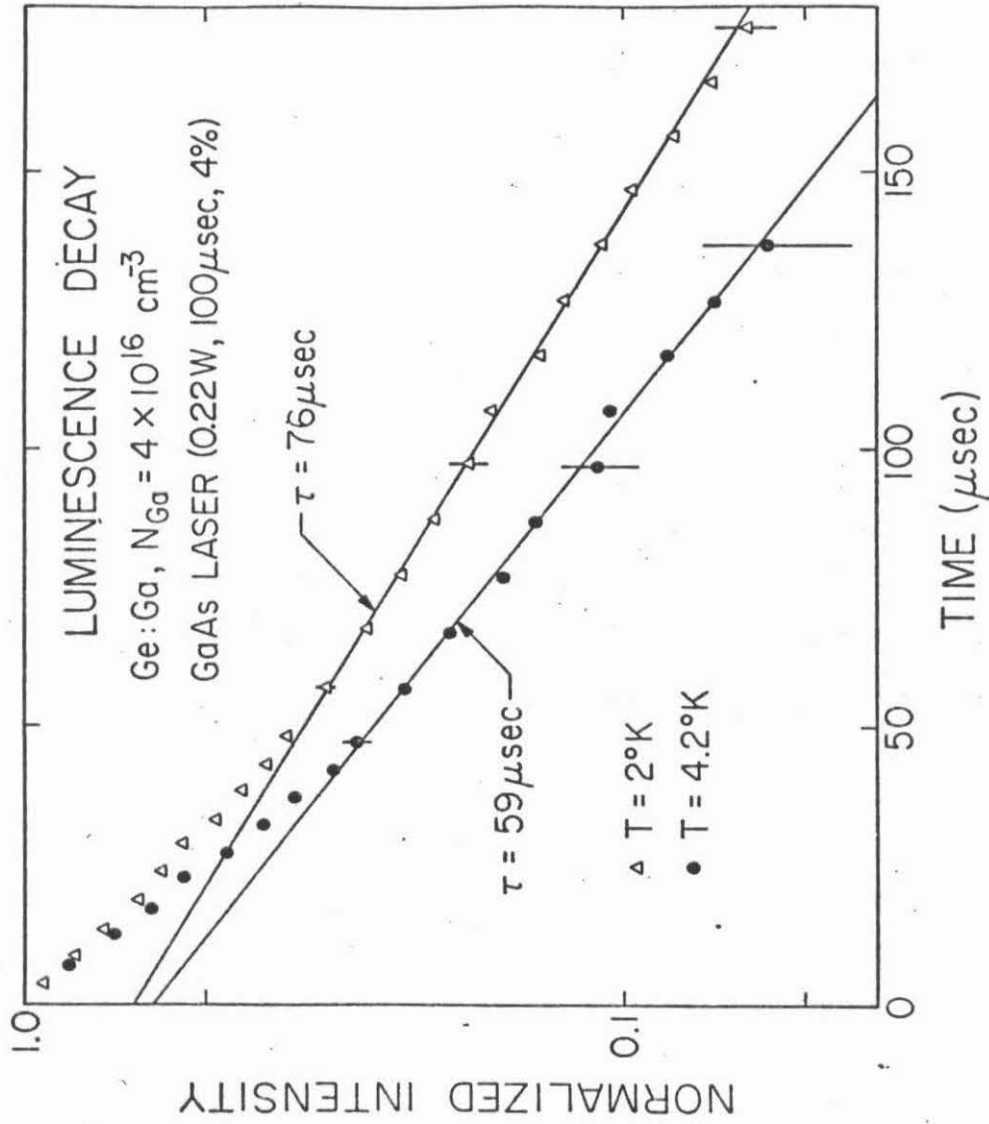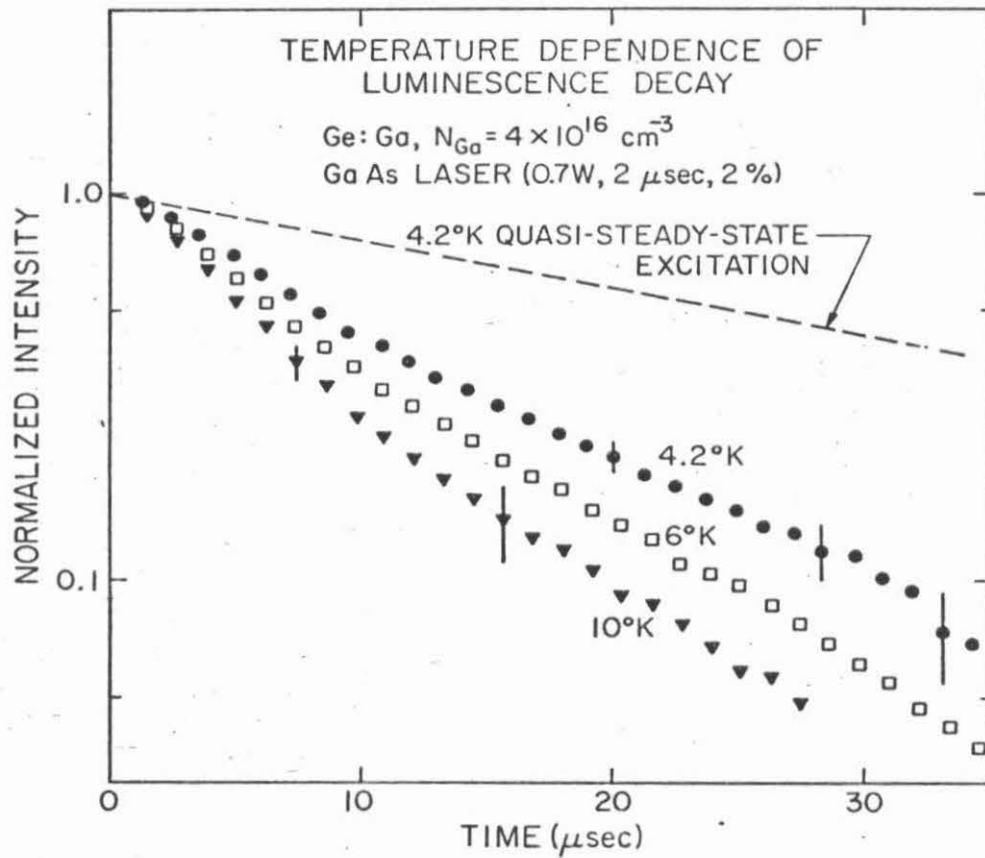data points for long delay times.

Figure 11

Figure 12

Decay of the luminescence intensity of the LA-
phonon-assisted line of Ge:Ga at various tem-
peratures. Pulsed GaAs laser excitation was
used. The quasi-steady-state-excitation re-
sult at 4.2°K in Fig. 11 is reproduced here
for reference. The time zero is approximately
the time the LA line intensity reached its
maximum.

It should be noted that, although two exponentials are sufficient to fit the decay transients, the possibility of the presence of more than two decay times cannot be excluded. Experimentally it is difficult to resolve the decay of more than two components, especially if some decay times are not too different from each other.

In Figure 13, the t = 3 μsec spectra of the LA-phonon-assisted line of the $2.5 \times 10^{16} Ga/cm^3$ sample for various pump powers at 4.2°K are shown. The peak of this line shifts towards lower energy and its line-width increases with increasing excitation level. At 4.2°K, a factor of 10 change in excitation power produced a 0.5 meV shift of the peak and a 0.5 meV change in the FWHM. At 6°K, a factor of 4 change in pump power caused the peak to shift by 0.5 meV and the FWHM to change by 0.2 meV.

(d) Ge:Sb

Figure 14 shows the 2°K LA-phonon-assisted EHD line from high-purity Ge and the LA lines from Ge:As, Ge:Ga and Ge:Sb samples. These results show that (for a constant excitation level) the peak in the emission line for Ge:Ga and Ge:As are close to the peak of the EHD line in pure Ge. In contrast, the data show that the peak of the emission line in Ge:Sb is shifted to lower energy by about 0.5 meV. This shift to lower energy is not understood at present, although calculations[13] for the properties of the EHD in doped Ge suggest that such a shift of the EHD might occur when impurity concentration approaches the Mott density.

The temperature dependence of the spectrum of the Ge:Sb sample is
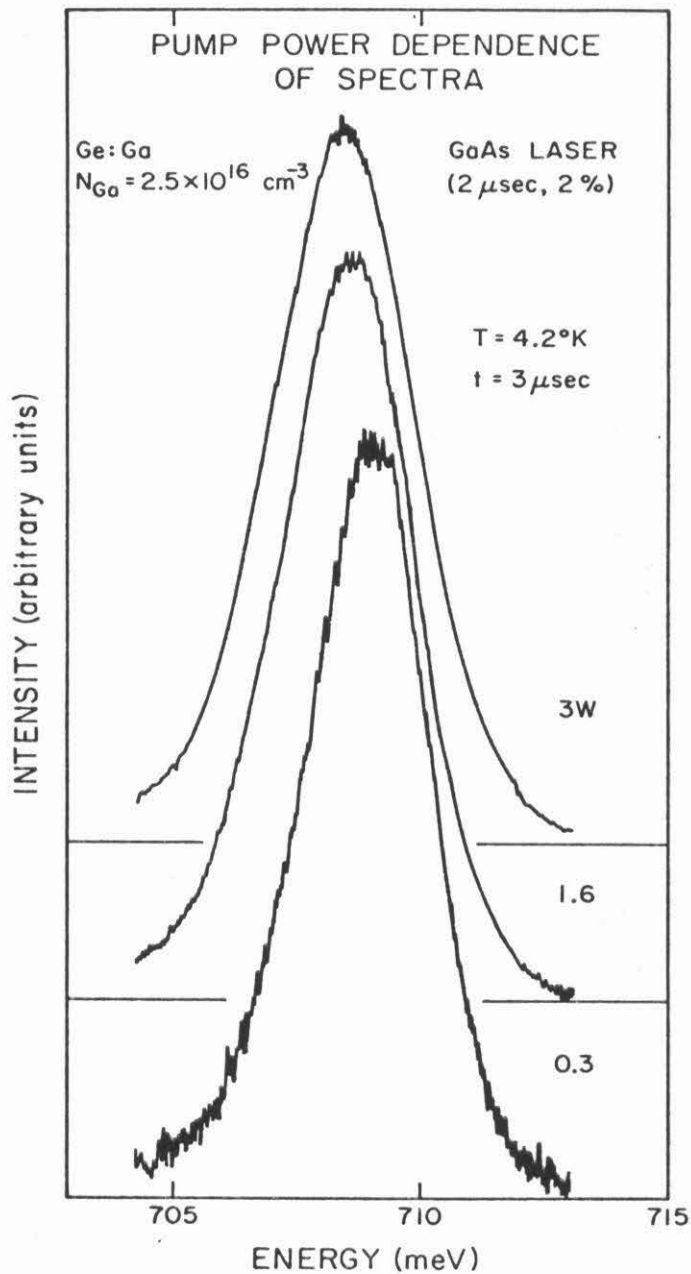
Figure 13

Excitation-power dependence of the LA-phonon-assisted line of Ge:Ga
at a delay time of 3 μsec. The pump-power is shown at the right
baseline of each spectrum. Relative intensities of the spectra
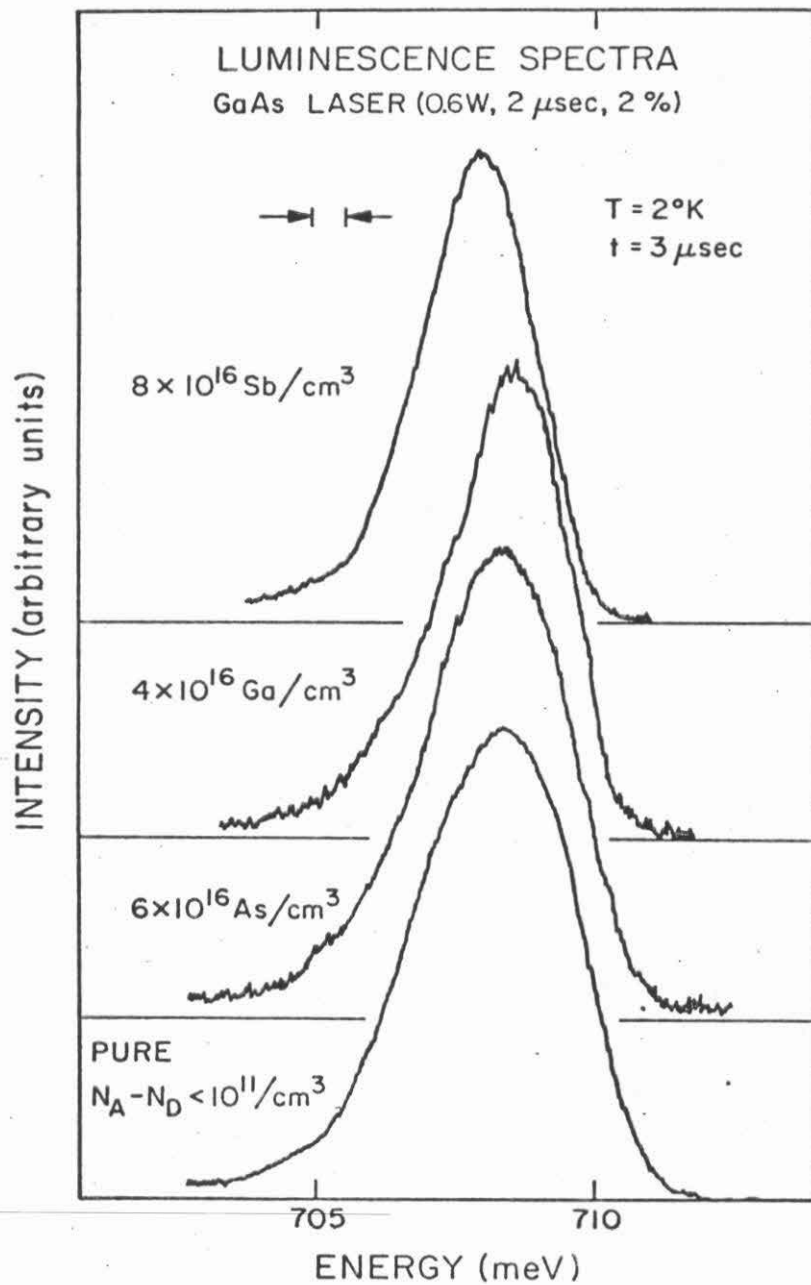are arbitrary.

Figure 14

Photoluminescence spectra of the LA-phonon-assisted lines of samples moderate-heavily doped with Sb, Ga and As as well as a high-purity Ge sample. The relative intensities of the spectra are arbitrary.

qualitatively similar to that of the 4×10^{16}Li/cm^3 sample shown in Figure 1(d). Time-resolved spectra at 4.2°K from the Ge:Sb sample showed a peak position independent of time delay. However, the line-width decreased from 3.1 meV at t = 2 μsec to 2.5 meV at t = 15 μsec.

In Figure 15, decay transients from the Ge:Sb sample are shown. The 2°K decay is nearly exponential with a time constant of 34 μsec. The 4.2°K data show two time constants. Following the laser turn-off, the decay is fast for about 20 μsec before it becomes exponential with time constant of 28 μsec. When pumping-power was decreased to 0.07 W, the transients remained essentially unchanged.

At 4.2°K the FWHM of the EHD-like line decreases from 2.7 meV to 1.9 meV with a reduction of pump power by a factor of 6. This is in good agreement with the observation of Martin and Sauer[8]. The position of the peak of the line is observed to be independent of the pump power.

IV. SUMMARY AND DISCUSSION

For Ge with impurity concentrations up to a few times 10^{15}cm^{-3}, we have observed no changes of the properties of the EHD line from those of the high-purity Ge. At temperatures close to the critical tempera-ture of EHD formation, some impurity induced emission can be seen which should not be confused with the EHD line. The decay transients of the EHD line in these lightly doped Ge crystals are quite different from those in the high purity Ge and are dealt with in the next chapter.

The properties of the EHD-like line in moderate-heavily doped Ge are rather complicated. The results are most easily interpreted by
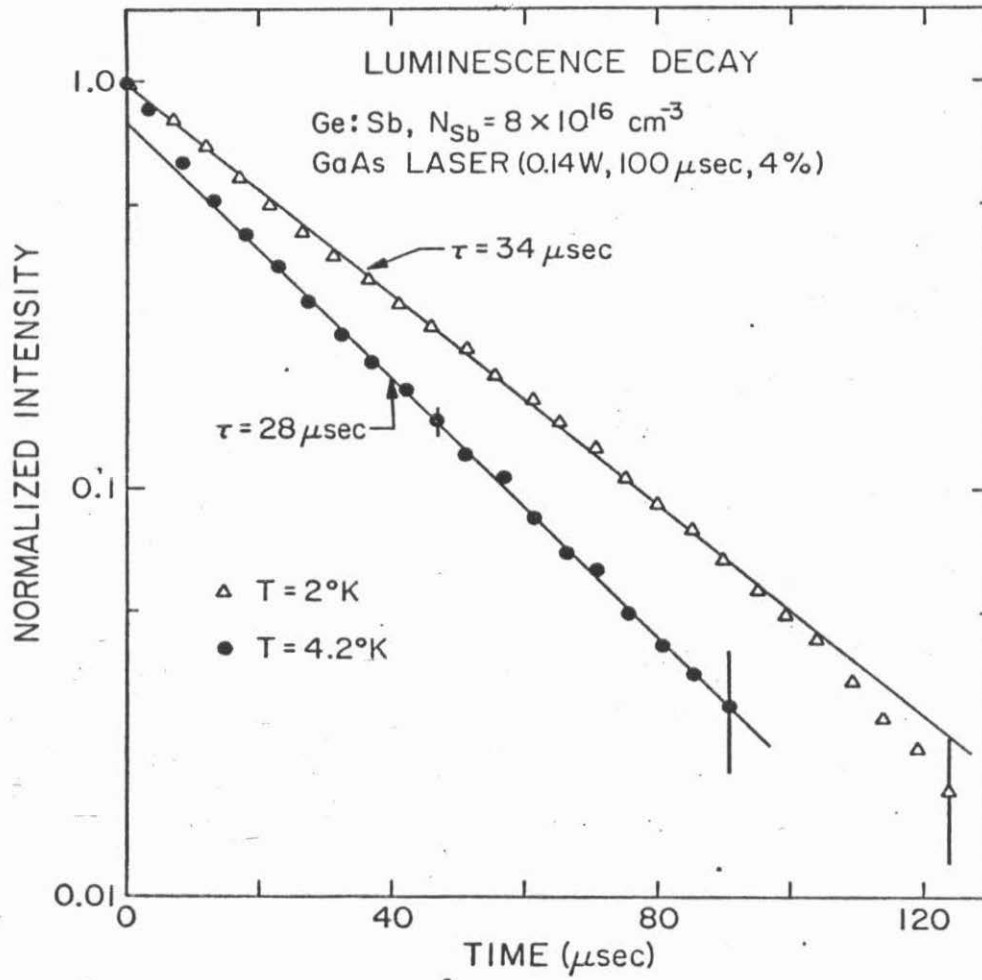
Figure 15

Photoluminescence intensity decay of the
LA-phonon-assisted line of Ge:Sb at 2
and 4.2°K.

assuming the existence of impurity-induced emissions:

1. LA line in Ge:As

The LA line in Ge:As is least affected by impurity-induced emissions. For $T \lesssim 4.2°K$, we found the shape and position of this line to be essentially excitation-power and delay-time independent as would be expected for an EHD line. Fitting the LA line to the well known EHD line shape[11], we obtained roughly linear decreases of both the density and chemical potential of the EHD as functions of increasing doping concentration. A comparison of the results of the line-fits to the theoretical prediction of Reference 12 is shown in Figure 16. Good agreement between the experiment and theory is obtained. We interpret the LA line in Ge:As for $T \lesssim 4.2°K$ to be due mostly to EHD emission. The lifetime of the EHD in moderate-heavily As-doped Ge is about 23 µsec which is considerably shorter than the 37 µsec for EHD in pure Ge[23].

At temperatures higher than about 4.2°K, the FE and impurity-induced emissions dominate the spectrum of Ge:As. The impurity-induced emission has a broad, structureless line shape similar to the EHD line shape.

2. The NP line in Ge:As and LA lines in Ge:Ga, Ge:Li, and Ge:Sb[24]

Impurity-induced emissions play a large role in the NP line of Ge:As and in the LA lines of Ge:Li, Ge:Ga and Ge:Sb. Their presence spectroscopically unresolvable from the EHD, cause the above lines to show pump-power and time dependences as well as two decay times.

Figure 16

Comparison of theoretically predicted properties of the
electron-hole-droplet of As-doped Ge with experiment.
The theoretical lines, for As-, Ga- and Sb-doped Ge, are
obtained from reference 12. The triangles (▲) are den-
sities (n) and chemical potentials (μ) obtained from
fitting the experimental LA line of Ge:As. The circles
(●) are density data for Ge:As given in reference 7.
The densities are in units of the electron-hole-droplet
density in pure Ge ($n_o = 2.4 \times 10^{17} cm^{-3}$). All data were
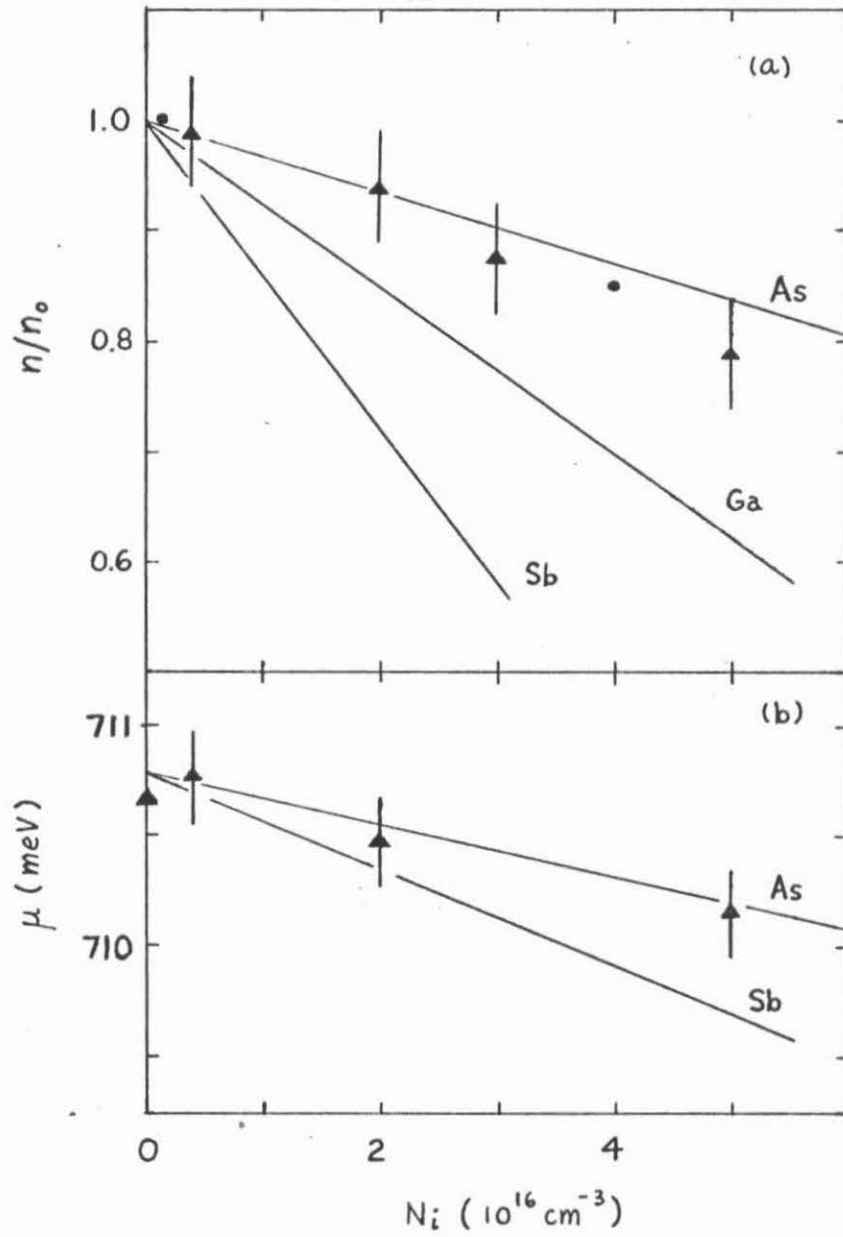obtained from spectra at $\sim 2°K$.

Figure 16

There are many possible mechanisms for the impurity-induced changes in the emission. We shall discuss some in detail and only mention others.

A.   "Multi-Exciton Complexes".

In Si samples with impurity concentration $\lesssim 10^{16} cm^{-3}$, a series of narrow lines between the BE line and the peak of the EHD line have been observed[11,25,26]. These lines have been attributed to, but as yet un-proven, emissions arising from transitions from neutral centers with n bound-excitons to centers with n-1 bound-excitons. They are usually referred to as "multi-exciton complex" (MEC) lines. Martin[22] has reported observation of a similar series of lines in Ge with about $10^{15} cm^{-3}$ As and P impurities. He found that MEC lines in Ge are emitted without phonon assistance and have extremely low intensities. In Ge doped with $\gtrsim 10^{16} cm^{-3}$ of impurities, MEC, if they exist, would most likely emit a broad line rather than a series of sharp lines for two reasons. First, the MEC lines in Si have been observed to broaden and merge[27] at doping level of 10^{16}-$10^{17} cm^{-3}$. At these doping levels, impurities may cluster. As a result many MEC's may overlap several impurities. This would lead to the observed broadening of MEC lines at high doping levels. Since the sizes of the exciton[27] and shallow-impurity states[29] in Ge are a factor of 2 to 3 larger than in Si, one would expect broadening and merging of the MEC lines to occur at doping levels of 10^{15} -$10^{16} cm^{-3}$ in Ge. Second, the total energy-spread of the MEC lines in Ge is only about 3 meV compared to greater than 10 meV in Si, so the spacings between successive MEC lines in Ge are much

smaller in Ge than in Si.

Provided that the doping levels are appropriately scaled as dis-
cussed in the preceding paragraph, many similarities between the doped
Ge and Si spectra can be observed. The data on the pump-power depen-
dence of the NP line $(1.8 \times 10^{17} P/cm^3)$ and the TO-phonon-assisted line
$(1.7 \times 10^{17} Sb/cm^3)$ of doped Si, taken from Reference 30, are shown in
Figure 17. Comparison of Figure 17(a) with Figure 9 and Figure 17(b)
with Figure 13 suggest that the NP line of Ge:As and the LA lines of
Ge:Ga, Ge:Li, and Ge:Sb could have the same origin, viz., luminescence
from both MEC and EHD. The temperature dependence of the EHD and MEC
lines in doped Si $(7 \times 10^{16} B/cm^3)$, also taken from Reference 30, are
shown in Figure 18. The possible presence of MEC lines in Ge is again
suggested by a comparison of Figure 18 with Figure 3(d) and 6. Measure-
ments of the MEC decay times in Si show that different MEC lines have
different decay times; the decay times monotonically decrease for lines
approaching the EHD peak[25]. The intensity decay of these lines
almost always show two decay constants. The time-resolved spectra
in Figure 11 of Reference 26 show a shift towards higher energies
and a narrowing of the combined width of the lines with increasing
delay time. These time-dependent properties of the MEC and EHD in
doped Si are also observed for the LA lines of Ge:Ga and Ge:Sb and for
the NP line of Ge:As, as given in Section III. Finally, at constant
excitation, the BE intensity in Ge is maximum for doping level of about
$10^{15} cm^{-3}$ whereas the FE is a monotonically decreasing function of
increased doping. Both the BE and FE lines are absent from the spectra
when doping level exceeds about $10^{16} cm^{-3}$. Similar observations have

Figure 17

Pump-power dependence of the spectra from broadened multiexciton complexes in doped Si (taken from reference *30*).

(a) Si:P ; emissions without phonon assistance.
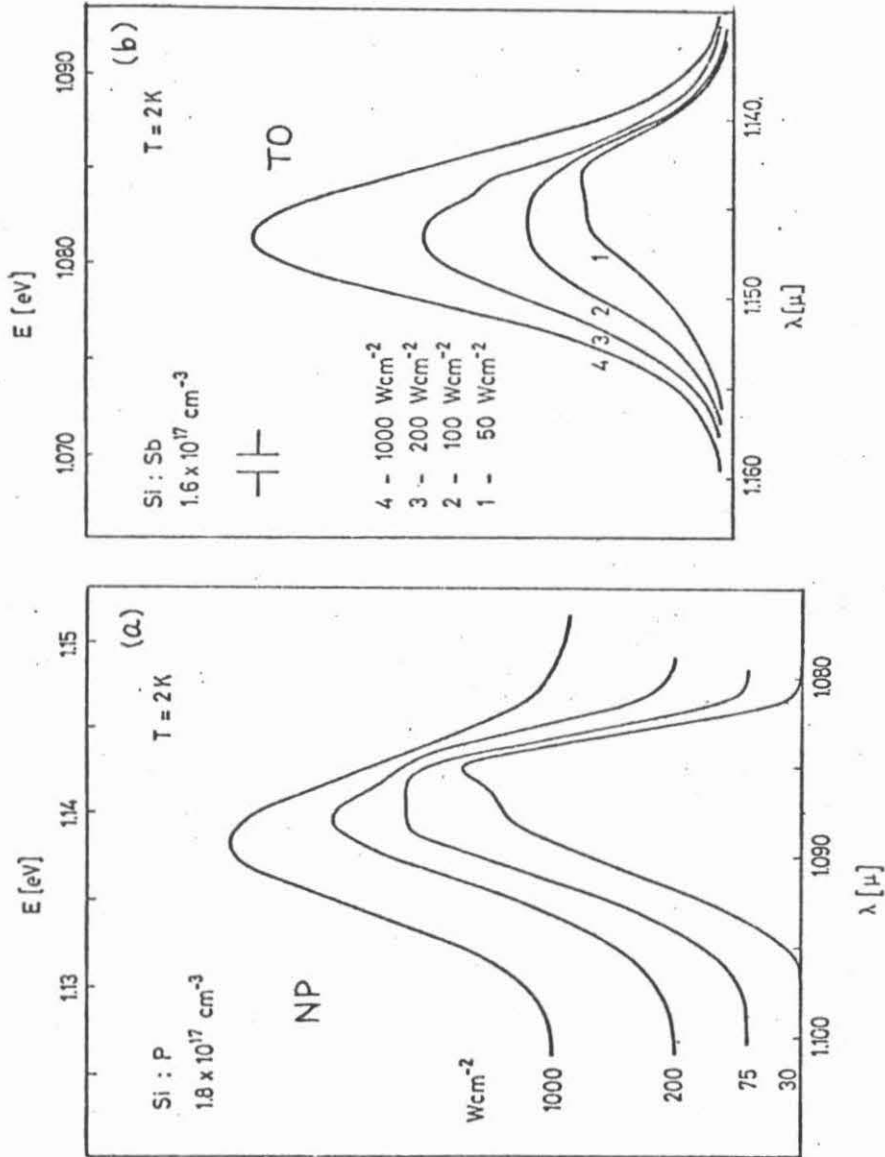
(b) Si:Sb; TO-phonon-assisted emissions.

66

Figure 17

67
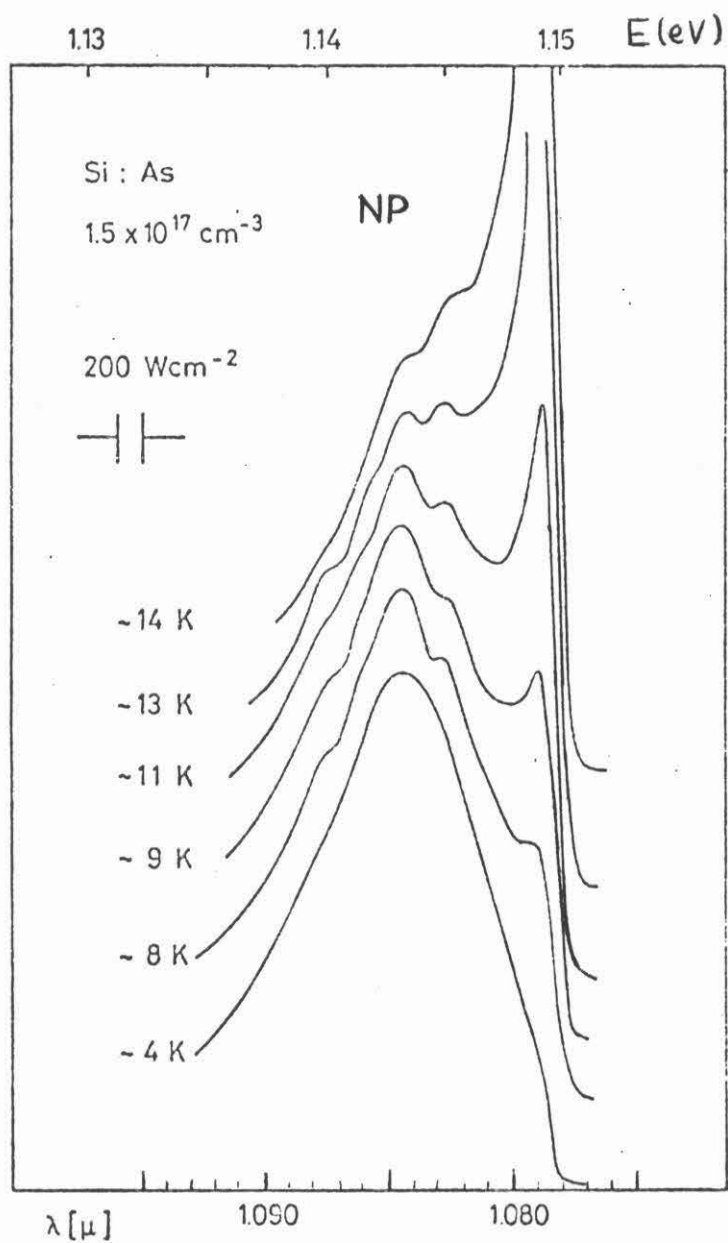
Figure 18

Temperature dependence of the phonon-
less emission spectrum of the electron-
hole-droplet and multiexciton complexes
in As-doped Si (taken from reference 30).

been reported for Si in reference 30.

On the basis of the comparisons in this subsection, one would expect that, in heavily doped ($N_i \gtrsim 10^{17} cm^{-3}$) Si:As or Si:P, where only broad NP and TO lines from the "EHD" are observed, the broad lines may actually be composed of differing amounts of EHD and broadened MEC radiation. There should be qualitative differences in all the properties of NP and TO lines. Verification of this point would strengthen the case for the MEC explanation for Ge.

It should be noted that, since the binding energy of MEC relative to FE in Ge is no more than about 2 meV, one would not expect to see much MEC emission above about 25°K. Thus, MEC alone could not explain the data above about 25°K in doped Ge.

B. Bound-Exciton Banding

In addition to a MEC band, a possible contribution to the impurity-induced emission comes from a broadened BE line. In analogy with the phenomenon of impurity banding in semiconductors[31], we might expect that the interaction between an exciton and more than one impurity would lead to a bradening of the BE line. This interaction with a number of impurities will produce a broadened BE line in two ways. First, consider a single exciton interacting via an attractive interaction with a number of nearest neighbor impurities. The energy of the ground state of the system made up of the exciton and a cluster of neutral impurities will depend on the number and spatial distribution of the neutral impurities. Since the impurities are distributed randomly, there are fluctuations in the spatial distribution of the nearest

neighbor impurities about any given impurity center. This leads to a distribution of values for the ground state energy of a <u>single</u> exciton interacting with an impurity and its nearest neighbor impurities. This interaction will lead to a broadening and shifting of the BE line with increased impurity concentrations. Estimates of the magnitude of this effect for impurity density of $\sim 10^{16} cm^{-3}$ gives broadening of the BE line on the order of 1 meV[32]. Second, as the pump power is increased, we are likely to increase the average number of excitons bound a given impurity center. Hence, we will be looking at the emission from varying number of excitons interacting with the impurity centers. This system will emit a line which broadens and shifts with increasing pump power.

C. Plasma Emission

Spatially-resolved luminescence scan measurements on doped Ge show that the excited region extend beneath the surface to a depth of $\sim$ 500 μm in $\sim 10^{15} cm^{-3}$-doped and $\sim$ 200 μm in $\sim 10^{16} cm^{-3}$-doped Ge[33,34]. In high-purity Ge, the penetration of excited carriers into the crystal is about 1 mm. Thus, a much higher density of carriers is generated in doped Ge than in pure Ge. The excited-carrier density is highest near the excited spot at the surface of the crystal and decreases with distance from the excited spot. Consider now an excited, doped Ge crystal whose temperature is above the droplet critical temperature ($\sim$6.5°K). Away from the excited spot, FE's are formed. Near the excited spot, the carrier density may be sufficiently high so that screening of the Coulomb attraction of electrons and holes can make the FE state un-

stable relative to a plasma state. Thus, spectra of doped Ge at temperatures higher than the droplet critical temperature, such as those shown in Figure 3, could be due to a combination of the emission from the plasma near the excited spot and the FE emission away from the excited spot.

The density n_{MI} at which the FE state is screened out can be estimated by equating the Debye screening length of the plasma to the Bohr radius of the exciton[35]. This density is

$$n_{MI} = \frac{kT}{8\pi E_x a_o^3} \qquad (1)$$

where k is the Boltzmann constant, T is the absolute temperature, E_x is the exciton binding energy and a_o is the exciton Bohr radius. For Ge, E_x = 4.15 meV and a_o = 114 Å[36] so that n_{MI} = 5.6X10^{14}T. When the duration of the excitation is much shorter than the carrier lifetime, the average density of pairs generated by each laser pulse can be estimated by

$$n = \frac{P\tau}{h\nu V} \qquad (2)$$

where P is the power absorbed by the Ge crystal, τ is the pulse length, $h\nu$ is the photon energy and V is the volume occupied by the excitation. The value of V is estimated by taking the product of the illuminated area, ~ 1 mm^2, and the depth of penetration. For 1 W absorbed power in a 2 μsec pulse at GaAs laser wavelength (8500 Å), we get n=2X10^{16}cm^{-3} for N_i ~ 10^{15}cm^{-3} and n=4X10^{16}cm^{-3} for N_i ~ 10^{16}cm^{-3}. If the excited

carrier density were uniform then we would expect, by equating n to n_{MI}, the FE state to be unstable below about 30°K and 75°K for lightly ($10^{15} cm^{-3}$) and moderate-heavily doped Ge, respectively. The actual density of carriers is spatially non-uniform so that these estimated temperature may not be very accurate. Nevertheless, there is indeed a trend for the impurity-induced peak next to the FE peak to persist to higher temperatures with increasing doping concentration (see Figure 3).

Due to the small extent of the volume occupied by the excited carriers, it is difficult to measure spatially-resolved spectra and our attempts have not led to conclusive results. At temperatures below the droplet critical temperature, the existence of the liquid phase complicates the situation, and we feel one of the other listed mechanisms in this section needs to be considered.

D. Others

1. Heating - Device heating by the exciton can be ruled out as the cause of the observed pump-power and delay-time dependence of the broad EHD-like lines in doped Ge. Increase of delay-time and decrease of pump-power cause the broad line to shift to lower energy whereas heating causes shifts in the opposite direction. In addition, if one assumes that the broad lines are due to EHD and carry out line fits, the results shown in Table I is obtained. It is necessary to use not only high temperatures but also larger densities to obtain fits to the spectra for larger pump-powers.

2. Donor-Acceptor Transition - For phonon-assisted donor-acceptor

excitation power (W)	Ge:Sb $8 \times 10^{16} \mathrm{cm}^{-3}$		Ge:Ga $4 \times 10^{16} \mathrm{cm}^{-3}$	
	$T(^\circ K)$	$n(10^{17} \mathrm{cm}^{-3})$	$T(^\circ K)$	$n(10^{17} \mathrm{cm}^{-3})$
1.3	3.0	1.4	3.5	2.1
1.1	2.9	1.4	3.0	1.9
.9	3.0	1.3	3.0	1.8
.7	2.8	1.2	2.5	1.6
.5	2.3	1.1	2.5	1.3
.2	2.0	0.9		

Table I.

Densities and temperatures obtained from theoretical linefits [a] to "EHD" spectra at t = 3 μsec and various excitation powers for two doped Ge samples. The bath temperature was 2°K. Excitation was provided by GaAs laser with 2 μsec pulse duration and 2% duty cycle. The density of states effective masses for electrons and holes were taken to be 0.5G and 0.37, respectively [b].

a. R. B. Hammond, T. C. McGill and J. W. Mayer, Phys. Rev. B13, 3566 (1976).
b. W. F. Brinkman and T. M. Rice, Phys. Rev. B7, 1508 (1972).

transition, the energy of the emitted photon is given by[37]

$$h\nu_{DA} = E_g - E_{ph} - (E_A + E_D) + \frac{e^2}{\kappa r} \qquad (3)$$

where E_{ph} is the phonon energy, E_A and E_D are respectively the donor and acceptor binding energies, e is the electronic charge, κ is the dielectric constant and r is the separation between the donor and acceptor. Donor-acceptor pairs with large separations give rise to a broad line which peaks at $r \simeq (4\pi|N_A-N_D|/3)^{1/3}$. For Ge, $E_g \approx 750$ meV, $\kappa \approx 16$, $E_A+E_D \approx 20$ meV, and $E_{ph}^{LA} = 27.4$ meV[17] so donor-acceptor line should peak for $|N_A-N_D| = 10^{16}$cm^{-3} at about 696 meV. The observed broad lines peak at about 709 meV and are not due to donor-acceptor transition.

3. Pressure - High densities of carriers are generated by surface excitation in doped Ge. The resulting pressure from the carriers may compress droplets in doped Ge leading to pump-power dependent droplet density and linewidth. The pressure required to lead to the observed changes of densities (see Table I) can be estimated from $\Delta n/n = \chi P$, where χ is the compressibility of the electron-hole liquid and has been measured[38] to be 3.7×10^{18}cm^3/meV. For $\Delta n/n$ of 30%, P is estimated to be about 10^{17}meV/cm^3. A carrier density of about 10^{17}cm^{-3} would be required to produce this pressure and such high density is not likely in our experiment.

The decay times for MEC in Ge:As and Ge:Ga are quite long (70 μsec in Ge:As at 1.5°K[10] and 76 μsec for Ge:Ga at 2°K). Further, experiments on Ge doped with impurity concentrations of $\sim 10^{15}$cm^{-3} of shallow

dopants exhibit decay times for free excitons which are essentially the same as those observed in pure Ge[39]. These results suggest a relatively slow rate of Auger recombination of the excitons bound to impurity centers in Ge. It is possible that the decay of free-excitons occurs in both the doped and pure sample via some center (e.g., dislocations) other than the shallow dopants. If this is the case, then immobile excitons bound on a shallow dopant will decay at a rate slower than that for the free excitons.

V. CONCLUSION

We have investigated the temperature, pump-power and time dependences of the photoluminescence spectra of Ge containing up to $8X10^{16}cm^{-3}$ of impurities. For impurity concentrations of less than about $10^{15}cm^{-3}$, few changes in the spectrum of EHD were observed compared to pure Ge. The broad LA-phonon-assisted line of Ge:As containing up to $5X10^{16}$ As/cm^3 has properties which can be explained by the existing theories of EHD for doped Ge. The broad NP line of Ge:As as well as the broad LA-phonon-assisted EHD-like lines of Ge:Li, Ge:Ga and Ge:Sb have properties unexpected of an EHD line when the temperature, pump-power or delay-time is varied. It is necessary to consider impurity-induced emissions in addition to that from the EHD to explain these results. A comparison of our data with those of doped Si suggests that emissions from multiexciton complexes and broadened bound-excitons make up part of the impurity-induced emissions. Additionally, at higher temperatures ($T \gtrsim 10°K$) the spectra of doped Ge may result from both emission from the free-exciton and a plasma of electrons and

holes. This plasma can exist near the excited spot on the crystal be-cause the large excited-carrier density there screens out the free- and bound-exciton states.

REFERENCES

1. C.D. Jeffries, Science 189, 955 (1975), and references contained therein.

2. J.C.V. Mattos, K.L. Shaklee, M. Voos, T.C. Damen and J.M. Worlock, Phys. Rev. B13, 5603 (1976), and references contained therein.

3. O. Christensen and J.M. Hvam, in Proc. Twelfth Int. Conf. Semicond. Phys., Stuttgart, 1974, p.56.

4. J.M. Hvam and O. Christensen, Solid State Commun. 15, 929 (1974).

5. A.S. Alekseev, V.S. Bagaev, T.I. Galkina, O.V. Gogolin and N.A. Penin, Fiz. Tverd. Tela. 12, 3516 (1971) [Sov. Phys.-Solid State 12, 2855 (1971)].

6. B.V. Novikov, R.L. Korchazhkina and N.S. Sokolov, Fiz. Tverd. Tela. 15, 459 (1973) [Sov. Phys.-Solid State 15, 326 (1973)].

7. C. Benoit a la Guillaume and M. Voos, Solid State Commun. 11, 1585 (1972).

8. R.W. Martin and R. Sauer, Phys. Status Solidi B62, 443 (1974).

9. R.W. Martin, Phys. Status Solidi B66, 627 (1974).

10. A.L. Karuzskii, K. Betzler, B.G. Zhurkin and V.P. Aksenov, in Molecular Spectroscopy of Dense Phases, Proceedings of the 12th European Congress on Molecular Spectroscopy, (Elsevier, Amsterdam, 1975), p.139.

11. Y.E. Pokrovskii, Phys. Status Solidi A11, 385 (1972).

12. D.L. Smith, Solid State Commun. 18, 637 (1976).

13. G. Mahler and J.L. Birman, Phys. Rev. B12, 3221 (1975); and Solid State Commun. 17, 1381 (1975).

14. We are grateful to Dr. R.N. Hall of G.E. Research Lab. who provided us with many samples.

15. Nucleonic Products Co., Inc. 6660 Variel Ave. Canoga Park, CA. 91303.

16. T.H. Yeh, in Atomic Diffusion in Semiconductors, (Plenum Press, New York, 1973), chap.4.

17. S.M. Sze, Physics of Semiconductor Devices, (John Wiley and Sons, New York, 1972), p.42 ff.

77

18. G.A. Thomas, T.M. Rice and J.C. Hensel, Phys. Rev. Lett. 33, 219 (1974).

19. See for example V.P. Varshni, Physica 34, 149 (1967).

20. J.R. Haynes, Phys. Rev. Lett. 4, 361 (1960).

21. E.F. Gross, B.V. Novikov and N.S. Sokolov, Fiz. Tverd. Tela. 14, 443 (1972) [Sov. Phys.-Solid State 14, 368 (1972)].

22. R.W. Martin, Solid State Commun. 14, 369 (1974).

23. J.C. Hensel, T.G. Phillips and T.M. Rice, Phys. Rev. Lett. 30, 227 (1973). It should be noted that, since no free-exciton emission is seen in the spectra of moderate-heavily doped Ge, it is somewhat speculative to assume that the decay of the electron-hole-droplets in moderate-heavily doped Ge is affected by free-exciton evaporation from droplets.

24. The wavefunction of an electron localized near a donor is an admixture of Bloch functions at different points in the conduction band. Because of the small energy difference between the minima at the Γ- and L-points of the conduction band of Ge, the strong potential associated with the deeper donors, As and P, mix in states at the Γ- point. This mixing makes the no-phonon recombination possible. The energy difference between the Γ- and L-points in the valence band of Ge is large so that one would not expect shallow acceptors to possess strong no-phonon transitions.

25. R. Sauer, Ref. 3, p.42.

26. K. Kosai and M. Gershenzon, Phys. Rev. B9, 723 (1974).

27. R. Sauer, Solid State Commun. 14, 481 (1974).

28. T.P. McLean and R. Loudon, J. Phys. Chem. Solids, 13, 1 (1960).

29. C. Kittel, Introduction to Solid State Physics, 4th ed. (John Wiley and Sons, New York, 1971), p.372 ff.

30. R. Sauer, thesis (Stuttgart, 1973) (unpublished).

31. V.I. Fistul', Heavily Doped Semiconductors (Plenum Press, New York, 1969), pp. 24-34.

32. D.S. Pan, D.L. Smith and T.C. McGill, (unpublished).

33. J.M. Ziman, Electrons and Phonons (Clarendon, Oxford, 1960), pp. 327-328, and references contained therein.

34. R.W. Martin, Phys. Status Solidi B61, 223 (1974).

35. N.F. Mott, <u>Metal-Insulator Transition</u>, (Barnes and Noble, New York, (1974).

36. G.A. Thomas, A. Frova, J.C. Hensel, R.E. Miller and P.A. Lee, Phys. Rev. <u>B13</u>, 1692 (1976).

37. J.I. Pankove, <u>Optical Processes in Semiconductors</u>,(Dover, New York, 1971), p.143.

38. G.A. Thomas, T.G. Phillips, T.M. Rice and J.C. Hensel, Phys. Rev. Lett. <u>31</u>, 386 (1973).

39. M. Chen, (unpublished).

Chapter 3

TRANSIENTS OF THE PHOTOLUMINESCENCE
INTENSITY OF THE EHD IN PURE AND
DOPED Ge

I. INTRODUCTION

The existence of a metallic liquid phase of electron-hole pairs in Ge at crogenic temperatures is by now well established[1]. A wide variety of experiments, mostly using optical excitation on high-purity Ge, have been used to determine many properties of this electron-hole liquid. Light scattering[2] and junction noise[3] experiments have demonstrated that the electron-hole liquid is produced in the form of a cloud of electron-hole-droplets (EHD's) in Ge. The size of the EHD can be as big as 10 μm[4]. The kinetics of formation and decay of these EHD's have been the subject of numerous investigations. The decay of the EHD has been carefully studied using cyclotron resonance[5], luminescence intensity decay[6,7], and far infrared absorption[8]. More recently, the growth of the EHD has been examined using both surface-excitation[9] and volume-excitation[10].

In the volume-excitation experiment[10], EHD's were observed to nucleate from a supersaturated free-exciton (FE) gas. The rate of growth of droplet intensity depends on temperature and is in qualitative agreement with theoretical predictions[11,12]. Inhomogeneous excitation and carrier-transport away from the excited surface complicates the situation in the surface-excitation experiments. To our knowledge, no quantitative explanation of the growth of the luminescence intensity of the EHD's exists in the literature. Pokrovskii[13] and Hensel et al.[5] have proposed a model for the decay of the EHD which may be applied to the surface-excitation experiments. This model is based on the average rate equations for the EHD

$$\frac{d\nu}{dt} = -\frac{\nu}{\tau} - aT^2 e^{-\phi/kT}\nu^{2/3} + b\nu^{2/3}\bar{n}_{ex} \quad , \tag{1}$$

and for the FE

$$\frac{d\bar{n}_{ex}}{dt} = -\frac{\bar{n}_{ex}}{\tau_{ex}} + \left(aT^2 e^{-\phi/kT}\nu^{2/3} - b\nu^{2/3}\bar{n}_{ex}\right)N. \tag{2}$$

In (1) and (2), ν is the average number of electron-hole pairs in a EHD τ and τ_{ex} are, respectively, the EHD and FE total lifetime, a is the Richardson-Dushman constant[14], ϕ is the work function of the EHD, T is the temperature, $\bar{n}_{ex}$ is the FE density, and N is the number density of droplets. The constant b is equal to $v_{ex}4\pi(3/4\pi n_o)^{2/3}$ where v_{ex} is the average thermal velocity of the exciton and n_o is the pair density of a EHD. The three terms on the righthand side of Eqn. (1) are, respectively, from left to right, bulk recombination, evaporation and FE backflow rates. Usually $\bar{n}_{ex}$ is assumed to be zero during the decay so that EHD's are decoupled from the FE and from each other. With the assumption of $\bar{n}_{ex}$ equal to zero, Eqn. (1) can be readily solved to yield

$$\nu(t) = \nu(o)\left[\frac{e^{(t_c - t)/3\tau} - 1}{e^{t_c/3\tau} - 1}\right]^3 \tag{3}$$

with

$$t_c = 3\tau \, \ell n \left[1 + \frac{\nu(o)^{1/3}}{AT^2 \tau e^{-\phi/kT}} \right] \qquad (4)$$

At low temperatures the evaporation rate is small compared to the recombination rate and the EHD decay is nearly exponential with a time constant equal to τ. At higher temperatures, evaporation becomes important, and, hence, the EHD decay is faster than the exponential decay expected at low temperatures. By adjusting t_c in Eqn. (3), one can fit the experimentally observed EHD decay transients quite well. However, if high excitation power is used[7], the value of t_c needed to fit the data leads to values for $\nu(o)$ or initial droplet radius which is too large compared with the results of lightscattering experiments[2].

In the case of doped Ge, very limited EHD luminescence decay data exist in the literature[15] and these data have not been used to extract any other information about the EHD and FE.

In this chapter, we present data on the growth and decay of the EHD and FE luminescence intensity in pure and doped Ge which are excited with long GaAs laser pulses (50-100 μsec). We found that it takes several tens of microseconds for the EHD luminescence intensity to reach a steady-state after the excitation is abruptly turned on (risetime < 1 μsec). The rise of the EHD intensity in our experiments cannot be adequately described by the nucleation theory due to the inhomogeneity of excitation. Our results of the decay of the EHD signal

for pure Ge and Ge doped with $10^{15} cm^{-3}$ of impurities show that the widely accepted single-drop model of decay is inadequate in many experimental situations. A new model based upon the existence of a cloud of EHD and the diffusion equation for FE's is presented. The diffusion equation approach can deal with the evaporation and backflow of FE across the surface of a droplet in a consistent manner. This model quantitatively explains the decay transients of EHD in both pure and doped Ge. In particular, it is found that a reduction of the FE diffusion coefficient in the $\sim 10^{15} cm^{-3}$-doped Ge can lead to the observed curtailment of FE evaporation by droplets.

This paper is organized as follows: Section II is divided into three parts and contains, respectively, the experimental results for pure, lightly doped (impurity concentration $N_i \sim 10^{15} cm^3$) and heavily doped ($N_i \sim 10^{16} cm^3$) Ge samples. In Section III, the model for the EHD and FE decay is presented. Discussion of experimental results and comparison of experiment with theory are presented in Section IV. The summary is in Section V. The experimental details have been described in Section II of Chapter 2 and are not repeated in this chapter.

II. EXPERIMENTAL RESULTS

(a) Pure Ge

In Figs. 1 and 2, respectively, we show the EHD luminescence intensity versus time at 2 and 4.2°K. The sample is a 2-mm thick, high-purity Ge crystal. At 2°K the transients for pump powers of 0.06 and 0.09W were identical. The rise of the EHD intensity was non-exponential

Figure 1

Transients of the photoluminescence intensity
of the electron-hole liquid in pure Ge at 4.2°K.
The thickness of the sample is denoted by †.

85

TRANSIENTS OF EHL LUMINESCENCE

$\lambda = 1.7495 \mu m$, $\Delta\lambda = 30\mathring{A}$

PURE Ge

$N_A - N_D \le 10^{11} cm^{-3}$

$T = 4.2°K$

$t = 2.0 mm$

—·—GaAs LASER PULSE

— — P = 0.22W

——— P = 0.09W

TIME (μsec)

INTENSITY (ARB UNITS)
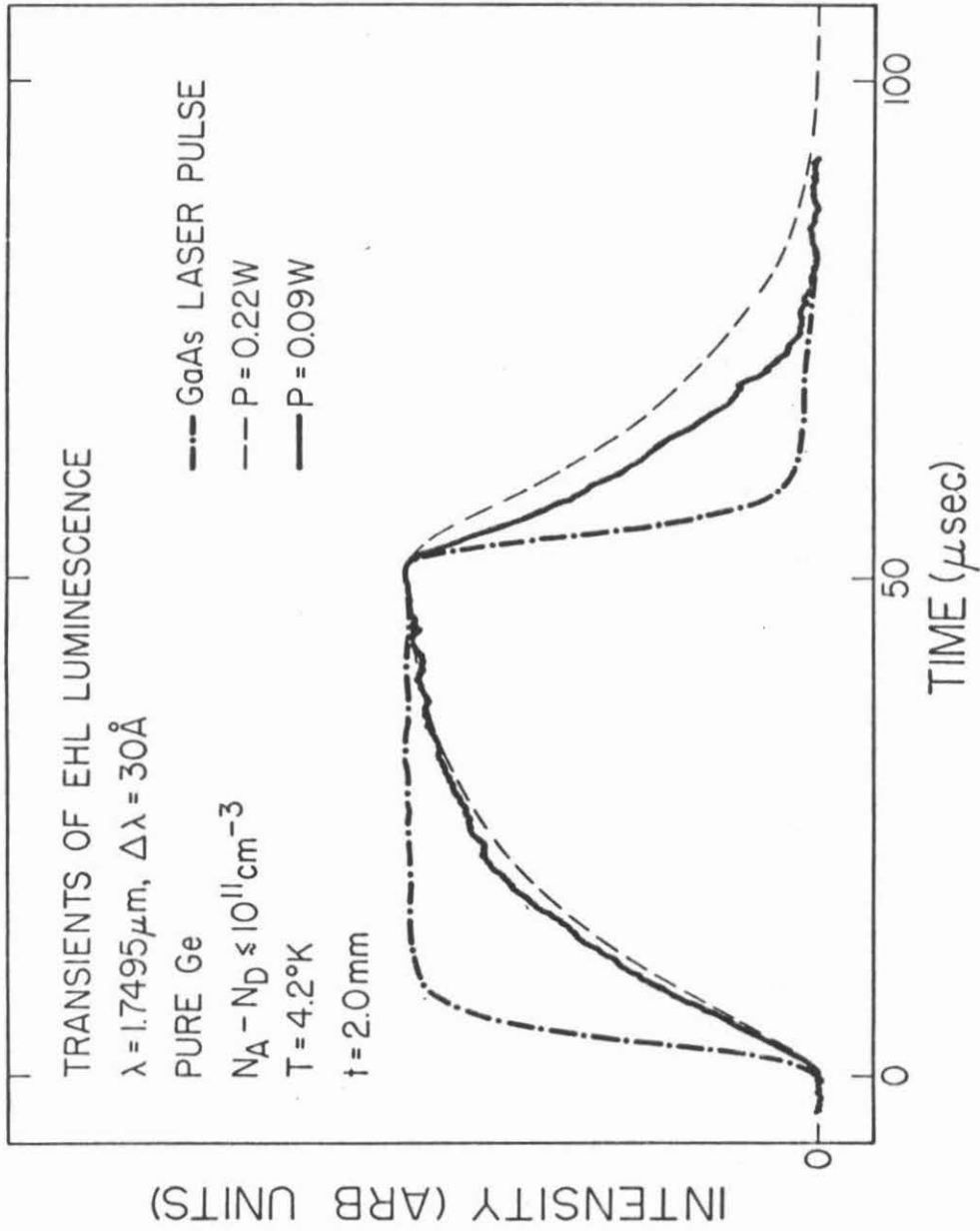
Figure 2

Transients of the photoluminescence intensity of
the electron-hole liquid. All parameters are the
same as those of Fig.1 except the temperature is
2 K. Note the difference in the horizontal scales
of this Fig. and Fig.1.

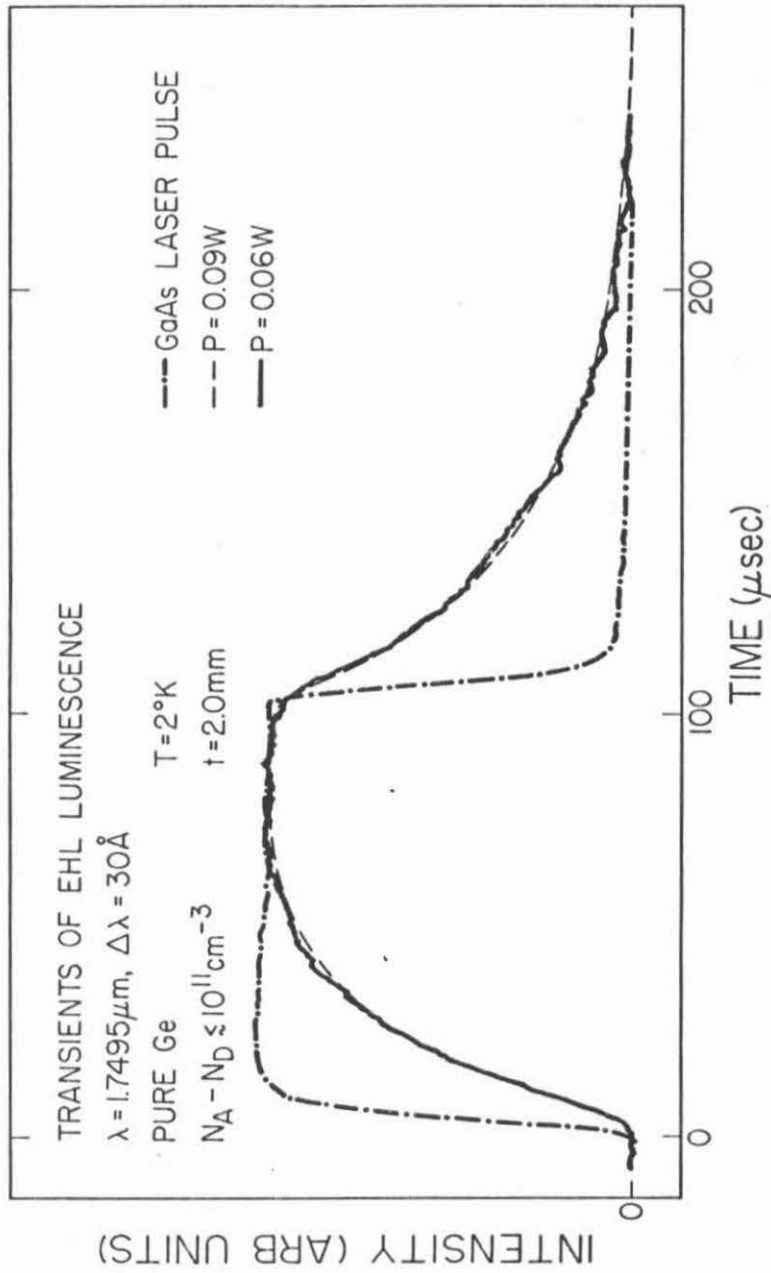and the 0-90% risetime was about 46 μsec. The decay was exponential with a lifetime of 37 μsec. This decay time is in good agreement with previous published results[5-7]. The 0-90% risetime of the EHD signal at 4.2°K was about 40 μsec. The decays at 4.2°K were non-exponential and showed finite cutoff times which increased with increased pump-power. The output of our GaAs laser, shown by the dash-dot curves, drooped during the current pulse as a result of the temperature rise of the laser. This droop reached a maximum of about 15% at the end of the laser pulse. Because of this droop, the risetime of the EHD signal that we measured was somewhat smaller than the step-response time of the EHD luminescence.

The qualitative behavior of the decay of EHD luminescence under our excitation conditions is similar to that observed using short, intense GaAs laser pulses[5-7]. The 4.2°K decay transients we observed can be fitted very well by Eqn. (3) using the observed EHD lifetime at 2°K and suitable t_c's. However, the required t_c's were between 45 and 60 μsec. These large t_c's yield, using Eqn. (4) and the values for the parameters given in Ref. 5, initial radius of the EHD of about 0.3 mm. In unstressed Ge, droplet radius of this order is in disagreement with the results of lightscattering experiments which show for a wide range of excitation conditions that the droplet radius does not exceed about 10 μm[2].

The sensitivity of the transients to sample thickness was checked by repeating the measurements for a 1-mm thick sample. In this 1-mm sample the growth and decay of the EHD signal were faster at both 4.2 and 2°K. We have also performed these experiments on the 2-mm sample after

we have damaged that sample's back surface by sandblasting. The transients of the EHD luminescence for this 2-mm sample were found to be unchanged by the damage to the back surface. Thus, we establish that the EHD cloud generated in the samples in our experiments extends between 1 and 2 mm away from the excited surface of the sample.

In Fig. 3, a transient of the FE luminescence signal along with the concurrent, normalized EHD signal from the 2-mm thick pure Ge sample is shown. We interpret the FE signal to be composed of the sum of two components. The first one is due to FE's created directly by the laser. This component has approximately a 7 μsec (FE lifetime)[7] rise and fall time at the beginning and the end of the laser pulse, and it is constant during the middle of the pulse. The second component is attributed to the increase of the volume occupied by FE's as the cloud of EHD's expand to its steady-state size. The growth and decay transients of the FE and EHD signal we observed are qualitatively different from the results of the volume-excitation experiment[10]. In particular, we detected no reduction in the FE intensity which should be associated with the nucleation and growth of EHD's[10]. We attribute these differences to the inhomogeneities of the excitation in our experiments.

The decay of the FE signal is approximately linear with time and the EHD's decay in the presence of a non-negligible concentration of FE's.

(b) Lightly doped Ge ($N_i \sim 10^{15} cm^{-3}$)

The EHD luminescence transients from a Ge sample with $4 \times 10^{15} As/cm^3$ at 4.2 and 2°K are shown in Fig. 4(a) and (b), respectively. The
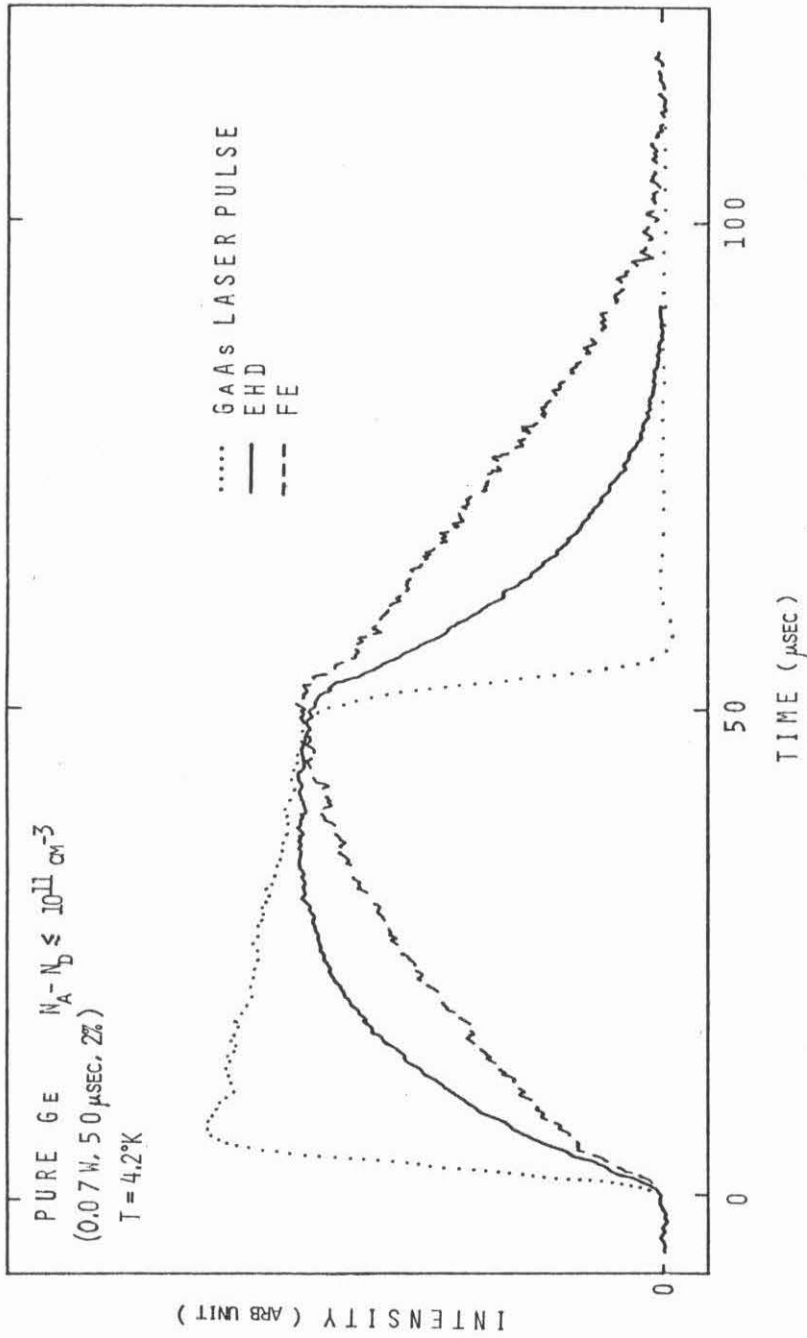
Figure 3

Transients of the photoluminescence intensity of
the electron-hole liquid and the concomitant free-
exciton. The intensities are normalized to the
same height at the end of the laser pulse. The
ringing on the laser pulse is an artifact caused
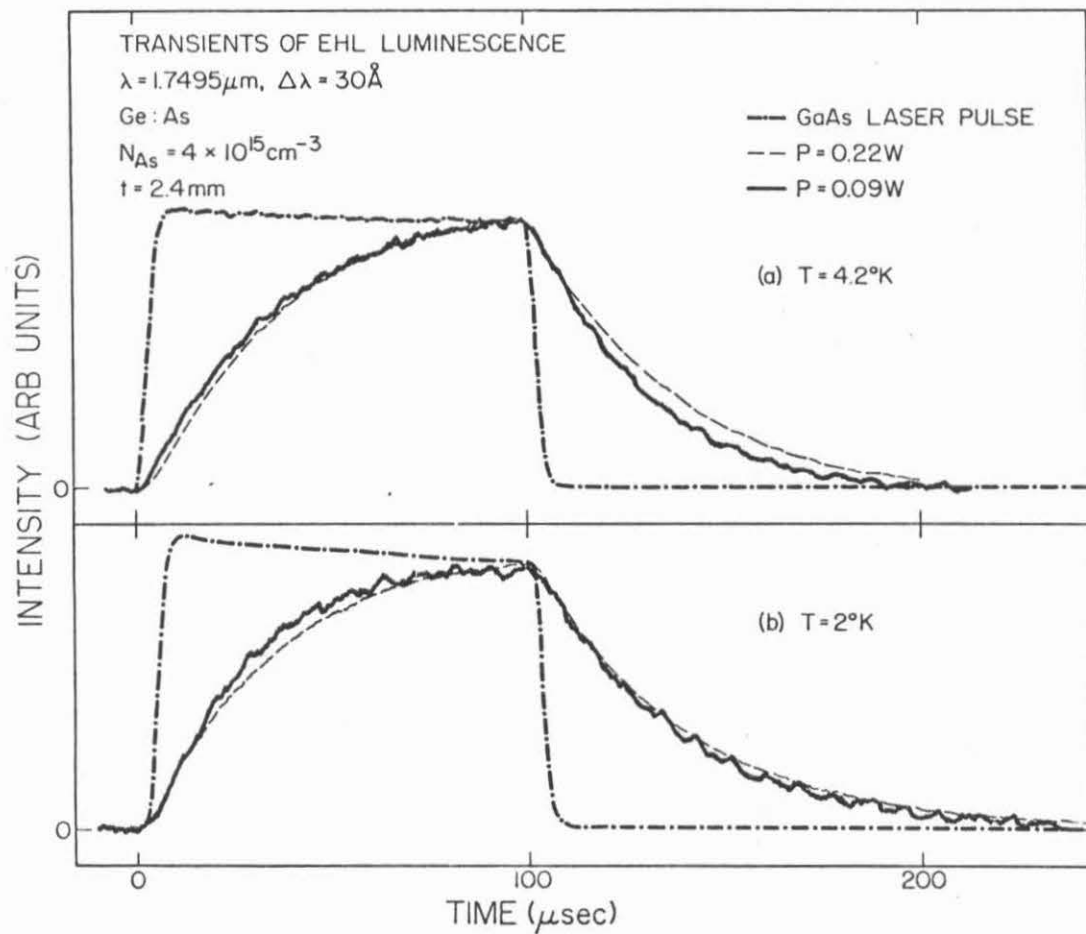by the amplifier for the detector.

Figure 4

Transients of the photoluminescence intensity
of the electron-hole liquid in lightly doped
Ge.

transients at 2°K for P = 0.09 and 0.06W were essentially identical. At 2°K the 0-90% risetime was ~65-70 μsec while the decay was exponential with a lifetime of 37 μsec. This lifetime is identical to the lifetime of EHD in pure Ge. However, unlike in pure Ge, the transients, in particular the decays,were not very sensitive to temperature between 2 and 4.2°K. In addition, the transients at both 2 and 4.2°K were only slightly pump-power dependent. Essentially identical results were observed for a 2×10^{15} Ga/cm^3 sample. Thus, for temperature at least as high as 4.2°K, the EHD luminescence intensity decay in lightly doped Ge is determined only by the EHD lifetime, i.e., FE evaporation from EHD's does not play a large role in the decay of EHD.

The work function of the EHD in Ge with $N_i \sim 10^{15}$cm^{-3} has been found, experimentally and theoretically[16], to be identical to that in pure Ge. We have shown above that the EHD lifetime was also unaffected by doping of this level. Thus, the recombination and evaporation terms in Eqn. (1) cannot be affected by doping level of ~10^{15}cm^{-3}. The reduction of the net evaporation rate for EHD in doped Ge must come about by an increase in the backflow rate caused by impurities. In the theory section of this paper, we shall show that a reduction of FE diffusion coefficient, caused by impurity atoms, could lead to increased backflow rate in doped Ge.

(c) Heavily doped Ge ($N_i \sim 10^{16}$cm^{-3})

The photoluminescence spectra of heavily doped Ge are complicated by impurity-induced emissions[17]. Only the phonon-assisted lines in Ge:As (and perhaps Ge:P) for T ≤ 4.2°K may be interpreted to reflect
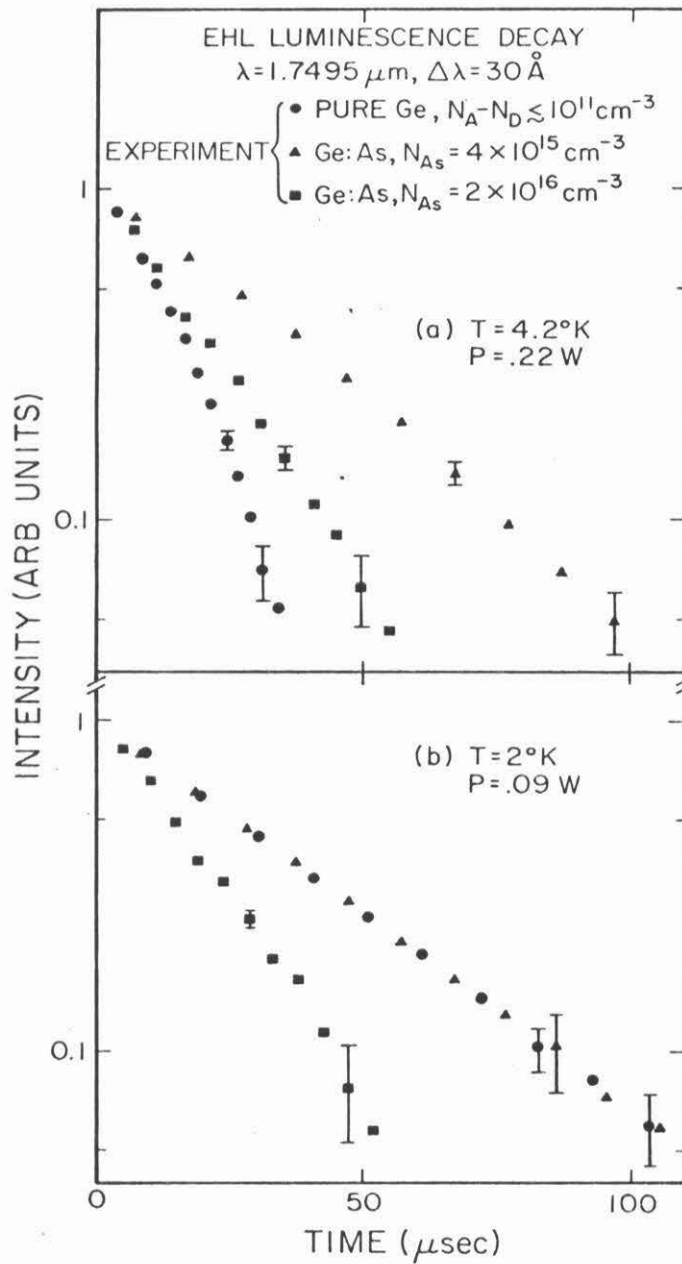
Figure 5

Normalized luminescence intensity of the electron-hole-droplets in heavily doped Ge on semi-log plot. The decay transients of the electron-hole-droplet luminescence of pure and lightly doped Ge are also shown for comparison.

the properties of the EHD in doped Ge. We report here the results for a Ge crystal with 2×10^{16} As/cm^3. The 0-90% risetime at 4.2°K was 50 μsec for 0.22W pumping and about 35 μsec for 0.09W pumping. While at 2°K, the risetime was 50 μsec for both 0.22W and 0.09W excitation power. The decay transients are shown on a semilog plot in Fig. 5 where we have also shown the decay curves for pure and lightly doped Ge for a comparison. We observed that the decay of the EHD at 2°K in heavily doped Ge:As was exponential with a time constant of about 23 μsec. This EHD lifetime is considerably shorter than the 37 μsec EHD lifetime in pure Ge. As in lightly doped Ge, the decays in heavily doped Ge showed very little effect of evaporation at both 2 and 4.2°K.

III. MODEL FOR DECAY

A. Description of Physics

The EHD distribution in the sample at the end of the excitation pulse is complex. The EHD cloud is spatially non-uniform and not simple in shape[2]. In addition, droplets may be in motion[18]. Nonetheless, we can gain an understanding of the decay of the EHD and FE using a somewhat idealized model which retains the essential physics.

In this model, the EHD cloud is assumed to be spherical in shape and situated in an infinite Ge crystal. Inside this sphere of radius R_c, the density of EHD's is assumed to be uniform while outside the radius R_c, the EHD density is taken to be zero. The exciton density inside the cloud is non-uniform due to the presence of EHD's. This spatially-varying exciton density is replaced by its average value

$\overline{n}_{ex}$. Outside the cloud, the exciton density is determined by exciton diffusion from the edge of the cloud. A schematic illustration of this model is shown in Fig. 6. Exciton concentrations in and out of the cloud are obtained through solutions to the exciton diffusion equation. This diffusion equation approach allows us to (1) treat the net evaporation rate, i.e., the sum of evaporation and backflow rates in Eqn. (1), in a reasonable way; and (2) incorporate flow of excitons outside of the cloud and the resulting shrinking of the cloud with time. Both of these aspects were not considered in the single-drop model.

There are three decay paths for electron-hole pairs: recombination inside a EHD, recombination of FE in the cloud, and recombination of FE after diffusing away from the edge of the cloud. To determine the rates for these three paths, two main problems have to be solved. First one is the diffusion of excitons away from the cloud, causing the cloud to shrink. For this, we solve the exciton diffusion equation outside the cloud with the boundary conditions that the exciton density be equal to zero at infinity and equal to $\overline{n}_{ex}$ at the cloud edge. The second problem is the calculation of $\overline{n}_{ex}$. The inset in Fig. 1 depicts the situation in the body of the cloud and is the basis for the calculation of the average exciton density. The close proximity of the droplets, inter-drop distances being much less than an exciton diffusion length for pure material, implies that each drop on the average only supplies excitons to its immediate vicinity. Each droplet is assigned a spherical volume of radius R_s as shown in the figure by the dashed line, and the condition is imposed that no excitons cross R_s. This boundary condition should be contrasted with that in a single drop picture in which

SCHEMATIC OF CLOUD
OF
ELECTRON-HOLE DROPLETS
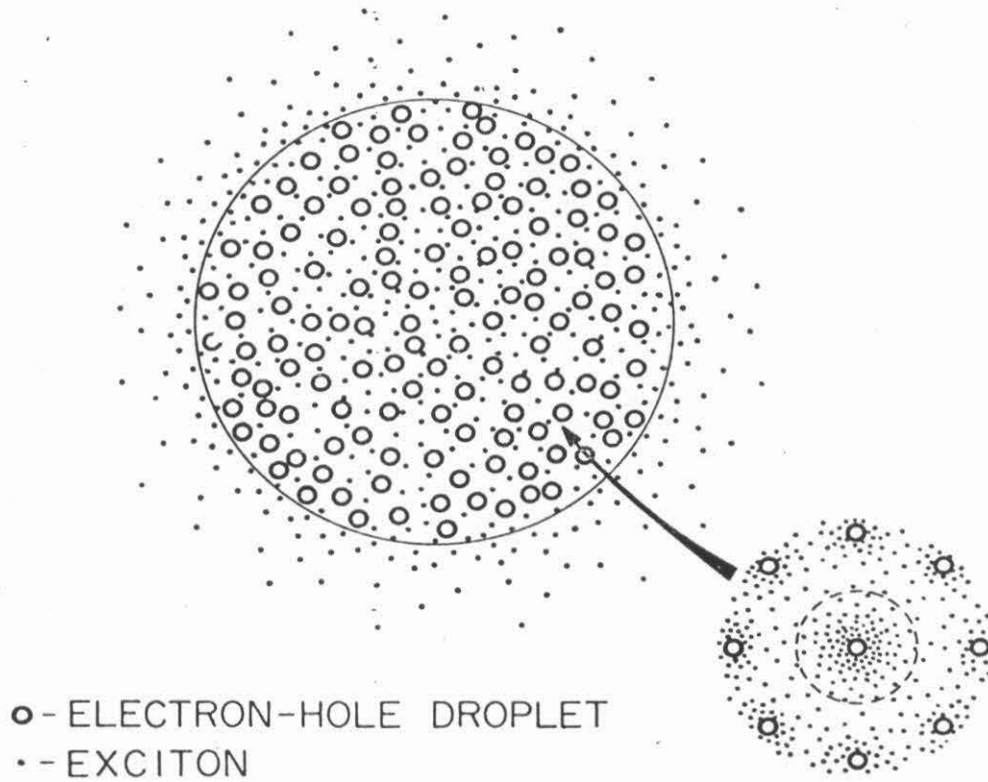

o - ELECTRON-HOLE DROPLET
• - EXCITON

Figure 6

Schematic illustration of the cloud of
electron-hole-droplets and free-excitons.
The radius of the cloud is R_c. Inset
shows an enlarged view of an electron-
hole-droplet surrounded by neighboring
electron-hole-droplets. The central
electron-hole-droplet needs to supply
excitons only into the volume bounded
by R_s (dashed line).

the excitons can diffuse out to infinity. Solving the diffusion equa-
tion within the region bounded by R_s and averaging the exciton density
over the volume of this region gives the average exciton density with-
in the cloud. Each droplet in the body of the cloud must shrink as it
must supply both the pair recombination current within itself and the
exciton recombination current in the volume bounded by R_s. Thus,
the number of pairs bound in droplets and the associated luminescence
signal decrease both through the shrinking of individual droplets and
the shrinking of the cloud as a whole.

B. Mathematical Description

The diffusion equation governing the FE's outside the EHD cloud is

$$\frac{\partial n_{ex}}{\partial t} = D\nabla^2 n_{ex} - n_{ex}/\tau_{ex} \quad , \tag{5}$$

where D is the exciton diffusion coefficient and n_{ex} is taken to be a
function of both t and the distance r from the center of the cloud.
The boundary conditions to be satisfied are

$$n_{ex} = \bar{n}_{ex} \text{ at } r = R_c(t) \quad , \tag{6}$$

and

$$n_{ex} = 0 \text{ at } r = \infty \tag{7}$$

Equation (5) is coupled to the equation for R_c through equation (6).
The equation for R_c is

$$\frac{dR_c}{dt} = \frac{(\text{diffusion flux of excitons away from cloud})}{(\text{density of pairs in cloud})}$$

$$= \frac{\left| D\nabla n_{ex} \right| \ r = R_c}{\bar{n}_{ex} + n_o \cdot FF} \tag{8}$$

In Eqn. (8), the fill factor (FF) is defined to be the fractional volume of the cloud containing electron-hole liquid. These equations can be solved for $\frac{dR_c}{dt}$ in terms of $R_c(t)$ and $\bar{n}_{ex}(t)$. To determine the decay of EHD and FE inside the cloud, it is necessary to solve the exciton diffusion equation (5) for the region surrounding a given droplet with two boundary conditions: (1) At the surface of the drop, $r = R_D(t)$, diffusion current away from the droplet equals evaporation rate minus backflow rate or

$$-D\nabla n_{ex} \cdot \hat{n} = aT^2 e^{-\phi/kT} - n_{ex}v_{ex}, \text{ at } r=R_D(t) \quad , \tag{9}$$

where $\hat{n}$ is a unit vector normal to and pointing out of the surface of the droplet; and (2) no exciton diffusion current flow across R_S, or

$$\nabla n_{ex} = 0 \text{ at } r = R_S(t) . \tag{10}$$

The FE evaporate rate can be estimated from the equilibrium density of FE ($\bar{n}^o_{ex}$) by detailed balance,

$$aT^2 e^{-\Phi/kT} = \bar{n}^o_{ex} v_{ex} \quad . \tag{11}$$

The excitons in the cloud are coupled to the droplets through the equation

$$\frac{d\nu}{dt} = -\nu/\tau - (\text{exciton diffusion current away from droplet}), \tag{12}$$

or

$$\frac{dR_D}{dt} = -\frac{R_D}{3\tau} - \frac{|D\nabla n_{ex}|_{r=R_D}}{n_o} \tag{13}$$

The exciton diffusion equation can be solved and substituted into (13) to yield dR_D/dt as a function of time

From the two parts of the problem outlined above, we obtain $\dot{R}_c$ and $\dot{R}_D$ in terms of $R_c(t)$ and $R_D(t)$.   A straightforward numerical

integration of $\dot{R}_c$ and $\dot{R}_D$ yields $R_c(t)$ and $R_D(t)$. From $R_D(t)$ and $R_c(t)$ we obtain

$$I_{EHD} \sim R_c(t)^3 \cdot FF(t) \tag{14}$$

and

$$I_{FE}(t) \sim \int n_{ex}(r,t) \, d^3r \quad , \tag{15}$$

where the integral extends over all space.

During and at the end of the laser pulse, a generation term must be added to the lefthand-side of Eqn. (9). This generation term drives the exciton gradient at each droplet surface negative so that excitons can flow into droplets during the time the laser is on. It is obvious that since we have not introduced the generation term, we cannot start out with the correct initial condition. In fact, our solution assumes an initial condition such that the exciton gradient is positive at the surface of each droplet. However, since FE decay is fast, we expect the exciton density to relax from that at the end of the laser pulse to the one we assume in about one exciton lifetime. This relaxation can be observed in the FE transient in Fig. 3. Thus, our solution should be accurate to describe the decay transients after about one exciton lifetime from the end of the laser pulse.

IV. RESULTS OF CALCULATION AND COMPARISON WITH EXPERIMENT

In this section, the calculated decay transients of the EHD and FE intensity will be presented and compared to experimental data.

The theoretical curves presented in Fig. 7 were calculated for three different initial cloud radii. Values of the parameters used in the calculation are listed in Table I along with the values of the same parameters reported in the literature. Within experimental uncertainty, the values we used to generate the curves in Fig. 7 are the same as those found in the literature. Figure 7(a) shows the calculated EHD luminescence decay transient, normalized to unity at the start of the decay. The corresponding curves for the FE are shown in Figure 7(b). At 4.2°K, increase of $R_c(o)$ causes the decay to be longer because for larger $R_c(o)$, the initial surface to volume ratio is smaller, and this lessens the importance of exciton diffusion away from the cloud. Spatially-resolved light absorption experiments at 4.2°K[19] show that different initial $R_c(o)$ can be created by using different excitation powers. It can be seen that there are clear differences between the three FE curves making them a sensitive, independent check on the model. In particular, these results are very different from the solutions to the average rate equations in which there is no boundary to the region occupied by EHD's. Experimental result of the EHD and FE decay transients for two different pump powers are also shown in Fig. 7. It can be seen that an excellent agreement is obtained for both the EHD and the FE curves when reasonable values for the parameters are used in the calculation. There are two points that should be noted,

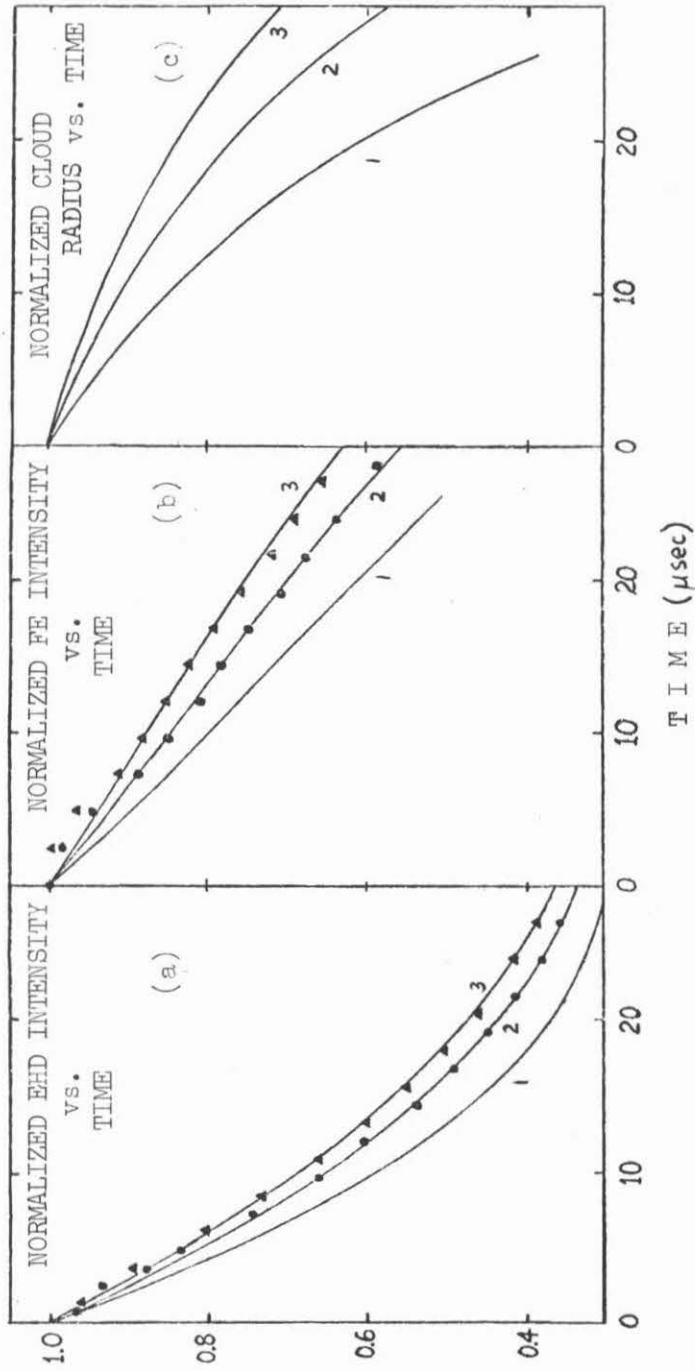Figure 7

Results of calculations of the Model for 4.2°K. The parameters used are appropriate for pure Ge and are given in Table I. The initial radii of the cloud for curves 1, 2 and 3 are 1.0, 1.4 and 1.8 mm, respectively. Experimental results for high-purity Ge are shown for comparison; pump-powers used are (▲) 0.14 W and (●) 0.09 W.

Table I   Values of parameters used in the Model.

Parameter	Values used in calculations for Fig. 7	Values found in the literature
EHD lifetime, τ	37 μsec	36 - 45 μsec [5-7]
FE lifetime, τ_{ex}	7 μsec	6 - 8 μsec [7,a]
Equilibrium density of FE, $\bar{n}_{ex}^{0}$		
2°K	$7 \times 10^{11} cm^{-3}$	$7 \times 10^{11} cm^{-3}$ [b]
4.2°K	$3 \times 10^{14} cm^{-3}$	$5 \times 10^{14} cm^{-3}$
Pair density in the EHD, n_0		
2°K	$2 \times 10^{17} cm^{-3}$	$2.1 \times 10^{17} cm^{-3}$ [b]
4.2°K	$2 \times 10^{17} cm^{-3}$	$2.4 \times 10^{17} cm^{-3}$
Initial EHD radius, $R_D(0)$		
2°K	2 μm	2 μm [c]
4.2°K	10 μm	~10 μm [4]
FE diffusion length, ℓ_x	0.8 mm	~1 mm [13,20]
Fill factor, FF	2%	1 - 2% [19,c]
Initial cloud radius, $R_C(0)$	1.4 - 1.8 mm	1 - 2 mm [2,19]

a. V. Marrello, T.C. McGill and J.W. Mayer, Phys. Rev. B13, 1607 (1976).

b. G.A. Thomas, A. Frova, J.C. Hensel, R.E. Miller and P.A. Lee, Phys. Rev. B13, 1692 (1976).

c. J.M. Worlock, T.C. Damen, K.L. Shaklee and J.P. Gordon, Phys. Rev. Lett. 33, 771 (1974).

however. First, different parameters can offset each other, e.g., re-
ducing the exciton diffusion length slows down the decays but this may
be offset by increasing the equilibrium density of excitons which
speeds up the decay. Second, light absorption experiments[19] have
shown that exciton recombination current at the Ge surface is not
negligibly small at 4.2°K. Thus, our model is qualitatively correct
in that much essential physics has been retained, but it is difficult
to get accurate quantitative results from our model. Figure 7(c) shows
plots of $R_c(t)$ corresponding to the cases shown in (a) and (b). At
4.2°K, it is seen that the shrinking of the cloud of EHD's is as im-
portant as the shrinking of individual droplets in causing the decay
in the droplet luminescence intensity. This collapse of the EHD cloud
has been observed in temporally and spatially resolved absorption ex-
periments[19].

Our model also correctly describes the EHD decay at 2°K. At this
lower temperature when the importance of exciton evaporation is reduced,
the EHD lifetime is the dominant factor in determining EHD luminescence
intensity decay. At 2°K, R_c does not change noticeably with time
because $\bar{n}_{ex}$ is so small that FE recombination current cannot affect
EHD decay.

Under the same excitation conditions, the initial cloud radius,
initial fill factor and exciton diffusion length can be different in
pure Ge and Ge doped with about $10^{15} cm^{-3}$ of impurities. Spatial
luminescence intensity scans show that the cloud of EHD's does not
penetrate as deeply in lightly doped Ge as in pure Ge[20,21], so $R_c(o)$

should be smaller in lightly doped Ge compared to pure Ge. This fact, coupled with the observation that the total luminescence intensity from pure and doped Ge does not differ significantly, implies a larger fill factor in doped Ge. Neutral impurity scattering of excitons can significantly alter the exciton diffusion length at the $10^{15} cm^{-3}$ doping level. Figure 8(a) shows calculations for 4.2°K for various initial cloud radii, fill factors and exciton diffusion lengths. For curve 1, an initial radius of 0.5 mm was assumed and the fill factor has been increased to 10% in keeping with the greater confinement of the EHD's. The exciton diffusion length is still $\ell_x = 0.8 mm$. The decay is seen to be slower in this case compared to pure Ge (Figure 7(a)) but is still far from being exponential. Curve 2 assumes $R_c(o)$ = 0.5 mm, fill factor = 2% and ℓ_x = 0.016 mm. Comparison of curves 1 and 2 shows the much greater importance of diffusion length over fill factor in slowing down the decay. Curve 3 incorporates all the expected changes for doped Ge with $R_c(o)$ = 0.5 mm, $\ell_x = 0.016$ mm, and a fill factor of 10%. As can be seen from the figure, altering the parameters to those for doped Ge dramatically changes the decay curves, causing the luminescence transients to become nearly exponential for temperature as high as 4.2°K. Excellent agreement with the experimental data, shown as dots in Fig. 8(a), is obtained. It should be noted that the value for exciton diffusion length in the doped material was determined through fitting the luminescence decays and has not been measured experimentally. Figure 8(b) shows the calculated decay curves for FE corresponding to the cases in Fig. 8(a). The decay time of the FE is controlled by the evaporation of excitons from droplets and is, therefore, directly

Figure 8

Results of calculations of the Model for $4.2°K$.
Curve 1: FE diffusion length = 0.8 mm, fill factor = 10%.
Curve 2: FE diffusion length = 0.016 mm, fill factor = 2%.
Curve 3: FE diffusion length = 0.016 mm, fill factor = 10%.
Initial cloud radius for all three curves is 0.5 mm, all
other parameters are the same as those for pure Ge given
in the text. Experimental results of the luminescence
intensity decay of the EHD in a Ge sample with $4 \times 10^{15} As/cm^{3}$
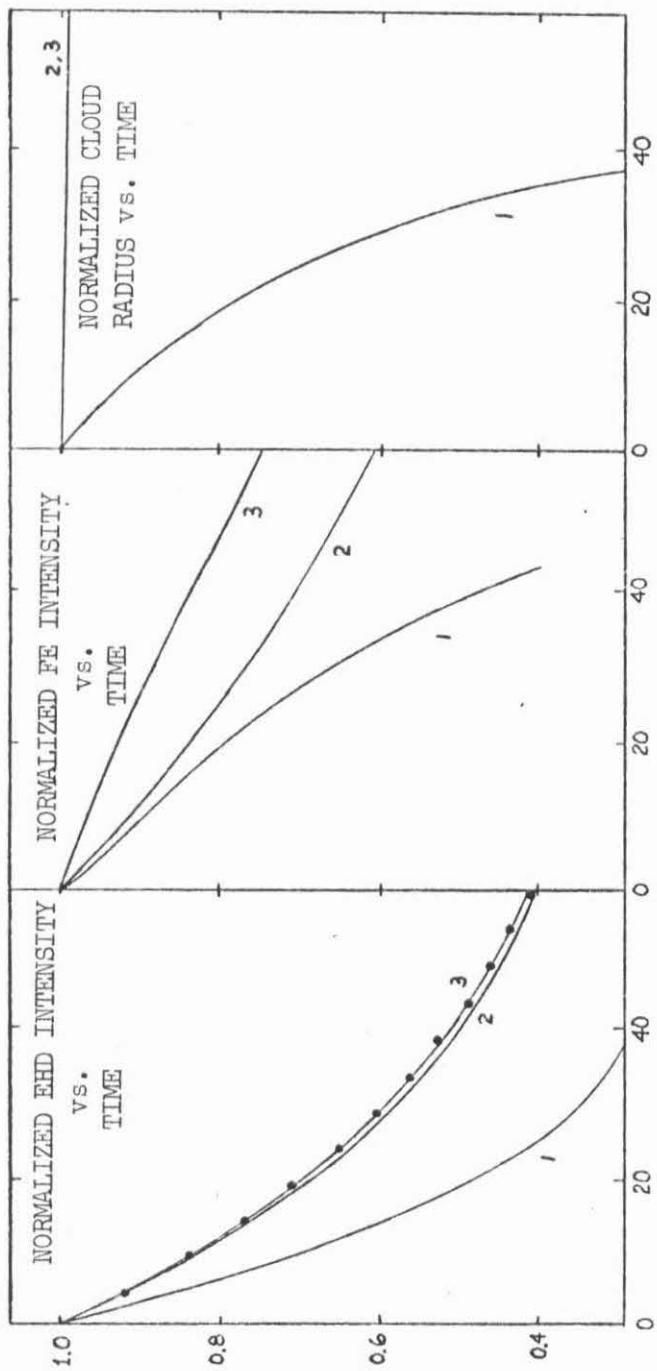is shown as the dots.

T I M E (μsec)

Figure 8

related to the EHD lifetime. For the case corresponding to lightly
doped Ge, curve 3, the FE decay is expected to be very slow compared
to pure Ge. Figure 8(c) shows the calculated $R_c(t)$ using the same
parameters as those used for the corresponding curves in Figure 8(a)
and (b). These curves illustrate clearly that reducing the diffusion
length stops the escape of excitons from the cloud and the reduction
of R_c with time. Merely increasing the fill factor as for curve 1
does not accomplish this and consequently the calculated decay is
much too fast compared to experiment. We emphasize that the evapora-
tion of excitons from droplets must be shut off in order to account for
the long decays observed for lightly doped Ge.

The reduction of free exciton diffusion length in doped Ge implies
a short exciton diffusion tail and, therefore, fewer excitons around
each drop. Therefore, it is expected that the relative EHD to FE
intensity should be small while EHD's are decaying. This reduction of
FE intensity for doped Ge is observed experimentally.

Our model predicts, as observed experimentally, that the decay
of the EHD in lightly doped Ge at 2°K should be determined by the life-
time of the EHD.

V. SUMMARY AND CONCLUSIONS

We studied the time evolution of the EHD luminescence from pure
and doped Ge using long surface-excitation pulses. We found the time
required for droplet luminescence intensity to reach a steady-state
after excitation turn-on to be several tens of microseconds in both

pure and doped Ge. The long excitation pulses used in our experiment produced EHD decays in pure Ge which are much too slow to be explained by the independent-droplet model extensively used previously. In addition, it is shown that this independent-droplet model cannot account for the observed turn-off of the FE evaporation from EHD's in lightly doped Ge.

A new model for the EHD luminescence intensity decay which takes into account both the existence of a cloud of droplets and exciton emission and capture by droplets is presented. This model explains qualitatively the experimental results. In the case of pure Ge at 4.2°K, evaporation from all the droplets in the cloud keeps the exciton density inside the cloud non-negligible after the excitation is turned off. This high exciton density causes the observed long EHD decay times at 4.2°K in pure Ge. Pump-power dependence of the decay time is a consequence of the different initial cloud radii generated by different pump powers. It is also shown that a reduction of the FE diffusion length in the lightly doped Ge can produce a large reduction of FE evaporation rate from droplets.

REFERENCES

1. C.D. Jeffries, Science 189, 955 (1975), and references contained therein.

2. J.C.V. Mattos, K.L. Shaklee, M. Voos, T.C. Damen and J.M. Worlock, Phys. Rev. B13, 5603 (1976), and references contained therein.

3. J.M. Hvam and O. Christensen, Solid State Commun. 15, 929 (1974).

4. V.S. Bagaev, N.A. Penin, N.N. Sibel'din and V.A. Tsvetkov, Fiz. Tverd. Tela. 15, 3269 (1973) [Sov. Phys.-Solid State 15, 2179 (1974)].

5. J.C. Hensel, T.G. Phillips and T.M. Rice, Phys. Rev. Lett. 30, 227 (1973).

6. C. Benoit a la Guillaume, M. Capizzi, B. Etienne and M. Voos, Solid State Commun. 15, 1031 (1974).

7. R.M. Westervelt, T.K. Lo, J.L. Staehli and C.D. Jeffries, Phys. Rev. Lett. 32, 1051 (1974).

8. K. Fujii and E. Otsuka, Solid State Commun. 14, 763 (1974).

9. J. Shah, A.H. Dayem, M. Voos and R.N. Silver, Solid State Commun. 19, 603 (1976).

10. J.L. Staehli, Phys. Status Solidi B75, 451 (1976).

11. R.N. Silver, Phys. Rev. 11, 1569 and 12, 5689 (1975).

12. R.M. Westervelt, Phys. Status Solidi B74, 727 and B76, 31 (1976).

13. Y.E. Pokrovskii, Phys. Status Solidi A11, 385 (1972).

14. To apply to the excitons, the Richardson-Dushman Constant for metals is corrected for exciton mass, binding energy and degeneracy. In addition, a factor $(36\pi)^{1/3} n_o^{2/3}$ is incorporated in a which converts $n^{2/3}$ to the droplet surface area.

15. C. Benoit a la Guillaume and M. Voos, Solid State Commun. 11, 1585 (1972).

16. D.L. Smith, Solid State Commun. 18, 637 (1976).

17. M. Chen, D.L. Smith and T.C. McGill, Phys. Rev. B15,___ (1977), (to be published).

18. J. Doehler, J.C.V. Mattos and J.M. Worlock, Phys. Rev. Lett. 38, 726 (1977).

19. K.R. Elliot, D.L. Smith and T.C. McGill, (to be published).

20. R.W. Martin, Phys. Status Solidi $\underline{B61}$, 223 (1974).

21. M. Chen, (unpublished).

Chapter 4

PROPERTIES OF THE EHD IN Ge DOUBLE INJECTION

DIODES

I. INTRODUCTION

Most of the studies of electron-hole-droplets in semiconductors to date have been performed using optical excitation [1]. The optical radiation used has most often been provided by photons from lasers in the energy range such that most photons are absorbed within about 1000 Å from the surface. The electron-hole pairs that are generated in this surface layer are driven further into the crystal by surface electric fields, density gradients, exciton wind or phonon wind. Thus, the condensation phenomenon often takes place in a region of the semiconductor where the density of electron-hole pairs is quite non-uniform.

It is also possible to generate electron-hole pairs in an intrinsic semiconductor electrically. This can be done by fabricating p- and n-contacts on an intrinsic crystal and biasing the resulting p-i-n diode so that electrons (holes) are injected into the intrinsic region through the n- (p-) contact (double injection). There are two reasons that this electrical means of generating electron-hole-droplets is important. First, in a p-i-n diode, electrons and holes are injected with approximately uniform density into the intrinsic region [2]. This allows one to study electron-hole condensation in a nearly homogeneous environment. Second, electrical excitation is more readily obtained than laser sources and possible practical uses of EHD's are likely to involve electrical devices.

To make injecting contacts work at liquid-He temperatures, the contacts must be degenerately doped. At the same time, in order not to contaminate the high-purity sample, only low temperature processes can be used. Marrello et al. [3-5] first developed methods for fabricating

double injection diodes and studied extensively the luminescence from these diodes. They found the spectra of optically and electrically excited Ge are different in many respects.

In this chapter, we explore various possible causes of the differences between electrically and optically excited spectra of Ge. We show that Li, introduced during device fabrication, is responsible for the observed differences. By properly choosing the device geometry so as to reduce Li contamination of the device to below about 10^{15} cm^{-3}, we were able to obtain very similar spectra from Ge using either optical or electrical excitation. We conclude that EHD's can indeed be generated in Ge using electrical double injection technique.

This chapter is organized in the following manner. In Section II, device fabrication procedure is described along with experimental details. The experimental results are presented in Section III. Section IV contains the summary and conclusions.

II. EXPERIMENTAL

Electrical excitation of the EHD was first reported by Marello et al. who developed the methods for fabrication of double injection diodes. These fabrication procedures are described in detail in Ref. 5. However, for completeness sake, the method will be briefly outlined here. High-purity Ge crystal slices were first prepared by lapping and etching. Then an Al film is evaporated on one face while Li, suspended in mineral oil, is painted on the opposite face of the Ge slices. The samples were heated at 350°C for about 30 minutes and then slowly cooled down. This procedure makes Li-diffused n^+-contacts and Al-regrown p^+-contacts on the Ge samples. The resulting device is appropriately called a p-i-n diode. To increase the current density for a given total device current, most of the Al contact is etched away, leaving only a mm^2-sized Al mesa contact. Figure 1(a) shows a schematic picture of such a mesa p-i-n diode. A typical separation between p- and n-contacts is 2 mm.

The double injection diodes used in this study were fabricated in such a way as to minimize the Li contamination of the intrinsic region. This is done in two ways. First, the separation between the p^+ and the n^+-contacts is made to be ~4 mm, about twice the typical contact separation distance of mesa p-i-n diodes. Second, instead of broad-area Li contact, Li is painted and diffused-in over a small area. Two device geometries were investigated: surface p-i-n and limited-area p-i-n. These devices are illustrated in Fig. 1(b) and (c). The surface p-i-n device consisted of two mesa type contacts, n^+ and p^+, on the same face of a pure Ge slice. A 4-mm spacing between the contacts

a) Mesa p-i-n

p^+

Ge

n^+ (Li-diffusion)

b) Surface p-i-n

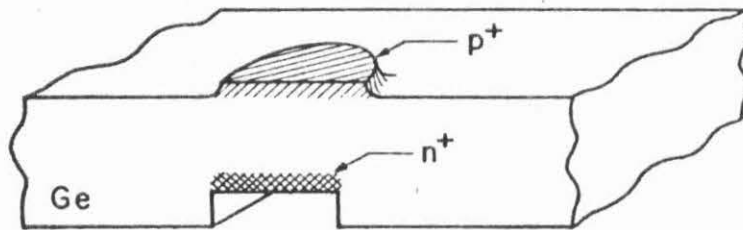p^+

n^+

Ge

c) Limited-area p-i-n

p^+

n^+

Ge
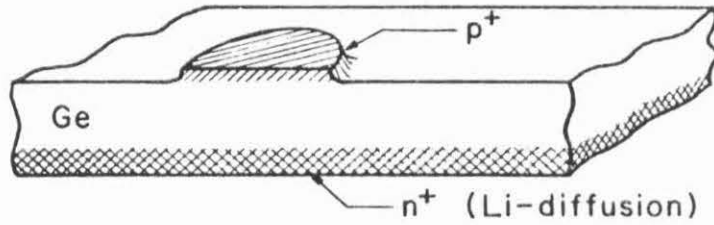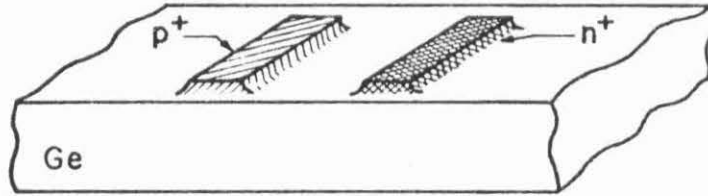
Figure 1

(a) Schematic representation of a mesa type p-i-n double injection device.

(b) Schematic representation of surface type p-i-n double injection device.

(c) Schematic representation of a limited-area p-i-n double injection device.

made it possible to laser excite the region between the contacts, and hence, to compare directly electrical and optical excitation. The contact structure was formed by protecting the n^+ and p^+ contacts with black wax prior to a final etch with 3 parts HNO_3 to 1 part HF which removed about 100 μm of the Ge surface. The limited-area p-i-n structure was produced by defining a n^+ Li contact which had a limited-area of approximately the same size as the area of the p^+ Al mesa contact. To allow a large flat area for thermal connection between the structure and the copper heat sink, the Li contact was recessed. The area of the Li diffusion was approximately 9 mm^2 which is approximately the same size as the p^+ contact. The contacts were separated by 4.4 mm.

The experimental apparatus used to investigate the luminescence spectra of these diodes is the same as that described in Chapter 2 of this thesis. A voltage pulser is connected directly to the double injection diode to provide electrical excitation.

III. EXPERIMENTAL RESULTS

In Fig. 2 we compare the luminescence spectra of laser-excited high-purity Ge and the mesa p-i-n. The laser-excited pure Ge spectrum is shown in (b). This spectrum is similar to published, optically excited recombination spectra at 4.2°K [1] in that in this energy range it contains peaks due LA- and TO- phonon-assisted recombination of excitons and electron-hole pairs in the condensate. The width of the line associated with the condensate is 3.3 meV which gives a density of $2.1 \times 10^{17} cm^{-3}$. The condensate line exhibited a well defined threshold. That is, a threshold value of laser excitation was required to see the condensate line. Below the threshold value in laser excitation, only the free exciton lines could be observed. A recombination spectrum from a p-i-n mesa structure is shown in Fig.2(a). The spectrum shows the well known LA- and TO- phonon-assisted recombination lines from the condensate. The line width of the LA-phonon-assisted line is 2.5 meV which corresponds to a density using the simple model of Pokrovskii of about $1.2 \times 10^{17} cm^{-3}$.

This density is somewhat less than the density previously observed in optical excitation experiments on pure Ge [6]. Also, no FE lines were observed even at this very low current level. Further, the line shapes are noticeably different. The line shape obtained from the double injection mesa structure is slightly narrower, has its low energy edge shifted to slightly higher energy, and has its high energy edge shifted to slightly lower energy when compared with the condensate line from the pure material. This narrowing of the line is reflected
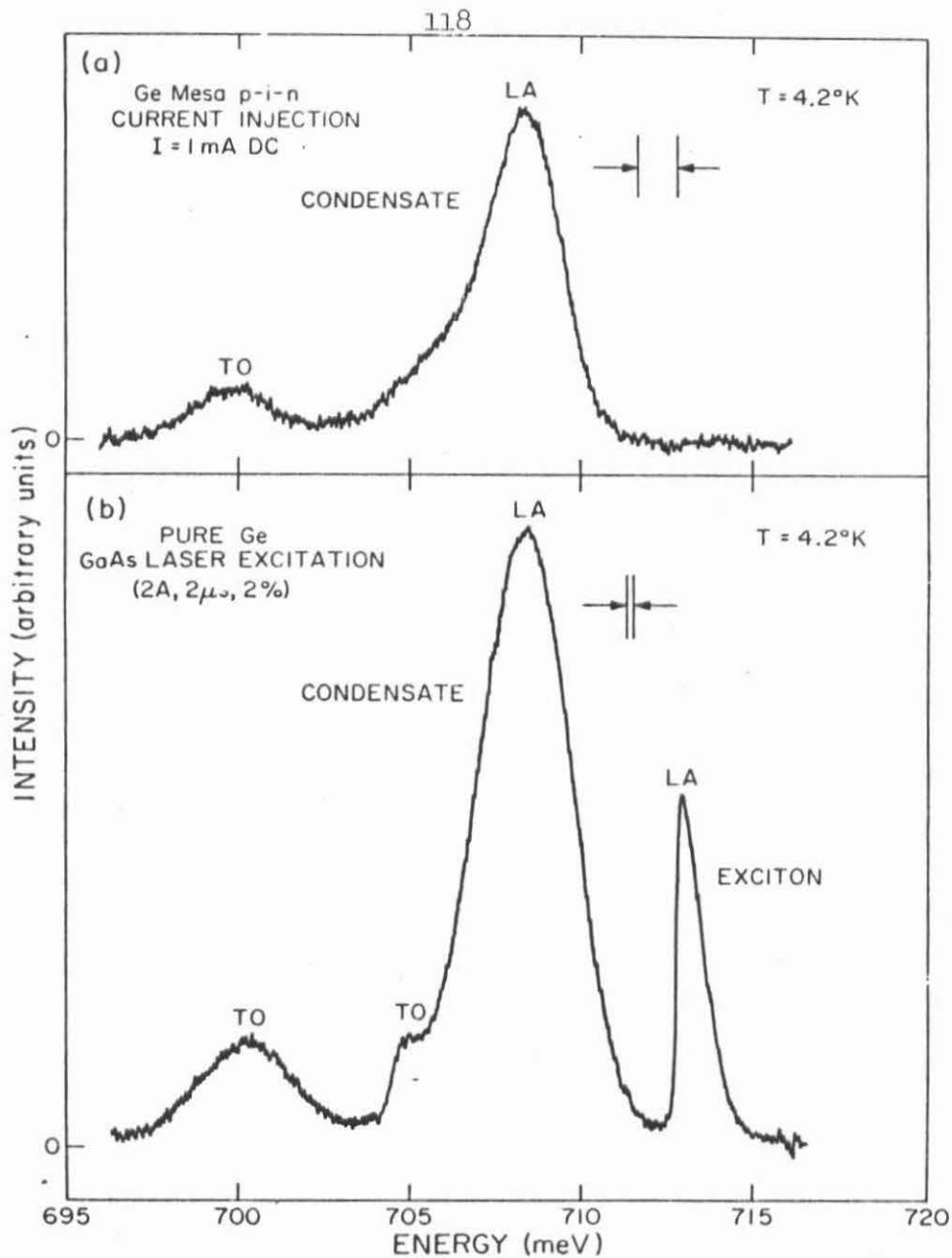
Figure 2

(a) Recombination Spectrum from a Ge mesa type double injection device. The spectrum was produced using electrical excitation.

(b) Recombination spectrum of a sample of high purity Ge produced by a GaAs laser excitation. Laser power ≈ 0.9 W.

in a lower density of $1.2 \times 10^{17} cm^{-3}$ as compared to $2.1 \times 10^{17} cm^{-3}$ obtained from the laser excited spectrum.

The results of the study on the effect of doping on the luminescence spectrum of Ge strongly suggest that the mesa double injection devices are contaminated by impurities. There are two ways impurities could be introduced into these devices. First, Li diffusion is involved in the diode fabrication so that the mesa diodes could contain significant amounts of Li in the active volume. Second, temperature cycling during the fabrication could introduce unknown impurities into the diode. In addition, electrical excitation requires fields and currents in the active region of the device which may not be present in optical excitation.

To test if temperature cycling is responsible for the dissimilarities between the spectra, high-purity Ge was subjected to the same heat treatment cycle that was used in device fabrication. The spectrum from this heat treated sample when it was excited by laser excitation was identical to that obtained from the pure Ge which had not been heat treated. Hence, the temperature cycles used in device fabrication are not responsible for the dissimilarities between the spectra in Fig. 2.

The influence of Li as the cause of the difference between electrical excitation of a mesa p-i-n and laser excitation of pure Ge was investigated by examining the spectra from the surface and the limited-area devices. As described in Sec. II, these devices were designed (see Fig. 1) so that minimal amounts of Li would be present in their active volumes.

Figure 3(a) shows the 4.2°K electrically excited spectrum from the surface p-i-n diode. This spectrum exhibits peaks due to the LA- and TO- phonon-assisted recombination of free excitons and electron-hole pairs in the condensate. The width of line associated with the condensate is 3.3 meV which yields a density of $2.1 \times 10^{17} cm^{-3}$ in good agreement with that obtained by using laser excitation of pure Ge[6]. In contrast to results obtained by electrical excitation of a mesa type structure, this spectrum contains a well defined free-exciton peak. The intensity of the optical signal from this device was much less than that obtained from the mesa structure or from the optical excitation of pure Ge. The rather small signal to noise ratio precluded a systematic search for current threshold in observation of the condensate recombination line. To compare directly electrical and optical excitation, we have excited the region between the contacts of this same p-i-n surface structure with a GaAs laser. The recombination radiation spectrum obtained in this fashion is shown in Fig. 3(b). The linewidth of the condensate line is 3.3 meV, again giving a density of about $2.1 \times 10^{17} cm^{-3}$. The spectral features of the spectrum in Fig. 3(b) are very similar to those of Fig. 3(a). This fact again indicates the similarity between the results obtained by optical excitation and double injection.

Finally, in Fig. 4 the recombination spectrum from a limited-area p-i-n structure using electrical injection is shown. The spectrum exhibits lines due to the LA- and TO- phonon assisted recombination from free excitons and electron-hole pairs in the condensate. The linewidth of the condensate line is about 3.3 meV which yields a density of

Figure 3

(a) Recombination spectrum from a surface p-i-n
    double injection structure. The sample was
    excited by illuminating the area between the
    p^+- and n^+- contacts. The laser power,
    uncorrected for reflection loss at the
    sample surface, was approximately 2.3 W.

(b) Recombination spectrum from a surface p-i-n,
    Ge double injection device. The device was
    excited by passing a current between the
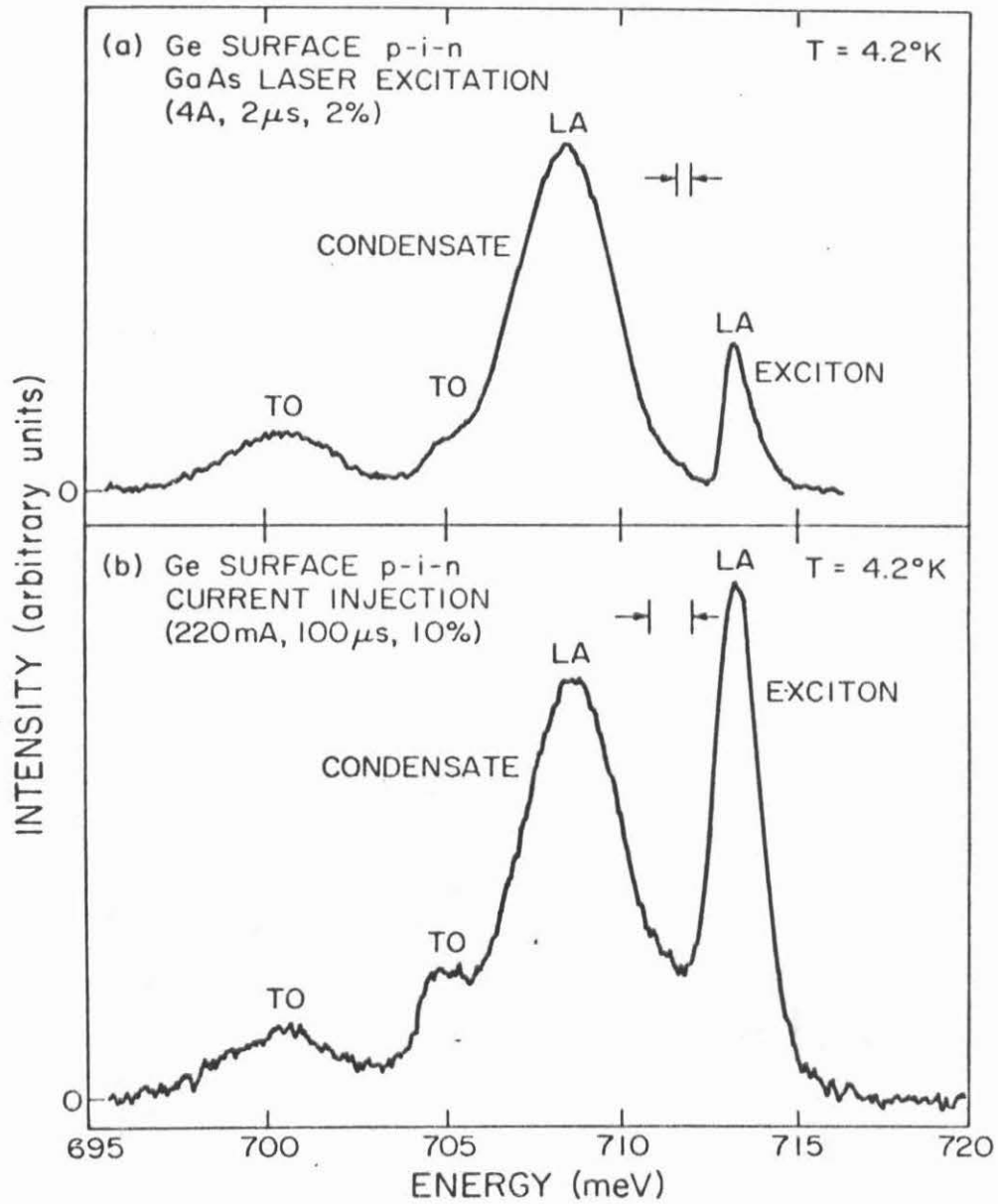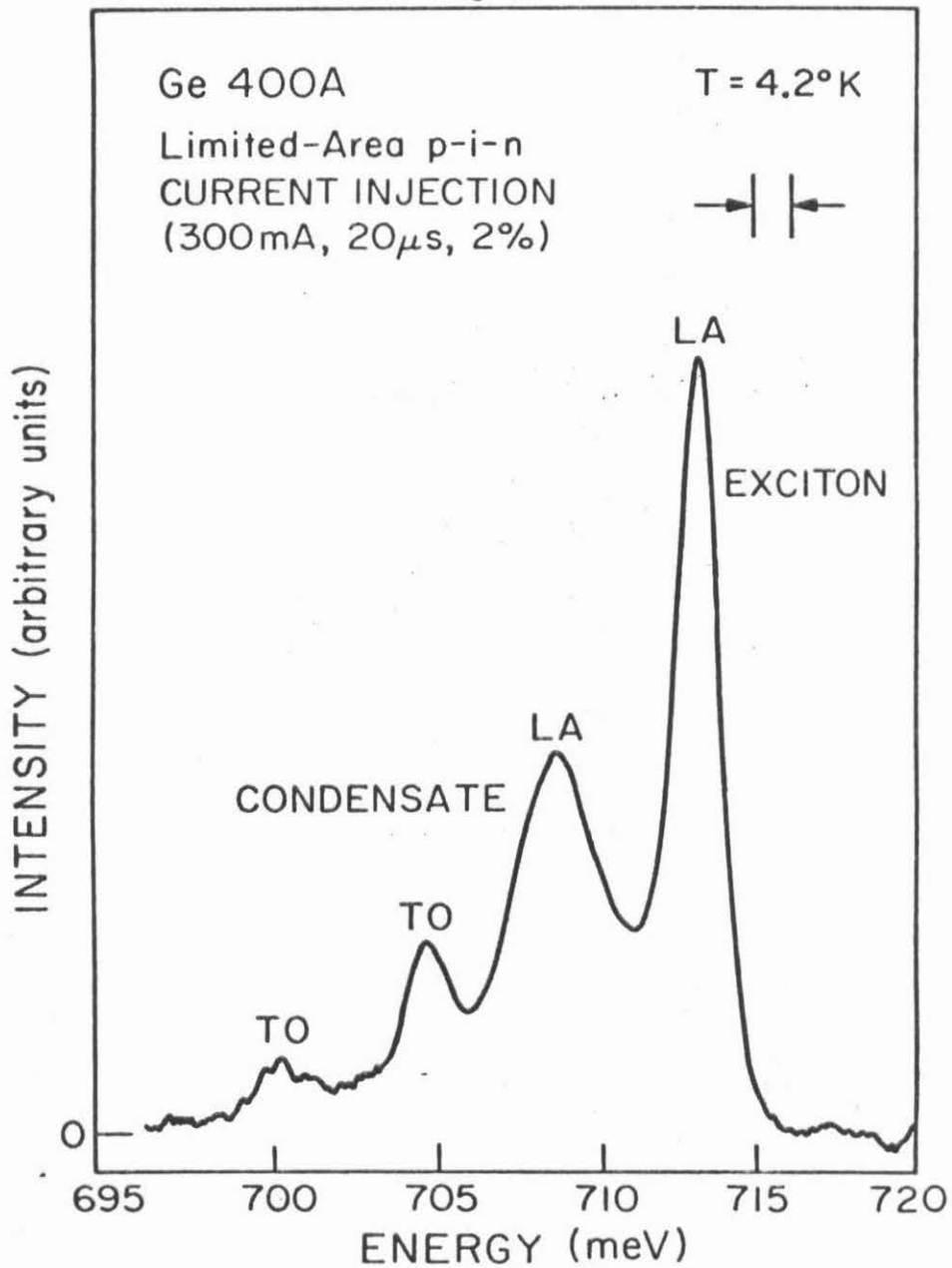   contacts.

Figure 3

Figure 4

Recombination spectrum from a limited-area p-i-n double injec-
tion device. The device was excited using electrical injection.

about $2.1 \times 10^{17} \text{cm}^{-3}$ in good agreement with that found in laser excitation of pure Ge[6]. The spectrum is qualitatively similar to that observed in the laser excitation from pure material and electrical injection in the surface p-i-n structure.

Although the features of the recombination spectra are similar we have noted some differences in the intensity of the recombination radiation between optically excited and double injection structures. In the surface and limited-area p-i-n structures, the signal to noise ratio as well as the ratio of condensate to exciton intensities are lower than in laser excited samples. These differences can be explained by the difference in the excitation level produced by the two methods of excitation. In the electrical excitation case, the injected density of carriers can be estimated from

$$J = ne\mu E \qquad (1)$$

where J is the current density in the device, e is the electronic charge, μ is the sum of electron and hole mobilities, and E is the electric field in the device. From a typical device current of 300 mA and the contact area of about 4 mm^2 we estimate J to be 5 A/cm^2. The value of μ at 4.2°K for pure Ge is about $6 \times 10^6 \text{cm}^2/\text{V-sec}$[7]. We take E to be 1 V/cm[8]. Thus, we estimate the injected pair density to be on the order of 10^{11}cm^{-3}. The intrinsic region of the crystal could be contaminated by as much as 10^{15}cm^{-3} of Li. Contamination of this level could reduce the mobility by as much as 100 and increase n by the same factor[9]. In the optical excitation case, we can calculate the number

of photons absorbed per laser pulse to be about 10^{13}. The volume occupied by the excited carriers can be estimated from the results of spatially-resolved infrared absorption measurements[10] to be about 1 mm^3. The pair density generated in the optical excitation experiments is estimated to be on the order of $10^{15} cm^{-3}$; and this value is much larger than that estimated for the double injection diodes. At lower optical excitation levels than that employed in the present experiment, one would expect to obtain spectra identical to those in Figs. 3(b) and 4. It should be noted, however, that at higher temperatures than 4.2°K, bound-exciton luminescence line is seen in both the surface and the limited-area p-i-n diodes. The existence of the bound-exciton line is an indication that the Li concentration in the active volume of these two devices may be as high as $10^{15} cm^{-3}$.

IV.   SUMMARY AND CONCLUSIONS

In this chapter we have examined possible causes of the dis-
similarities between the recombination spectra from electrically
excited mesa type p-i-n diodes and laser excited high-purity Ge.   We
produced spectra via electrical excitation from structures fabricated
to minimize the amount of Li in the device and compared these spectra
with those obtained by laser excitation of Li doped and high-purity Ge.
The spectral features in the recombination spectra from current
injection in low Li content devices were found to be the same as those
from laser excitation of high-purity Ge.   On the other hand, electrical
excitation of mesa type Ge p-i-n structures and laser excitation of
Li-doped Ge produced similar spectra.   We conclude that the features
of the recombination spectrum of the electron-hole condensate do not
depend on the method of excitation but on the impurity of the Ge.   We
have demonstrated that it is possible to generate EHD's in Ge electri-
cally by using double injection technique.

REFERENCES

1. C.D. Jeffriés, Science 189, 955 (1975), and references contained
    therein.

2. V. Marrello, M. Chen, T.C. McGill and J.W. Mayer, (unpublished).

3. V. Marrello, T.F. Lee, R.N. Silver, T.C. McGill and J.W. Mayer,
    Phys. Rev. Lett. 31, 593 (1973).

4. V. Marrello, R.B. Hammond, R.N. Silver, T.C. McGill and J.W.
    Mayer, Phys. Lett. 47A, 237 (1974).

5. V. Marrello, T.C. McGill and J.W. Mayer, Phys. Rev. B13, 1607,
    (1976).

6. G.A. Thomas, T.G. Phillips, T.M. Rice and J.C. Hensel, Phys. Rev.
    Lett. 31, 386 (1973).

7. G. Ottaviani, C. Canali, F. Nova and J.W. Mayer, J. Appl. Phys.
    44, 2917 (1973).

8. V. Marrello, (unpublished).

9. T.C. McGill and R. Baron, Phys. Rev. B11, 5208 (1975).

10. K.R. Elliot, D.L. Smith and T.C. McGill, (to be published).

Chapter 5

RATIO OF LA- TO TO-PHONON-ASSISTED LUMINESCENCE

INTENSITIES FROM THE EXCITON AND EHD IN Ge

I. INTRODUCTION

In a pure, indirect band-gap semiconductor, radiative recombination of electron-hole pairs must be assisted by phonons. These phonons are required for conservation of crystal momentum. Since it is possible for several phonons with different energies to supply the same amount of crystal momentum, recombination of electron-hole pairs can produce several replicated lines in different spectral ranges[1]. The low-temperature luminescence spectra of Ge, Si, and GaP have features due to exciton recombination and recombination of pairs in the electron-hole-droplet (EHD) with the assistance of different phonons. In Table I the different phonons that lead to the major lines for Ge, Si, and GaP are listed along with the energies of these phonons.

The intrinsic linewidths of the EHD luminescence line for Ge, Si and GaP are also listed in Table I. For Ge, the difference in energy between the phonons is much larger than the EHD linewidth. Thus, each phonon-replica of the EHD line can be fitted accurately to the theoretical line shape. This line-fitting procedure has been shown to be a convenient method for the determination of the electron-hole pair density, work function and the Fermi-liquid parameters of the EHD in Ge[2].

In Si and GaP, the several phonon-replicas of the EHD line are separated in energy by amounts smaller than the intrinsic EHD linewidth. Without a knowledge of the intensity ratios for the various phonon-replicas of the EHD line, it is impossible to accurately determine the EHD parameters from the luminescence line shape of the EHD.

material	phonon	energy (meV)	intrinsic EHD linewidth at $2°K$ (meV)
Germanium	TO LA	35.9 27.4	3.4
Silicon	TO LO	56.3 58.1	~12
Gallium Phosphide	TO LA TA	44.1 30.8 13.0	~17

Table 1

Energies of phonons which assist in the most intense recombination lines and intrinsic EHD linewidth for three semiconductors.

In contrast to the EHD lines, the width of the exciton (FE) lines are considerably narrower. This is because the FE linewidth is caused by the thermal motion of the FE's and is of the order of kT or 0.086 T(°K) meV[3,4]. The various phonon-assisted FE lines are easily resolvable from each other and their relative intensity ratios can be easily determined.

In this chapter, we report the results of an experimental determination of the ratio of the total integrated-intensities of the TO- to LA-phonon-assisted lines of the FE and the EHD as functions of temperature for Ge. (These ratios for the FE and the EHD will henceforth be denoted by γ_E and γ_{EHD}, respectively.) We verify the theoretical prediction of Smith and McGill[5] that γ_{EHD} is independent of temperature and is equal to the value of γ_E in the high temperature limit. Thus, in semiconductors such as Si and GaP, one can use $\gamma_E(T)$ to determine γ_{EHD} and perform accurate line fits of the EHD spectra.

II. THEORY

The theory of Smith and McGill[5] for the temperature dependence of γ_E is based on the ground state splitting of the exciton[6,7] combined with the differences in the phonon emission rates for the two exciton states. Since the exciton binding energy in Ge is only about 4 meV[8], an examination of the band structure of Ge shows that the ground state wavefunction of the exciton is largely an admixture of electronic states (L_1) near the conduction band minimum and hole states (Γ_8^+) near the valence band maximum. Since the conduction band minimum is anisotropic, the electronic charge density of an exciton is spatially anisotropic.

This anisotropic electron charge density causes the exciton ground state to split. Figure 1(a) schematically illustrates the electron and hole charge densities in real space for the two exciton ground states in Ge. In one of these two states, the hole charge density has the symmetry of $(L_4^+ + L_5^+)$ which is a mixture of the four Γ_8^+ states. This state takes maximum advantage of the electron-hole Coulomb interaction to reduce the total energy of the state. In contrast, the hole charge density in the other of the two exciton ground states has the symmetry L_6^+ and this state is less tightly bound than the state labelled by $(L_4^+ + L_5^+)$. The relative probability of the occupation of these two exciton states is proportional to a thermal occupation factor, $e^{-\Delta E/kT}$, where ΔE is the difference in energy between the two states. Figure 1(b) shows a high-resolution spectrum of the FE in Ge. In this spectrum, the presence of the two split ground states of the FE can be clearly seen. Usually, however, the two FE states cannot be resolved so that one observes only a single peak for each phonon-assisted FE line. In this latter case, $\gamma_E(T)$ is given by

$$\gamma_E(T) = \frac{R_{TO} + r_{TO}\, e^{-\Delta E/kT}}{R_{LA} + r_{LA}\, e^{-\Delta E/kT}} \tag{1}$$

where R_{TO} (R_{LA}) and r_{TO} (r_{LA}) are the rates for photon emission via TO- (LA-) phonon emission for the more tightly bound state and the less tightly bound state, respectively.

As illustrated in Figure 2, the two most likely recombination paths

Figure 1

(a) Schematic illustration of the charge densities in real space of an electron and a hole bound in an exciton.

(b) Free-exciton recombination spectrum of pure Ge showing the presence of both the upper ($L_6^\pm$) and the lower ($L_4^\pm + L_5^\pm$) excitons.

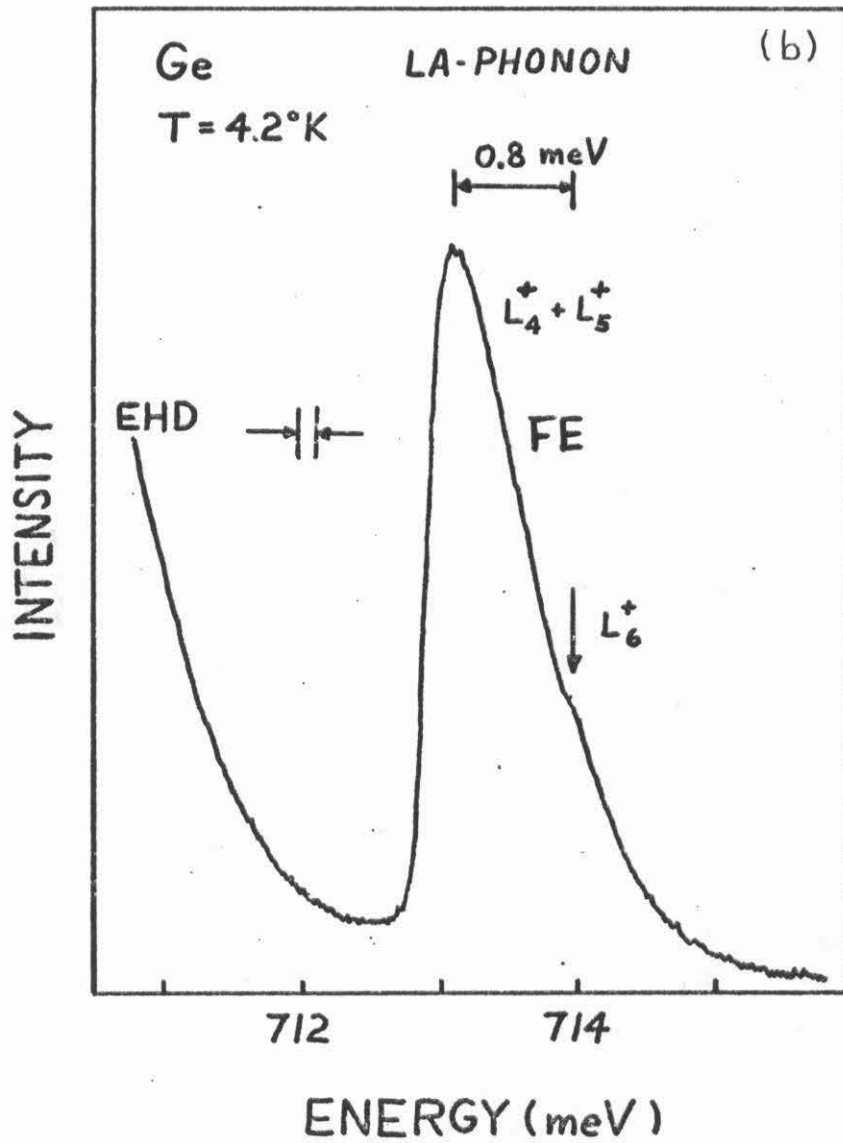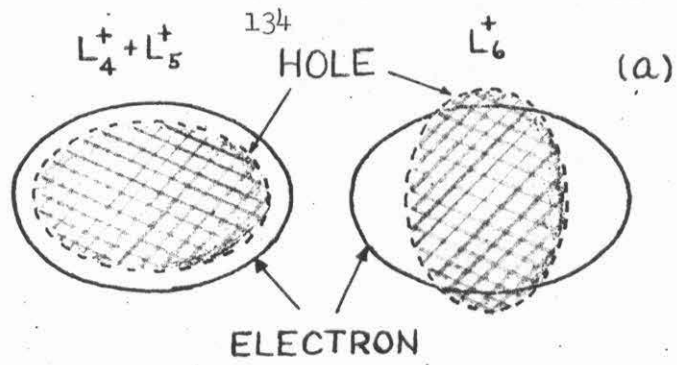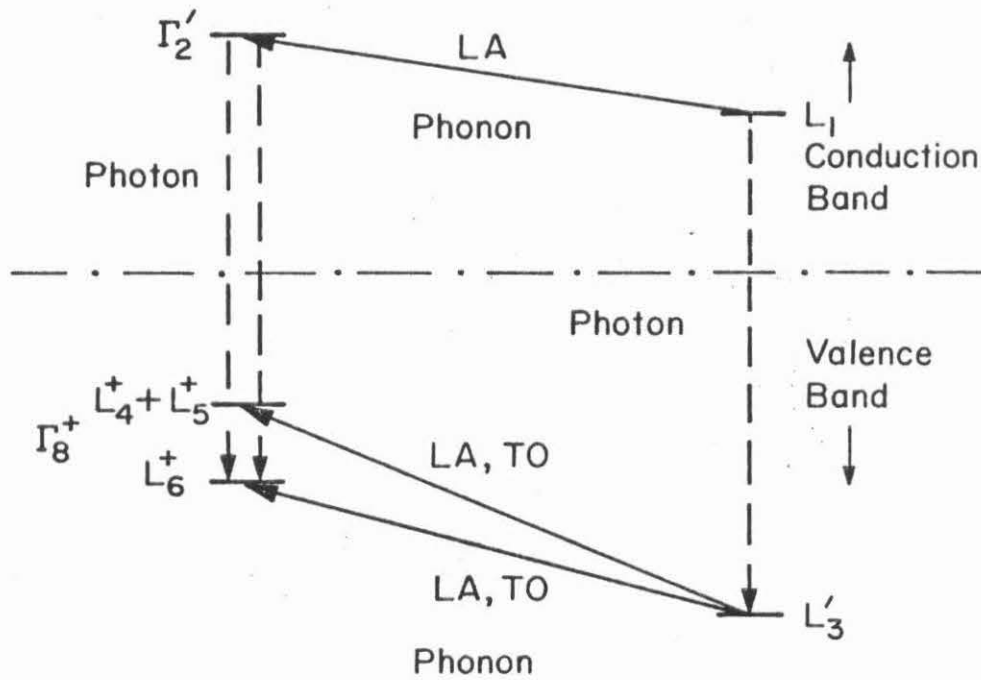Figure 1

Exciton Recombination Paths

Figure 2

Schematic diagram of the two recombination processes in Ge. The splitting of the exciton ground state is shown in the hole band where the 4-fold degeneracy of the Γ_8^+ states is split into two 2-fold degenerate states ($L_4^+ + L_5^+$) and L_6^+ which are labeled according to the irreducible representations of the group of $\vec{K}$ for $\vec{K}$ at L.

in Ge are: (1) The electron emits a phonon and makes a transition from the L_1 state in the conduction band to the Γ_2' state in the conduction band and then recombines with a hole in either the $(L_4^+ + L_5^+)$ state in the case of the more tightly bound exciton or the L_6^+ state in the case of the less tightly bound exciton. This process is allowed for LA-phonon emission only[1]. (2) The hole in either $(L_4^+ + L_5^+)$ or L_6^+ emits a phonon and makes a transition to L_3; it then recombines with the electron at L_1 emitting a photon. This process is allowed for LA- and TO-phonons.[1]

The matrix elements for the rates R_{TO}, R_{LA}, r_{TO} and r_{LA} are calculated using second-order perturbation theory. For example, the amplitude for r_{TO} is

$$\sim \frac{1}{\Delta E_v} \langle L_6^+ | H_{ep}^{TO} | L_3' \rangle \cdot \langle L_3' | P | L_1 \rangle, \tag{2}$$

while the amplitude for r_{LA} has two contributions:

$$\frac{1}{\Delta E_v} \langle L_6^+ | H_{ep}^{LA} | L_3' \rangle \cdot \langle L_3' | P | L_1 \rangle \tag{3a}$$

and

$$\frac{1}{\Delta E_c} \langle L_6^+ | P | \Gamma_2' \rangle \cdot \langle \Gamma_2' | H_{ep}^{LA} | L_1 \rangle. \tag{3b}$$

In Eqns. (2) and (3), P is the momentum operator, H_{ep}^{TO} and H_{ep}^{LA} are,

respectively, the TO- and LA- part of the electron-phonon interaction Hamiltonian, and ΔE_c and ΔE_v are the energy differences between the L- and Γ-points in the conduction band and valence band, respectively. Neither the electron-phonon interaction Hamiltonian nor the momentum operator couple spins, so the matrix elements for the rates, such as those in Eqn. (2) and (3), may be simplified by decomposing the electron and hole wavefunctions into spatial and spin parts by using Clebsch-Gordon coefficients. Thus, $\gamma_E(T)$ may be reduced to the form[5]

$$\gamma_E(T) = \frac{3}{2}|B|^2 \frac{3 + (1 + 2|A|^2)\, e^{-\Delta E/kT}}{3(1+C)^2 + (2+(1+C)^2)e^{-\Delta E/kT}} \qquad (4)$$

where A, B and C in terms of the reduced matrix elements[9] are

$$A = \frac{\langle L_3' \| H_{ep}^{TO} \| L_1 \rangle}{\langle L_3' \| H_{ep}^{TO} \| L_3 \rangle}, \qquad (5)$$

$$B = \left(\frac{\Delta E_c}{\Delta E_v}\right) \frac{\langle L_1 \| P \| L_3' \rangle \langle L_3' \| H_{ep}^{TO} \| L_3 \rangle}{\langle L_1 \| H_{ep}^{LA} \| \Gamma_2' \rangle \langle \Gamma_2' \| P \| \Gamma_{25}' \rangle}, \qquad (6)$$

$$C = \frac{\sqrt{3}}{2}\left(\frac{\Delta E_c}{\Delta E_v}\right) \frac{\langle L_1 \| P \| L_3' \rangle \langle L_3' \| H_{ep}^{LA} \| L_3 \rangle}{\langle L_1 \| H_{ep}^{LA} \| \Gamma_2' \rangle \langle \Gamma_2' \| P \| \Gamma_{25}' \rangle}. \qquad (7)$$

In absorption, the exciton states are the final states so that no thermal occupation factor needs to be considered. The intensity ratio γ_A is given by

$$\gamma_A = \frac{R_{TO} + r_{TO}}{R_{LA} \quad r_{LA}}, \qquad (8)$$

and is independent of temperature. For high temperatures such that kT >> ΔE, we have that $\gamma_E(T)$ approaches γ_A.

In an EHD, each hole is correlated with many electrons so that each hole sees a symmetric charge density and the hole states are not split, i.e., $\Delta E = 0$. As a result, the ratio of EHD emission intensities, γ_{EHD}, should be equal to the high temperature limit of the exciton emission intensity ratio (or equivalently the absorption ratio). Thus, we should have

$$\gamma_{EHD} = \gamma_A = \lim_{T \to \infty} \gamma_E(T). \qquad (9)$$

Hammond et al.[10] have shown that in Si $\gamma_E(T)$ has the form given by Eqn. (1). (In Si, the relevant phonons are the TO- and LO-phonons.) In addition, they have shown that $\gamma_E(T)$ does approach at high temperatures the value of γ_A as determined by earlier investigators. For reasons mentioned earlier, however, they could not verify the important, second equality in Eqn. (9).

III. EXPERIMENTAL

The luminescence data were taken using high-purity Ge with net impurity concentration $N_D - N_A \sim 2 \times 10^{10} cm^{-3}$. The spectra were obtained in the manner described in detail in Chapter 2. The spectra were independent of laser power and hence showed no evidence of heating. At temperatures less than 6.5°K, the exciton spectra were taken at excitation levels below the threshold for droplet formation. Since the lines are well separated in Ge, the relative integrated-intensities of the TO- and LA-emission lines were easily determined.

IV. EXPERIMENTAL RESULTS

The experimental values of the ratio for the exciton and EHD are

shown in Figure 3. The experimental values of the ratio for the
exciton show a temperature dependence as expected from the above dis-
cussion. On the other hand, the ratio for EHD shows no temperature
dependence within experimental error. Further, the high temperature
value of exciton ratio is found to approach the ratio for the EHD.

The results for exciton ratio predicted by Eqn. (4) are also shown
in Figure 3. The parameters ΔE and C were taken from previous experi-
mental investigations of Ge. The energy splitting ΔE has been measured
using a number of different experimental techniques and values between
0.7 meV and 1.1 meV have been reported[7,8,11-13]. We use the most re-
cent result obtained by Frova et al[8] using wavelength-modulated ab-
sorption (ΔE=1.01 meV). However, our result is not very sensitive to
small changes in ΔE and an equally good fit can be attained if one of
the other measured values of ΔE is used. The parameter C can be deter-
mined from the relative oscillator strengths of the LA-phonon assisted
$(L_4^+ + L_5^+)$ and L_6^+ exciton absorption measured by Frova et al[8] (C=0.25).
The values of the parameters A and B have not previously been measured
and were taken to produce the best agreement between theory and experi-
ment. (The parameter A could be determined from the relative oscilla-
tor strenghts of the TO-phonon assisted $(L_4^+ + L_5^+)$ and L_6^+ exciton absorp-
tion.) The values of A and B which produced the best fit were 0.52 and
0.45, respectively. The agreement between the theoretical and experi-
mental values of $\gamma_E(T)$ is quite good as illustrated in Figure 3.

We have also plotted the high temperature limit of Eqn. (4) for
the same parameters used for the exciton ratio. The comparison between
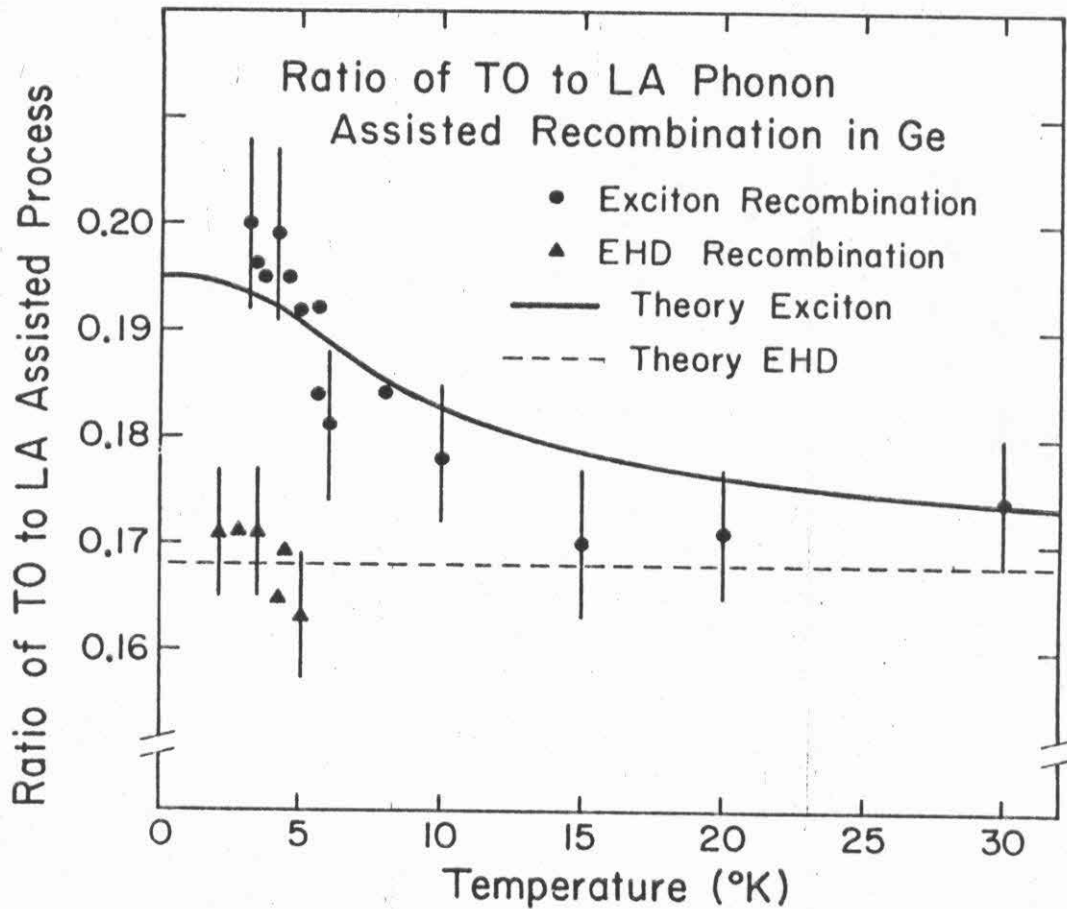this high temperature limit and the observed ratio for the EHD is given

Figure 3

The ratio of TO- to LA-phonon assisted exciton and EHD emission as
as a function of temperature. The experimental data labeled by (●) are
for free exciton emission and the data labeled by (▲) are for EHD
emission. Representative error bars are shown on some of the data
points. The theoretical curves are obtained by taking $\Delta E = 1.01$ meV,
$A = 0.52$, $B = 0.45$, and $C = 0.25$ (see Eqs. (4) and (9)).

in Figure 3. The agreement is well within the experimental error.

V. CONCLUSION

In conclusion, a temperature dependence of the TO- to LA-phonon assisted luminescence intensities in Ge has been systematically investigated and explained. This effect should be distinguished from the well understood temperature dependence in the intensity ratio of forbidden to allowed transitions (e.g., TA/LA in Ge)[1,14]. The EHD intensity ratio for allowed phonon processes has been explicitly shown to equal the high temperature limit of the corresponding exciton emission ratio. Therefore, in semiconductors where it is impossible to determine γ_{EHD} directly, one can use either $\gamma_E(T)$ or γ_A to determine γ_{EHD}. The correct value of γ_{EHD} should be used in attempting to determine parameters for the EHD from its luminescence line.

REFERENCES

1. The selection rules for various phonon-assisted transitions have been worked out in M. Lax and J.J. Hopfield, Phys. Rev. $\underline{124}$, 115 (1961).

2. G.A. Thomas, T.G. Phillips, T.M. Rice and J.C. Hensel, Phys. Rev. Lett. $\underline{31}$, 386 (1973).

3. R.J. Elliot, Phys. Rev. $\underline{108}$, 1384 (1957).

4. C. Benoit a la Guillaume and M. Voos, Solid State Commun. 12, 1257 (1973).

5. D.L. Smith and T.C. McGill, Phys. Rev. $\underline{B14}$, 2448 (1976).

6. T.P. McLean and R.J. Loudon, J. Phys. Chem. Solids $\underline{13}$, 1 (1960).

7. N.O. Lipari and A. Baldereshi, Phys. Rev. $\underline{B3}$, 2497 (1971).

8. A. Frova, G.A. Thomas, R.E. Miller and E.O. Kane, Phys. Rev. Lett. $\underline{34}$, 1572 (1975).

9. G.F. Koster, J.O. Dimmock, R.G. Wheeler and H. Statz, Properties of the Thirty-Two Point Groups, (M.I.T. Press, Cambridge, MA., 1963), p.133 ff. The states L_1 and L_3 in eqn.(5) and L_3 in eqns. (6) and (7) refer to the spatial part of the hole wavefunction.

10. R.B. Hammond, D.L. Smith and T.C. McGill, Phys. Rev. Lett. $\underline{35}$, 1535 (1975).

11. E.F. Gross, V.J. Safarov, A.N. Titkov and I.S. Shlimak, Pis'ma Zh. Eksp. Teor. Fig. $\underline{13}$, 332 (1971) [JETP Lett. $\underline{13}$, 235 (1971)].

12. T. Nishino, M. Takeda and Y. Hamakawa, J. Phys. Soc. Japan $\underline{37}$, 1016 (1974).

13. K.J. Button, L.M. Roth, W.H. Kleiner, S. Zwerdling and B. Lax, Phys. Rev. Lett. $\underline{2}$, 161 (1959).

14. C. Benoit a la Guillaume and O. Parodi, in Proc. Int. Conf. Semicond. Phys., Prague, 1960, p.426.